الجمهورية الجزائرية الديمقراطية الشعبية
People's Democratic Republic of Algeria
وزارة التعليم العالي والبحث العلمي
Ministry of Higher Education and Scientific Research
جامعة البليدة1
University of Blida 1

Faculty of Nature and Life Sciences

Department of Biotechnology

Laboratoire de Biotechnologie des Productions Végétales

End of study thesis

For the obtention of the Academic Master degree qualification

Option

Biotechnology and Molecular Pathology

Theme

Contribution of Epstein-Barr virus to the pathogenesis of classical Hodgkin lymphoma: Highlighting of key genes and associated signaling pathways

By

Ms. Bensafi Fella

Ms. Chabane Fatma Zohra

Assessment Committee members:

Mme A. KANANE	***M.C.B***	***SNV, Blida I***	***Chair***
Mme I. RAHIM	***M.C.A***	***SNV, Blida I***	***Examiner***
Mme F. BENAZOUZ	***M.A.A***	***SNV, Blida I***	***Supervisor***
Mr. A. BELARBI	***Professor***	***DOUERA hospital***	***Co-promoter***

Session 2020/2021

Acknowledgments

We would like to thank the following people, without whom we would not have been able to complete this research, and without whom we would not have made it through our Master's degree!

First, we would like to thank our parents for standing with us to the last moment!

May Allah keep you always by our side.

Mme BENAZOUZ F for having supervised this work of research, whose guidance, support, insight and knowledge steered us through this research.

The chief of Anatomy Cytopathology unit of DOUERA hospital, Pr Bellarbi A for giving us the chance in such a global pandemic to join the Anatomy Cytopathology team and for guiding us in our experimental work as co-promoter, we are very thankful for his valuable advice and guidance in the development of this thesis.

All the members of the jury for having accepted to judge this work Mme KANANE A for having accepted to chair the members of our jury. Mme RAHIM I for having kindly examined this work and for her support.

A special thanks for the Anatomy Cytopathology team especially Dr Kassa, Mr Kherroubi.H and Mr Maazouz.L

The Biotechnology and Molecular Pathology team of the Biotechnology department, especially to Dr Mokrane A for her support!

The owner of the Anatomy Cytopathology laboratory of Blida Pr Khamsi D for helping us to reach our results, that was very kind from you doctor!

Our brothers, sisters, friends and colleagues who have supported us and had to put up with our stresses for the past 8 months of study!

Thank you all…

Table of content

List of tables

List of Figures

List of abbreviations

Ab: Monoclonal antibody

APC: Antigen-presenting cells

BHRF1: fragment H rightward open reading frame 1

CCL17: C-C Motif Chemokine Ligand 17

CCL22: C-C Motif Chemokine Ligand 22

CCL5: C-C Motif Chemokine Ligand 5

CCT: Cytoplasmic C-terminal Tail

CHL: Classical Hodgkin lymphoma

CTARs: carboxy-terminal activating region sites

CtBP: C-terminal-Binding Protein

CXCL10: C-X-C motif Chemokine ligand 10

DDR1: Discoidin Domain Receptor 1

Down Reg: Downregulated

E2A: Transcription factor E2-alpha

EBER1: EBV-Encoded small RNAs 1

EBER2: EBV-Encoded small RNAs 1

EBNA-3A, Epstein – Barr Virus Nuclear Antigen 3A

EBNA-3B, Epstein – Barr Virus Nuclear Antigen 3B

EBNA-3C: Epstein – Barr Virus Nuclear Antigen 3C

EBNA-LP: EBV Nuclear Antigen-Leader Protein

EBNAs: Virus Nuclear Antigens

EBV miRNAs: Epstein – Barr Virus- encoded microRNAs

EBV: Epstein Barr virus

EC: Endothelial cell

FASCIN1: Actin-bundling protein Fascin

GATA3: Trans-acting T-cell-specific transcription factor GATA-3

GC: Germinal center

GP: glycoproteins

HL: Hodgkin's lymphoma

HRS: Hodgkin Reed Sternberg

HL-CHILD-N: Hodgkin's Lymphoma--Child/EBV—Negative

HL-CHILD-P: Hodgkin's Lymphoma--Child/EBV—Positive

HL-N: Hodgkin's Lymphoma--Adult/EBV—Negative

HL-P: Hodgkin's Lymphoma--Adult/EBV—Positive

ID2: DNA-binding protein inhibitor ID-2

IgV: Variable Immunoglobulin gene

LCV: Lymphocryptovirus

LD: Lymphocyte Depleted

LMP1: Latent Membrane Protein 1

LMP2A/B: Latent Membrane Protein 2

LR: Lymphocyte Rich

MC: Mixed Cellularity

MHCII: Major Histocompatibility Complex class II

miRNAs: MicroRNAs

NcRNAs : non-coding RNAs

NF-Kb: Nuclear Factor κB

PAX5: Paired box protein 5

PD-L1: Programmed death- Ligand 1

RIP: Receptor Interacting Protein

Thy-1: Thy-1 membrane glycoprotein

TM1-6: six transmembrane domains

TNF: Tumor Necrosis Factor

TNFRSF21: Tumor necrosis factor receptor superfamily member 21

TRADD: TNFR-Associated Death Domain proteins

TRAFs: Tumor necrosis factor Receptor -Associated Factors

Treg: regulatory T cells

Up Reg : Upregulated

Abstract

Classical Hodgkin Lymphoma is widely accepted to be a malignant clonal proliferation of B-lymphocytes. 50% of cHL are caused by Epstein - Barr virus infection. In the present study, it has been demonstrated that classical Hodgkin Lymphoma affects people of all age groups, and a specification was made for EBV positive age groups. Nodular sclerosis subtype was remarkably abundant in the cohort of study with absence of Lymphocyte Depleted subtype. The presence of H and RS cells in the lymph node infiltrate indicated the presence of a malignant B lymphoma. Results have shown that the diagnosis of cHL requires both histological and IHC testing to avoid misdiagnosis of other B cell lymphomas. The total of immunohistochemical staining tests for the markers CD15, CD30 and CD20 was done to confirm the diagnosis of cHL. To investigate the incrimination of EBV in cHL oncogenesis, a IHC technique was established to highlight the presence of LMP1; subsequently the detection of EBERS using Chromogenic *In situ* hybridization approving the contribution of EBV as straight risk factor in the pathogenesis of classical Hodgkin lymphoma. In order to highlight other molecules that might be directly or indirectly related to cHL, specifically, in cHL - Positive cases, a bioinformatics analysis of an NCBI Geo DataSet, which is based on molecular profiling of classical Hodgkin Lymphoma tissues, was performed with the aim to explore key genes and signaling pathways associated with this pathogenesis through EBV. Results showed significant signaling pathways including chemokine pathways, NF-κB pathways, MAPK pathways and other significant signaling pathways that are essential for cHL's malignant progression. Our study also revealed a high expression of some key molecules such as CXCL-10 and CCL20 that need to be highlighted in the future to understand its mechanism through EBV in cHL patients with unfavorable outcome.

Key words: cHL, EBV, Immunohistochemistry, Differentially Expressed Genes, CISH, LMP1, Signaling pathways

Résumé

Le lymphome hodgkinien classique est largement reconnu comme étant une prolifération clonale maligne de lymphocytes B. 50 % des LHC sont causés par une infection par le virus d'Epstein-Barr. Dans la présente étude, il a été démontré que le lymphome de Hodgkin classique touche les personnes de tous les groupes d'âge, et une spécification a été faite pour les groupes d'âge EBV positifs. Le sous-type scléronodulaire était remarquablement abondant dans la cohorte étudiée avec absence de sous-type à déplétion lymphocytaire. La présence de cellules H et RS dans l'infiltrat des ganglions lymphatiques indique la présence d'un lymphome B malin. Les résultats ont montré que le diagnostic du LHC nécessite à la fois un test histologique et un test IHC afin d'éviter un diagnostic erroné avec d'autres lymphomes B. L'ensemble des tests immunohistochimique pour les marqueurs CD15, CD30 et CD20 a été effectué pour confirmer le diagnostic de LHC. Pour étudier l'incrimination d'EBV dans l'oncogenèse du LHC, une technique d'IHC a été établie pour mettre en évidence la présence de la protéine LMP1 puis la détection des EBERS par hybridation *in situ* chromogénique approuvait la contribution d'EBV comme facteur de risque direct dans la pathogenèse du lymphome de Hodgkin classique. Afin de mettre en évidence d'autres molécules qui pourraient être directement ou indirectement liées au lymphome hodgkinien classique, en particulier dans les cas de lymphome hodgkinien EBV-positif, une analyse bioinformatique d'une série du NCBI Geo DataSet basée sur le profiling moléculaire des tissus de lymphome hodgkinien classique a été réalisée dans le but d'explorer les gènes et les voies de signalisation clés associés à cette pathogenèse par le biais de l'EBV. Les résultats ont montré des voies de signalisation importantes, notamment la voie de des chimiokines, des NF-κB et la voie des MAPK qui sont essentielles pour la progression maligne du LHC. Nos observations ont également révélé une forte expression de certaines molécules clés telles que les CXCL-10 et CCL20, qui doivent être mises en évidence dans le future pour comprendre plus leur mécanisme par le biais d'EBV chez les patients atteints du LHC dont le bilan est défavorable.

Mots clés : LHC, EBV, Immunohistochimie, Gènes Exprimés différentiellement, CISH, LMP1, Voie de signalisation.

ملخص

من المعروف وعلى نطاق واسع بان سرطان هودجكن الكلاسيكي (cHL) يشكل تكاثر نسيلي خبيث في الخلايا اللمفاوية البائية. 50بالمئة من سرطان هوجكن الكلاسيكي ناتج عن عدوى فيروس ابستاين- بار (EBV). في هذه الدراسة ثبت بان هذا السرطان يصيب اشخاص من جميع الفئات العمرية، مع تحديد الفئات العمرية المصابة بفيروس ابشتاين-بار. كان النوع الفرعي للتصلب العقدي وفيرًا بشكل ملحوظ مع غياب النوع الفرعي المستنفد للخلايا الليمفاوية ضمن مجموعة الدراسة. يشير وجود الخلايا الهودجكنية (Hodgkin) وخلايا ريد ستيرنبرغ (Reed-Sternberg) في تسرب العقدة الليمفاوية على وجود ورم لمفي خبيث للخلايا البائية. أظهرت النتائج أن تشخيص لمفومة هودجكين يتطلب كلا من التحليل النسيجي بتقنية التلوين الهيما توكسيلين-ايوزين وعلى تحليل النمط الظاهري المناعي بتقنية الكيمياء النسيجية المناعية لتجنب التشخيص الخاطئ للأورام اللمفاوية للخلايا البائية الأخرى. تم إجراء إجمالي اختبارات التلوين المناعي (immunohistochemistry)للعلامات CD15 و CD30 و CD20 لتأكيد التشخيص. لإبراز دور فيروس ابشتاين-بار في تكوين ورم هوجكن الكلاسيكي، تم استخدام تقنية التلوين المناعي لتسليط الضوء على بروتين الكمون الغشائي لفيروس ابشتاين-بار LMP1 , بعد ذلك تم الكشف عن وجود الحمض النووي الريبوزي EBERS لهذا الأخير بواسطة تقنية التهجين الموضعي (CISH) الذي سمح بتأكيد مساهمة فيروس ابشتاين-بار كعامل خطر مباشر في التسبب في ورم الغدد الليمفاوية هودجكين الكلاسيكي. من أجل تسليط الضوء على الجزيئات الأخرى التي قد تكون مرتبطة بشكل مباشر أو غير مباشر ب cHL على وجه التحديد، في الحالات الإيجابية لـ cHL، تم إجراء تحليل المعلوماتية الحيوية لمجموعة بيانات جغرافية NCBI، والتي تعتمد على التنميط الجزيئي لأنسجة هودجكين الليمفاوية الكلاسيكية ، بهدف استكشاف الجينات الرئيسية ومسارات الإشارات المرتبطة بهذا المرض من خلال EBV. أظهرت النتائج مسارات اشارة مهمة بما في ذلك مسارات الإشارة الكيميائية. كشفت دراستنا أيضًا عن تعبير مرتفع لبعض الجزيئات الرئيسية مثل ; CCL20 . CXCL-10 التي تحتاج إلى تسليط الضوء عليها في المستقبل لفهم آليتها من خلال EBV في مرضى المصابين ب cHL مع نتائج غير مواتية.

الكلمات المفتاحية: سرطان هودجكين كلاسيكي، ابستاين-بار، الكيمياء النسيجية المناعية، الجينات المعبر عنها تفاضليًا، تهجين الموضعي، بروتين الكمون الغشائي لفيروس ابستاين-بار، مسارات الإشارة.

Introduction

More than 170 years ago, Thomas Hodgkin first described the disease named after him. Hodgkin Lymphoma (HL) is one of the most frequent lymphomas in the western world, representing about 2-5 cases per 1000.000 persons annually in Europe. For several reasons, HL is; despite recent progresses, still one of the most fascinating hematopoietic malignancies **(Stephan et *al*., 2016)**. This lymphoid malignancy involves peripheral lymph nodes and can also affect organs such as liver, lung, and bone marrow. In Algeria, HL is the most frequent lymphoma (70.3%) **(National Institute of Public Health.,2017)**, its incidence is in progression since it passes from 0.7/105 inhabitants in 2006 to 1.8/105 in 2012, however, it remains lower than in France where it is 2.4 x 105 new cases per year **(Algerian review.,2015)**.

In classical HL, the malignant cells are referred to Hodgkin and Reed-Sternberg (HRS) cells, these cells are believed to be originated from the germinal center. EBV infection of B cells has a different malignant transformation path, with its latent genes; EBV is capable of causing damages to the host B cell. Changes in cell fate are driven by EBV encoded proteins LMP1 and LMP2 to promote a high immunogenicity **(Vrzalikova et *al*., 2018)**.

Currently IHC technique and *In Situ* Hybridization techniques are considered as gold standards to reveal and confirm EBV presence in cHL patients with the aim to provide a suitable prognosis. On the molecular level EBV LMP1/2A proteins have a major contribution to favor malignant progression.

The question of how the Epstein - Barr virus contributes to the pathogenesis of classical Hodgkin Lymphoma was the purpose of the first part of this work by reviewing the previously highlighted EBV- Encoded-Latent Membrane Protein 1 (LMP1) and by prospectively highlighting the EBV- Encoded small RNAs (EBERs) in different cHL subtypes using immunohistochemistry for the LMP1 protein revelation and Chromogenic *In situ* hybridization to detect EBERs non-coding transcripts.

Some signaling pathways involved in cHL call for molecules that deleteriously affect the surrounding microenvironment, thus provide tumor progression, in order to reveal these molecules, new refined tools can be helpful. Bioinformatics is now considered as a prominent field that favorably contributes to biological sciences by aiding in comparing, analyzing and interpreting genetic and genomic data. Therefore, to uncover proteins that were not pointed to in other researches of a specific subject. In the present study, we focus on establishing classical

Hodgkin Lymphoma link with EBV through several bioinformatics tools on a published data giving a new perspectives and understandings of the involved processes in cHL malignancy.

CHAPTER I
Literature review

I. Classical Hodgkin lymphoma

Hodgkin's lymphoma (HL), formerly known as Hodgkin's disease, is the first malignant lymphocyte tumor that has been described , which mainly affects the lymph nodes **(Mathas et *al*.,2016)** , is a malignant lymphoid neoplasm derived from the germinal center of B cells , it is the unique type of lymphoma that is characterized by neoplastic cells with a number less than 1% of the total cell population that are found in a microenvironment rich with T cells, eosinophils, neutrophils, plasma cells, fibroblasts and histiocytes, but despite this abundance, these immune cells cannot induce an anti-tumor response, instead, they will protect the neoplastic cells from anti-tumor attacks and provide it with survival signals **(Hudnall and Küppers.,2018)** .

Classical Hodgkin lymphoma is distinguished with the presence of neoplastic typical cells which are called REED-STERNBERG cells, it represents about 95% of all HL cases and 30-40% Epstein Barr virus (EBV) positive cases in western countries. CHL manifests as enlarged lymph nodes in the cervical region or mediastinum accompanied with fever and night sweat, despite its advanced stage, it is highly curable thanks to frontline therapy: chemotherapy with or without radiotherapy. Based on histological differentiation, cHL is subdivided into four major subtypes: Nodular Sclerosis (NS), Mixed Cellularity (MC), Lymphocyte Depleted (LD) and Lymphocyte Rich (LR) **(Oviedo et *al*.,2020).**

I.1. Epidemiology

In 2018, HL was classified worldwide as the 27th most frequently diagnosed cancer with nearly 80,000 individuals and the most frequent cause of death with over 26,000 people **(Ferlay et *al*.,2018)**. The incidence of Hodgkin lymphoma is lower in Asian and developing countries than in Western industrialized countries where the incidence is higher **(Fig.01)**, Conversely, death from HL is higher in some developing countries than in industrialized countries **(Fig.01) (Ferlay et *al*.,2018)**. Hodgkin's lymphoma occurs more often in men (in whites than in African Americans), so the discordant incidence and death reflect the fact that modern therapy can cure most Hodgkin lymphomas and that the access to this therapy depends on the level of socioeconomic development **(Ferlay et *al*.,2018)**.

- **In Algeria**

According to the distribution of cancer cases by age range and diagnostic groups in Algiers region in 2017:

In girls under 20 years of age malignant lymphomas represent 14.3% of childhood cancers which are more often observed in 15-19 years of age with 63.6%. Majority of cases were diagnosed as Hodgkin's disease **(Fig.01) (National Institute of Public Health.,2017)**.

In boys under 20 years of age lymphomas account for 17.7% of childhood cancers and are more often seen in 10-19 years old with 70.8%. Hodgkin's lymphoma is the most common with 70.3% **(Fig.01) (National Institute of Public Health.,2017)**.

Fig.01.Estimated worldwide age-standardized incidence and mortality rates of Hodgkin's lymphoma for both sex combined with an accurate distribution of HL cases by age group in Algiers region for the year 2017 **(Original illustration)** Upper Cartography reproduced from **(Ferlay et *al.*,2018)**

I.2. Risk factors

- **Childhood Socio-Economic Environment.** In children, adolescents and young adults' dirty environment (pathogens) and low socio-economic level are among the reasons of Hodgkin's lymphoma **(Engert and Younes.,2020)**.
- **Epstein-Barr Virus Infection.** Among suspected pathogens, the human herpesvirus Epstein-Barr virus, which is shown to be the main cause of infectious mononucleosis after its isolation for the first time from Burkitt lymphoma **(Engert and Younes.,2020)**.

- **Anthropometry.** This risk is associated with increased weight birth: In a Californian register-based investigation, Hodgkin lymphoma risk in the age group 0–19 years was found to increase by 16% per kilogram increase in birth weight **(Triebwasser et *al*.,2016)**.
- **Primary and Secondary Immune Deficiencies.** Hodgkin lymphomas occur excessively among patients suffering from certain primary and secondary immune deficiencies in which; the risk of Hodgkin lymphoma is between 4 and 16-fold increase in cohort studies of HIV-infected people and between 2 and 7-fold increase in cohort studies of solid organ transplant recipients **(Engels and Hildesheim.,2018)**.
- **Autoimmune and Allergic/Atopic Diseases.** Several studies have reported an increased risk of Hodgkin lymphoma among patients with autoimmune diseases **(Engels and Hildesheim.,2018)**.
- **Medications.** In one American **(Chang et *al*.,2004)** and in two partly overlapping Danish studies **(Chang et *al*.,2011)**, reported increased Hodgkin lymphoma risk among users of nonsteroidal anti-inflammatory drugs such as selective Cox-2 inhibitors or acetaminophen **(Chang et *al*.,2004,2011)**.
- **Ultraviolet Light.** An association between ultraviolet radiation exposure and Hodgkin lymphoma risk is supported **(Mondul et *al*.,2017; Bowen et *al*.,2016)**.
- **Tobacco**. Given that of the many effects of tobacco on the human immune system, it is conceivable that it is also associated with the risk of Hodgkin's lymphoma **(Engert & Younes.,2020)**.

II. Physiology of lymph nodes

Lymph nodes are small secondary lymphatic organs distributed all over the human body, more precisely they are interposed along the lymphatic vessels, grouped in certain strategic points (regional lymph nodes) to drain different regions. In the first place allow to filter the lymph during its return to the bloodstream. It is the site of activation of T and immunocompetent lymphocytes **(Rehfeld et *al*.,2017).**

The lymph node is 1-20 mm long, flat in structure, kidney bean shaped. Lined by a thin capsule of dense connective tissue, where the trabeculae are extended from the capsule to the lymph node, hilum (at the concave border), afferent and efferent blood vessels **(Rehfeld et *al*.,2017)**. Which consists of:

Capsule: dense connective tissue that encloses the nodule, formed by subcapsular sinus, trabeculae and trabecular sinuses **(Brelje and Sorenson.,2005)**.

Cortex: which contains three compartments; outer cortex (nodular), inner cortex (paracotex) and the subcapsular (region between the outer cortex and the medulla that is free of nodules) **(Rehfeld et *al*.,2017; Brelje and Sorenson.,2005)**.

Medulla is the inner part of the node formed by anastomosing cords: medullary cords and medullary sinuses that form an intervening space by which lymph circulates before exiting the node through efferent lymphatic vessels **(Fig.02) (Appendix I) (Rehfeld et *al*.,2017; Brelje and. Sorenson.,2005)**.

The lymph node in the first place allows to filter the lymph during its return to the bloodstream. It is the site of activation of T and immunocompetent lymphocytes **(Rehfeld et *al*.,2017).**

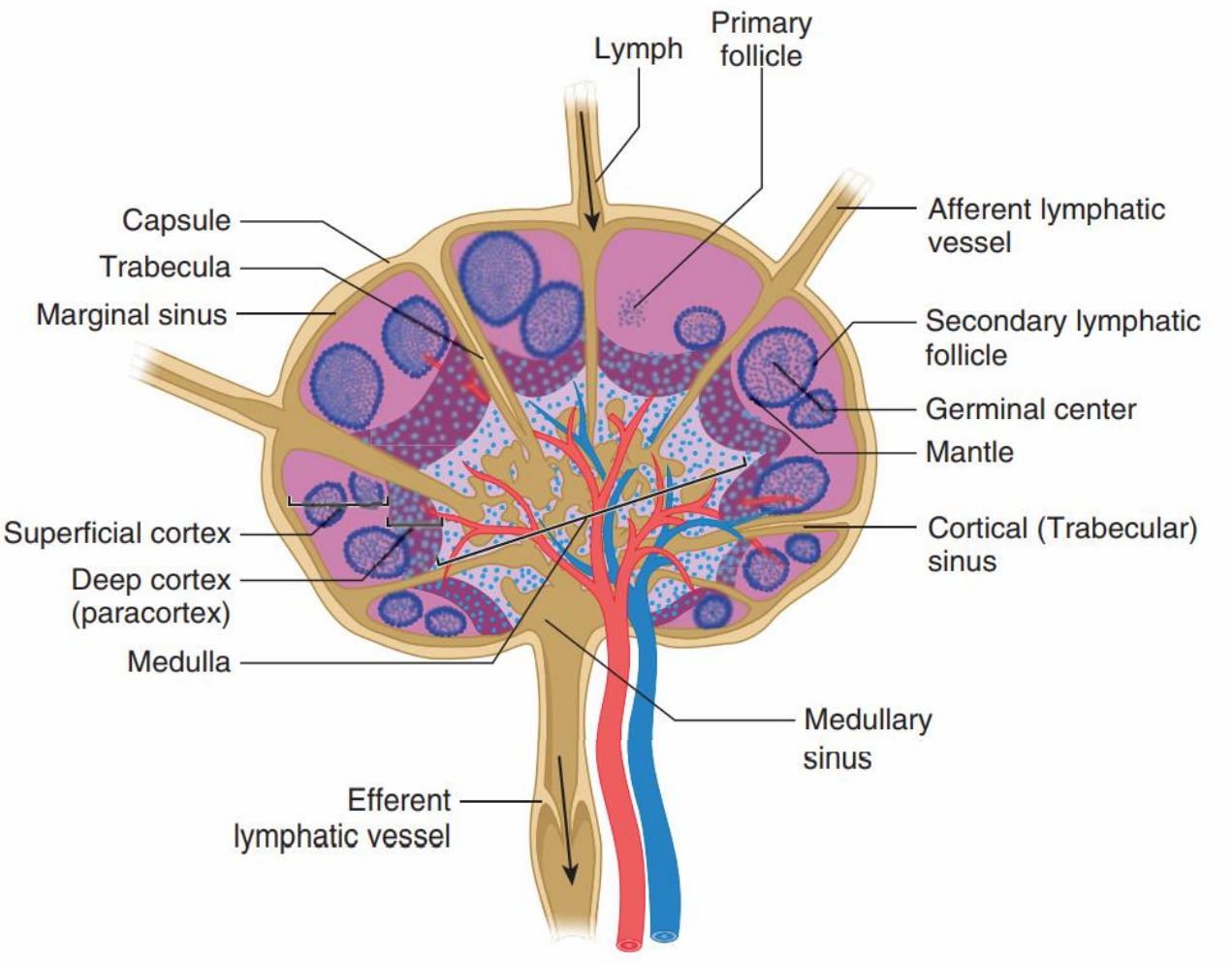

Fig.02. Lymph node **(Rehfeld et *al*.,2017)**

- **Light microscopy: (Table.01 (Appendix I))**

III. Physiopathology and molecular pathology of cHL

III.1. Classical Hodgkin lymphoma: HRS cells

Hodgkin/Reed-Sternberg cell appears with a large shape of approximately 20-60 µm that contains at least two irregular enlarged nuclear lobes or nuclei, often surrounded by a prominent nuclear membrane **(Swerdlow et *al*.,2008)**.

The nucleoli (one or more) of HRS cells are usually eosinophilic with little DNA condensation. However, HRS is characterized by abundant cytoplasm with a large Golgi apparatus **(Swerdlow et *al*.,2008)**.

HRS cell is featured by two central diagnostic markers that are; CD30, CD15 with a co-expression in most cases. **(Swerdlow et *al*.,2008)**.

Immunohistologically, HRS cell is positive for CD30, CD15, CD20 and sometimes shows prominent staining in the Golgi zone. However, CD15 is negative in 20-25% of cases of cHL which might remove this marker in the establishment of diagnosis **(Oviedo et *al*.,2020, O'Malley et *al*.,2019)**.

For the expression of CD20, it is observed in 7- 44% of cases with a variable intensity in different parts of the cell membrane while the expression of CD79a is observed less frequently **(Oviedo et *al*.,2020, O'Malley et *al*.,2019)**.

The HRS cell is often negative for CD45 so as for the B-cell transcription factors BOB-1 and OCT-2**(Engert and Younes.,2020)** .

At the nuclear scale HRS cells of the B lineage is positive for PAX5/BSAP with usually, a weak staining compared to the reactive B cells present in the background of the infiltrate **(Engert and Younes.,2020)**.

Another marker is requisite to identify the distribution and activity of cells in CHL microenvironment as a pan T cell marker is frequently CD3 which is not expected to be positive in the HRS cells **(O'Malley et *al*.,2019)**.

A significant positive immunohistochemical staining in a proportion of cHL for LMP1 (latent membrane protein 1) or for EBER with *In Situ* hybridization indicates an EBV-associated infection **(Oviedo et *al*.,2020).**

III.2. Sub-classification of cHL

Based on growth patterns, HRS cell morphology and background infiltrate composition, cHL is divided into four histological subtypes, including Nodular Sclerosis, Mixed Cellularity, Lymphocyte-Rich and Lymphocyte-Depleted **(Engert and Younes.,2020).**

III.2.1 Nodular sclerosis classical Hodgkin's lymphoma (NScHL)

This is the most common subtype in about 80% of cHL cases, it usually affects women more than men **(Oviedo and Moran.,2016).**

Microscopically the affected lymph node undergoes a complete effacement of the lymphoid architecture, a distinctly thick capsule and nodular infiltrate in which individual nodules are surrounded by broad fibrous bands of collagen crossing the lymph node at the cell-rich areas: a mixture of small lymphocytes , eosinophils, macrophages, neutrophils, plasma cells, and large HRS cells that may be multi or binucleated , a large eosinophilic nucleolus , open-chromatin , bilobed or multilobed , irregularly contoured , and an eosinophilic cytoplasm **(Fig.03) (Leeds Virtual Pathology Library.,2013)** .

Occasionally these large cells are surrounded by T cells which will form T cell rosettes around HRS cells **(Leeds Virtual Pathology Library.,2013)**, this may vary in one case of NScHL to another within the same infiltrated lymph node.

Sometimes HRS cells form sheets that may be associated with necrosis and a fibrohistiocytic reaction, a variant lacunar cell expression of HRS cells may occur in cases of NScHL that results from formalin-induced retraction of the cytoplasmic membrane. Lacunar HRS cells are typical of NScHL but can be found in other cHL subtypes **(Engert and Younes.,2020)**. Sometimes a significant granulomatous reaction or abundant acute inflammation can mask HRS cells in NScHL **(Oviedo et *al*.,2020)**.

However, association with EBV is less common compared to other subtypes of cHL, most of which are MCcHL **(Oviedo and Moran.,2016)**. Other cells may be abundant in this case called "mummified" cells **(Gelvez and Smith.,2015)**.

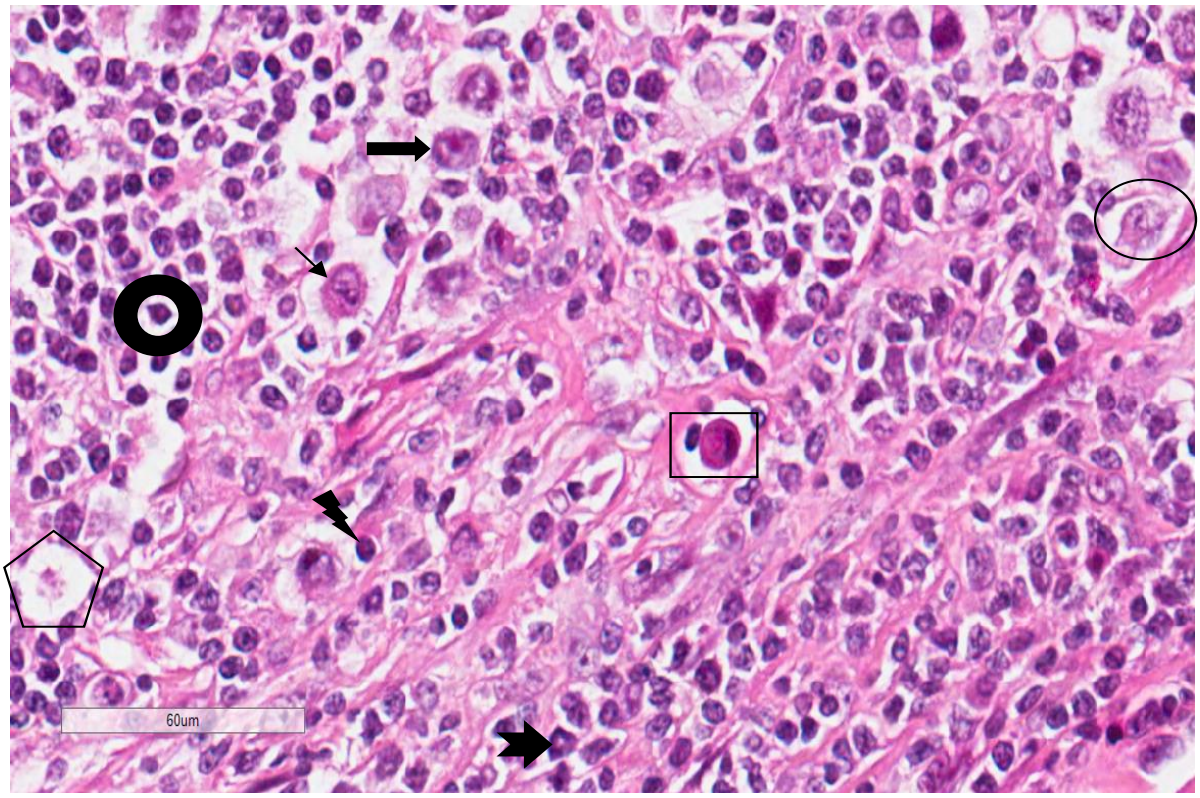

Fig. 03. Microscopic appearance of nodular sclerosis classical Hodgkin lymphoma (Virtual slide of a left neck lymph node biopsy from a 45-year-old woman under light microscopy; G:40×. HE staining) **(Leeds Virtual Pathology Library.,2013)**

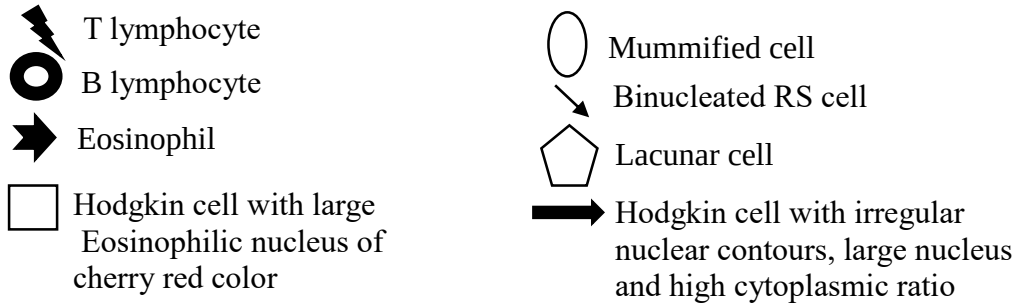

III.2.2. Mixed-cellularity classical Hodgkin lymphoma (MCcHL)

This is the second most common subtype after NScHL with 15% of cases especially in developing countries. It usually affects children and the elderly. MCcHL is the most common subtype associated with EBV and can reach up to 75% of cases **(Oviedo et *al*.,2020),** this disease frequently affects lymph nodes and mediastinum in around 5 to 10%. This subtype has the same morphological characteristics as Nodular Sclerosis cHL. In contrast, sometimes the architecture of the lymph nodes and especially some areas of B-cells are partially preserved showing rarely light collagenous fibrous bands. HRS cells are more abundant than lacunar or mummified cells and scattered in a background that may contain small lymphocytes,

eosinophils, neutrophils, plasma cells and histiocytes **(Fig. 04) (Leeds Virtual Pathology library.,2014)**.

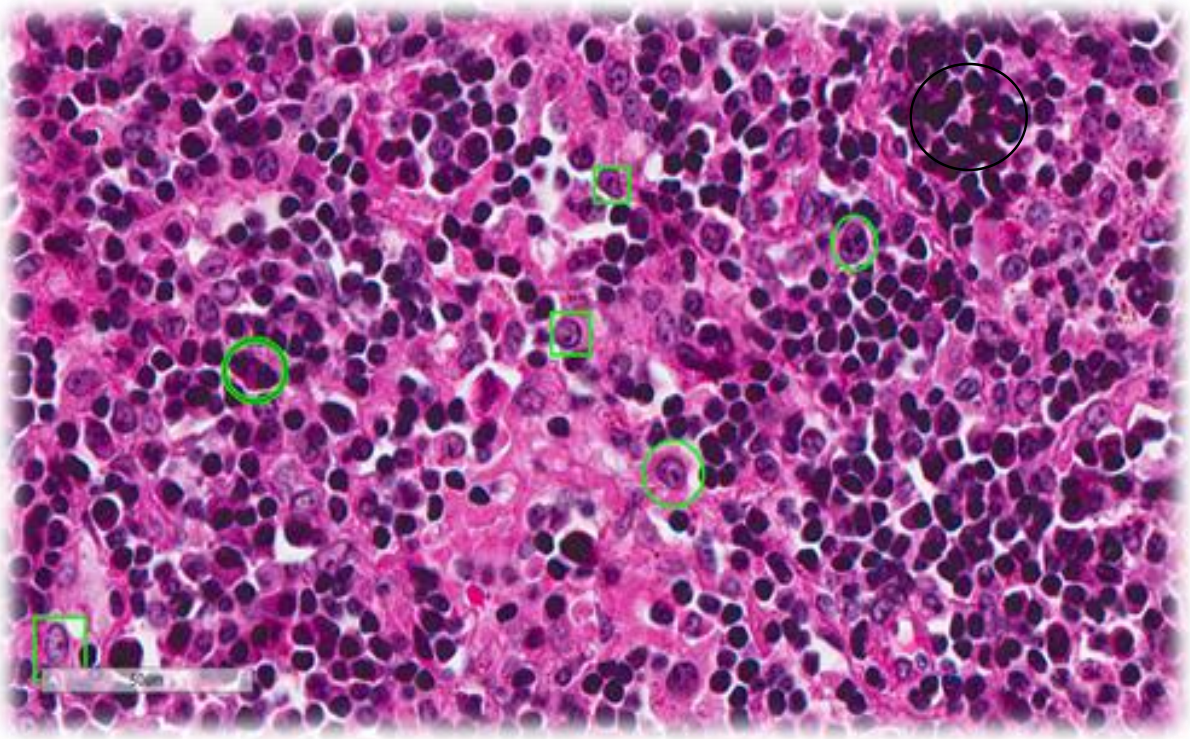

Fig.04. Microscopic appearance of Mixed Cellularity classical Hodgkin Lymphoma (Virtual slide of cervical lymphadenopathy from a 35-year-old woman under light microscopy; G: 40×.HE staining) **(Leeds Virtual Pathology Library, 2014)**.

III.2.3. Lymphocyte-rich classical Hodgkin's lymphoma (LRcHL)

This subtype is rare (3% -5%) **(Younes et *al*.,2014)**, usually affects older individuals involving peripheral lymph nodes. There is a strong association between LRcHL and EBV infection, but even with treatment, prognosis still can be intermediate to poor for the patient. **(Carbone et *al*.,2016)**. Microscopically, it manifests in two forms: nodular or rarely diffuse. Often, B-cell follicles are partially preserved with recognizable GC, HRS cells are found in extensive mantle tissues, abdomen, germinal centers of residual lymphatic follicles and interfollicular areas in monotonous background full of small lymphocytes and macrophages scattered in a polymorphic background with absence of fibrosis **(Fig.05).** Morphologically,

HRS cells of LRcHL may resemble the lymphocyte-predominant cells of lymphocyte-predominant Hodgkin's lymphoma, which requires the use of an appropriate set of markers to diagnose LRcHL (see paragraph 'HRS cells') **(Oviedo et *al*.,2020)**.

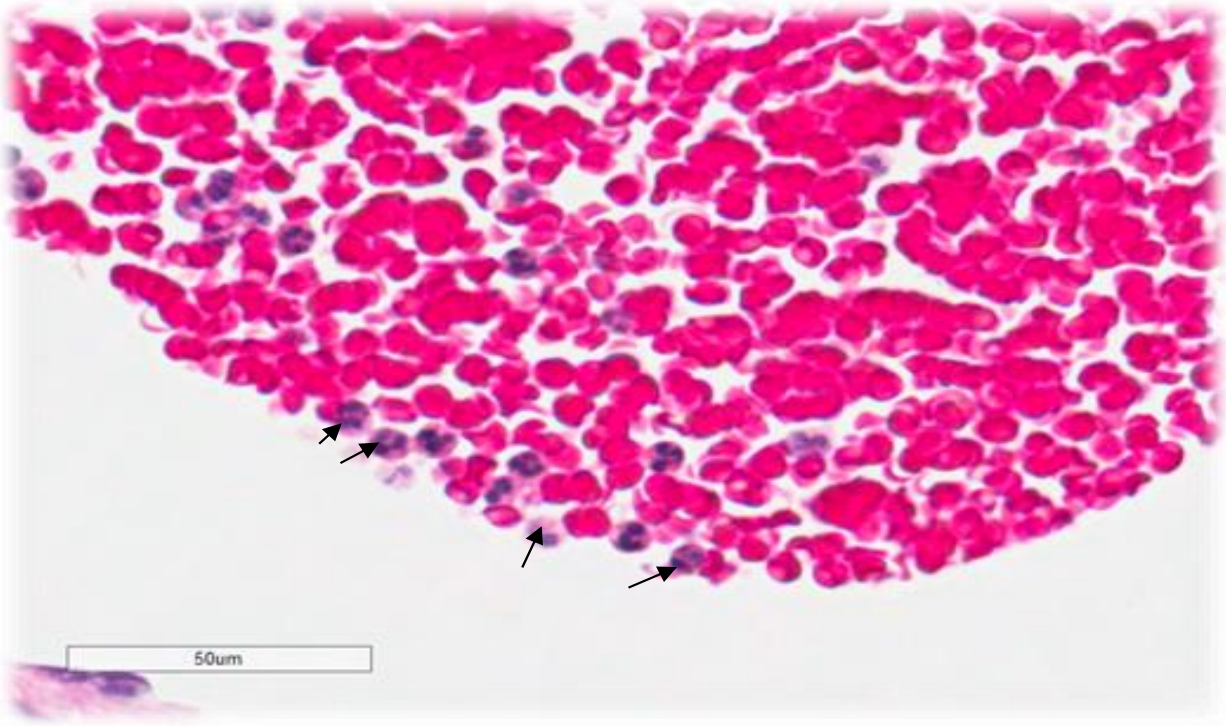

Fig.05. Microscopic appearance of Lymphocyte Rich classical Hodgkin Lymphoma (virtual slide of Large left groin lymph node of a 41-year-old Mal under light microscopy; G: 40×) **(Leeds Virtual Pathology library, 2013)** /Pink background indicates the abundance of lymphocytes.HRS at the mantle zone (arrow)

III.2.4. Lymphocyte-depleted Classical Hodgkin's lymphoma (LDcHL)

Lymphocyte-depleted cHL is the rarest histological subtype of cHL (1% of cases), it is more difficult to be diagnosed because the polymorphic background is limited or absent, hence the name "depletion". It usually affects the elderly and its association with EBV is inconsistent. Frequently presented as peripheral lymphadenopathy or a large abdominal mass, rarely involving the mediastinum. This is the variant with the poorest prognosis **(Olszewski.,2014).** Microscopically, it is characterized by an increased number of HRS cells scattered in an infiltrate and/or a reduction of small lymphocytes in the background population. Sometimes, HRS cells are anaplastic in their appearance and sometimes there is extensive diffuse or reticular fibrosis formation but without fibrous band formation **(Engert and Younes.,2020).** HRS cells are usually few and scattered in diffuse fibrosis and more prominent in reticular fibrosis **(Oviedo et *al*.,2020)**

III.3. Origin of HRS cells

The immunophenotype of HRS cells may share the same expression of immune cells, e.g. B cell markers (PAX5- Paired box protein 5, E2A - Transcription factor E2-alpha), T cell markers (GATA3 - Trans-acting T-cell-specific transcription factor GATA-3), natural killer cell markers (ID2- DNA-binding protein inhibitor ID-2), and markers of dendritic cells (CCL17- C-C motif chemokine 17). The cell derivation of HRS cells could be identified via the detection of clonal rearrangements of immunoglobulin heavy and light chains that occur specifically in developing B cells and thus represent genetic markers for this cell type. **(Murray and Bell.,2015)**. When cells isolated from the cHL cellular milieu were tested for the presence of such gene rearrangements; they were identified in almost all cases ascertaining the B origin of HRS cells **(Hudnall and Küppers.,2018)**. However, as the genes in the IgV (Variable Immunoglobulin gene) region are very diverse and represent clonal markers, the detection of identical IgV genes in HRS cells of a given case was also a strong demonstration of the monoclonality of HRS cells in another given case. Indeed, normal B cells activate the somatic hypermutation process when they are engaged in T-dependent humoral immune responses and differentiate into germinal center (GC) B cells. Subsequently, B cells will acquire numerous somatic mutations during their clonal expansion in the GC, which indicates the differentiation process which, therefore is a characteristic of post-GC B cells (memory B cells and long-lived plasma cells). In addition, a quarter of the cases revealed "disabling" mutations at the level of rearranged immunoglobulin sequences that lead to the nonfunctionality of the surface immunoglobulin molecule (B cell receptor (BCR) **(Murray and Bell.,2015)**. Such "disabling" mutations occur physiologically in GC B cells but normally cause immediate apoptotic cell death **(Hudnall and Küppers.,2018)**. This indicates that HRS cells are derived from GC B cells prone to apoptosis, but have been somehow rescued from apoptosis by cell transformation events **(Fig.06)** since B cells that underwent unfavorable mutations, e.g. reduce the antigenic affinity of BCR, premature codon arrest or frameshifts, must be eliminated by Fas-mediated apoptosis. However, these pre-apoptotic germinal center B cells can be rescued by a combination of EBV and cellular genetic alterations, generating a pool of cells that the researchers believe to be the progenitors of HRS cells **(Murray and Bell.,2015)**.

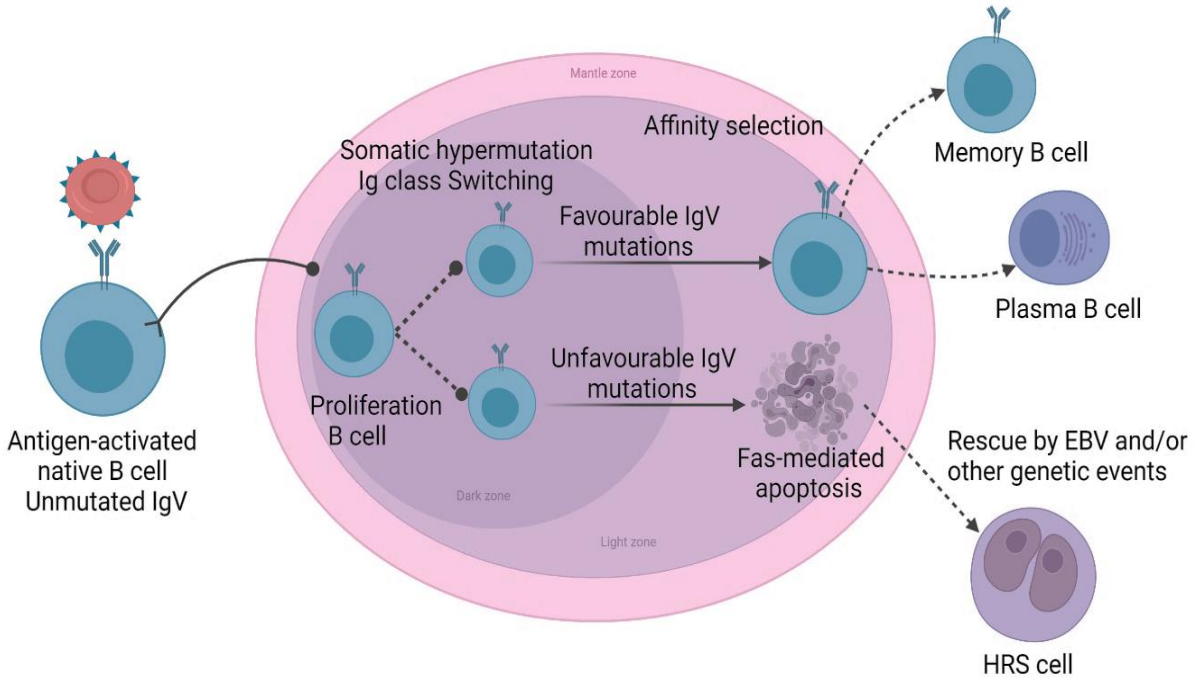

Fig.06. HRS cells originate from pre-apoptotic germinal centre B cells**. (Original illustration)** Reproduced from **(Murray and Bell.,2015.)**

III.4. Lost B-cell phenotype of HRS cells

HRS cells derived from mature B cells, show a global downregulation of the B cell gene expression program, which is unique among B cell lymphomas in its extent. The initial event that causes this extensive reprogramming is unknown, but several contributing factors have been identified. HRS cells downregulate expression of numerous B cell transcription factors, such as OCT2, PU.1, BOB1 and PAX5, early B-cell factor 1 (EBF1) and TCF3/E2A that regulate B-cell development **(Nutt and Kee., 2007; Bohle et *al*.,2013).** likely causing downregulation of their respective target genes **(Murray and Bell.,2015)**. B cell–specific genes are also silenced by epigenetic mechanisms in HL. Furthermore, HRS cells aberrantly express master regulators of other hematopoietic cell lineages that suppress B cell genes, in particular the T cell factor Notch1 and the NK cell factor ID2 **(Hudnall and Küppers.,2018)**. The transcription factors STAT5A and STAT5B are also involved in the downregulation of B cell genes in HRS cells. Expression of multiple key transcription factors of HSCs (hematopoietic stem cells) may further contribute to the peculiar phenotype of HRS cells. HRS cells express multiple members of the polycomb group family 1 and 2 complexes, these factors may play a role in the downregulation of B cell genes and the expression of markers of other lineages in

HRS cells **(Fig.07)**. specific feature may contribute to the consistent downregulation of the B cell program in HRS cells which is directly linked to the fact that HRS cells are derived from pre-apoptotic GC B cells. It is also possible that, for GC B cells with low-affinity BCRs or complete loss of BCR expression, a strong selection pressure to undergo apoptosis may select for loss of the B cell identity, so that these "failed" B cells escape the apoptosis **(Hudnall and Küppers.,2018)**. In addition, EBV-encoded LMP2A can induce Notch expression in human B-cell lines, suggesting that EBV infection may also contribute to increased Notch activity in HL **(Portis et *al*.,2003; Portis and Longnecker.,2004)**.

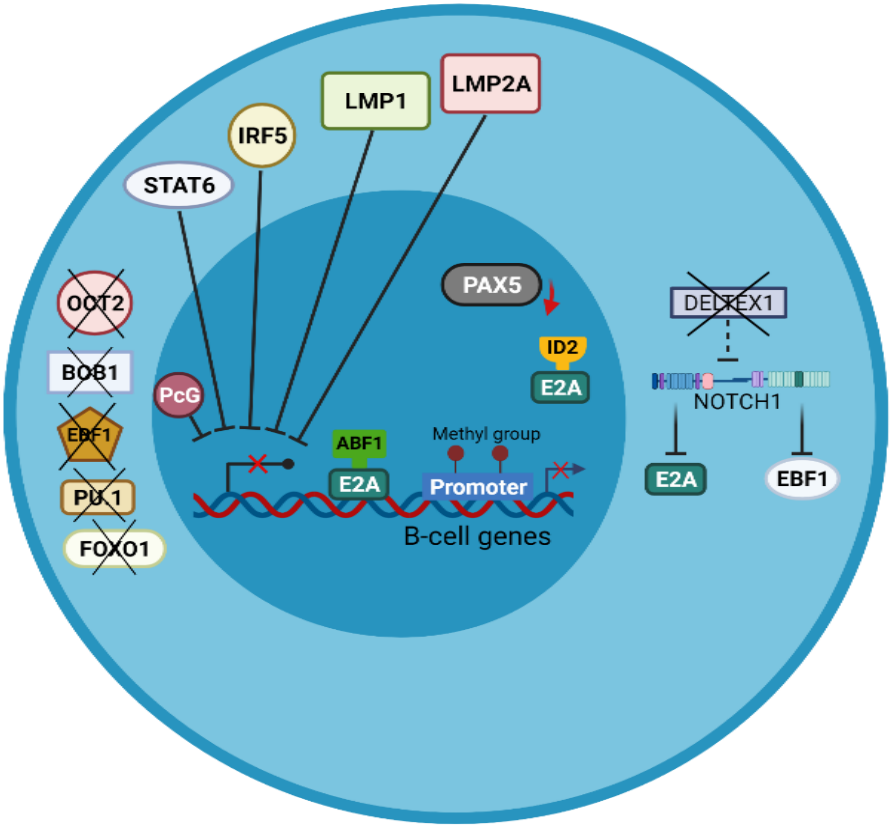

Fig.07.Factors contributing to the lost B cell phenotype of HRS cells. HRS cells have downregulated the expression of several key B cell transcription factors, including OCT2, BOB1, EBF1, FOXO1, and PU.1. PAX5 is still expressed, but at lower level than in normal B cells. The activity of the E2A transcription factor is inhibited by binding to ABF1 and E2A. The T cell transcription factor NOTCH1 is constitutively active in HRS cells and inhibits the B cell factors EBF1 and E2A. NOTCH1 signaling is presumably induced by its ligand JAGGED1 and promoted by high-level expression of MAML2, whereas the NOTCH1 inhibitor DELTEX is downregulated in HRS cells. The activity of many B cell genes is furthermore inhibited by expression of the transcription factors STAT5a, STAT5b, and IRF5, by members of the polycomb group family (PcG), and inEBV-positive cases by the EBV-encoded latent membrane proteins LMP1 and LMP2a. Many B cell genes are epigenetically silenced by methylation of promoter elements **(Original illustration)** Reproduced from **Hudnall and Küppers.,2018)**

IV. Epstein - Barr virus in classical Hodgkin Lymphoma

IV.1 Classification and virion structure

In formal taxonomy, EBV belongs to the « lymphocryptovirus » (LCV) genus, where it was classified with the « lymphotropic Gammaherpesvirinæ » sub-family of the « Herpesviridæ family ». EBV virion's diameter is between 120 and 180 nm; composed of 172 kb linear dsDNA and surrounded by an icosahedral nucleocapsid that comprises 162 shell particles (a.k.a capsomeres). This nucleocapsid is incorporated in a protein tegument that is walled by an envelope with a composition consisting of lipids and glycoproteins (gp); these glycoproteins are responsible of mediating viral infection. **(Fig.08 a & b) (Young.,2020. Yin et *al* 2018)**

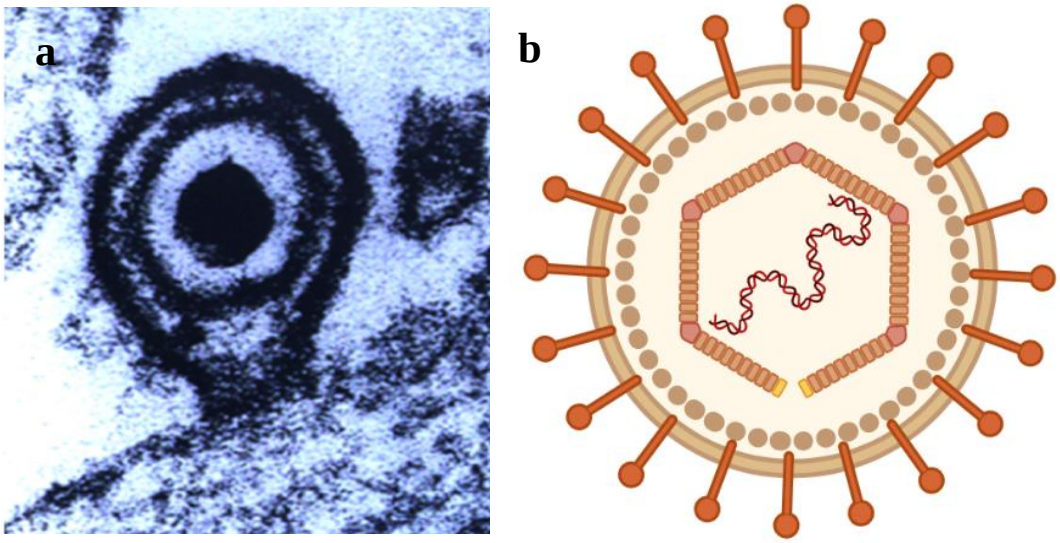

Fig. 08: Morphology and Structure of Epstein Virus -Barr. **(a)** Electron microscope photo of the EBV virion **(Young., 2020). (b)** Structure of the EBV with its different compartments: linear double stranded DNA, the nucleocapsid, the protein tegument and the outer envelope showing all the glycoproteins around it**. (Original illustration)**

IV.2 EBV infection

IV.2.1 Early B cell infection: Initial events

EBV is equipped with a system that allows it to enter the host cell, in which it induces numerous dysregulating mechanisms leading to a malignant transformation. In B cells; the viral interaction is driven by surface molecules, where EBV requires its five glycoproteins (gp), starting with gp350 that permits the virus attachment to the host cell, by binding to CD21, this interaction leads to the alteration of central signaling pathways which prepare the infected cell to establish viral latency. Additionally, gp350/CD21 complex appears to damage the expression of specialized histones transcripts. gp42 is also needed to launch EBV entry into B-cell by

attaching the Major Histocompatibility Complex class II (MHCII) to it. The heterodimer gH/gL with gB are utilized for the EBV core fusion to guarantee the EBV entry into the cytoplasm with a mechanism so-called "endocytosis". Once inputted in the intracellular environment. A following fusion process occurs between the EBV's virion membrane and the endosomal membrane, which liberates the tegument protein BNRF1. Arriving to the nucleus, EBV's double stranded leaner DNA is deposed and starts circulating to reprogram the nucleus and to amplify its genetic material **(See Fig.09)**. A refined study by Tsai and colleagues **(2011)** demonstrated that the EBV's tegument protein BNRF1 interacts with the host nuclear protein Daxx to disrupt the formation of the chromatin remodeling complex Daxx/Atrx leading to early viral gene expression. **(Price & Luftig.,2015; Stanfield & Luftig.,2017; Tsai et *al*.,2011; Chiu et *al*.,20**

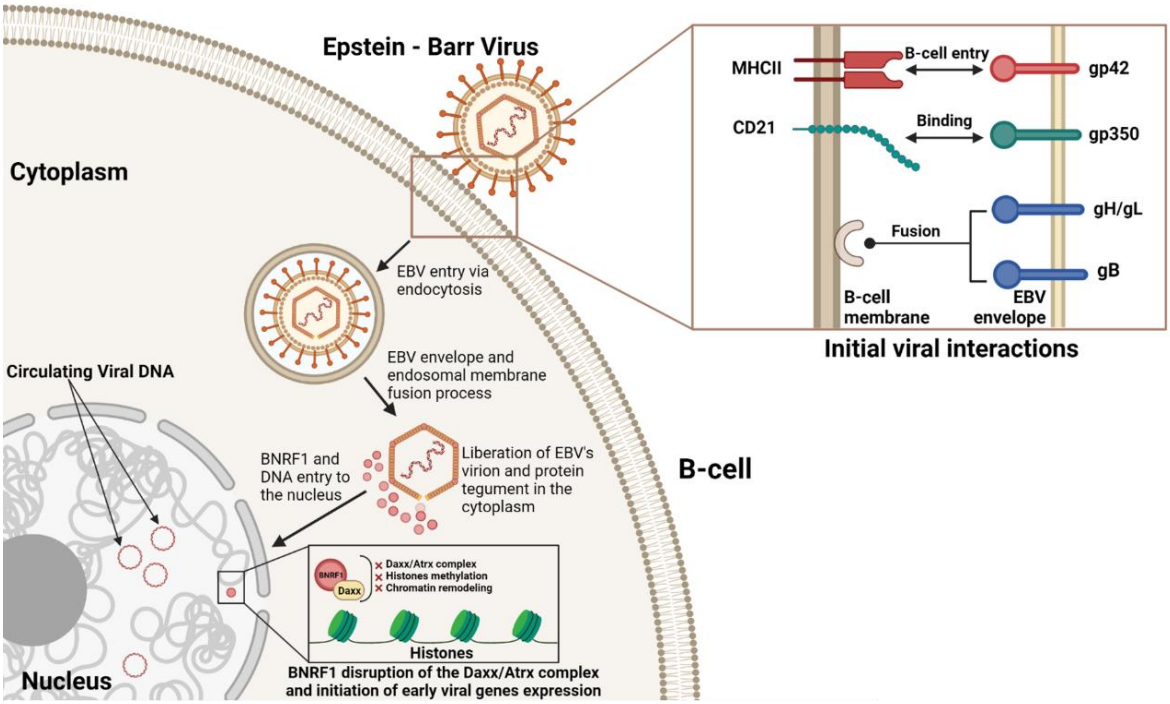

Fig.09 Schematic representation of early B-cell infection by the Epstein - Barr virus. **(Original illustration)** Reproduced from **(Stanfield and Luftig.,2017)**

IV.2.2. EBV latent genes and their mission in the establishment of classical Hodgkin Lymphoma

Up to nine viral proteins have been identified to cover the Epstein – Barr Virus oncogenicity; each viral protein carries a particular function with the aim of aiding and assuring the expansion of viral infection within B-cells. Together, EBV latent genes form a threatening cluster for the immune system. Here, we review all the Epstein - Barr virus latent genes with a

spotlight on EBV encoded Latent Membrane Protein 1 (LMP1) and the EBV-Encoded small RNAs 1 & 2 (EBER1 and EBER2). **Fig.10** below shows EBV episome and its latent genes location.

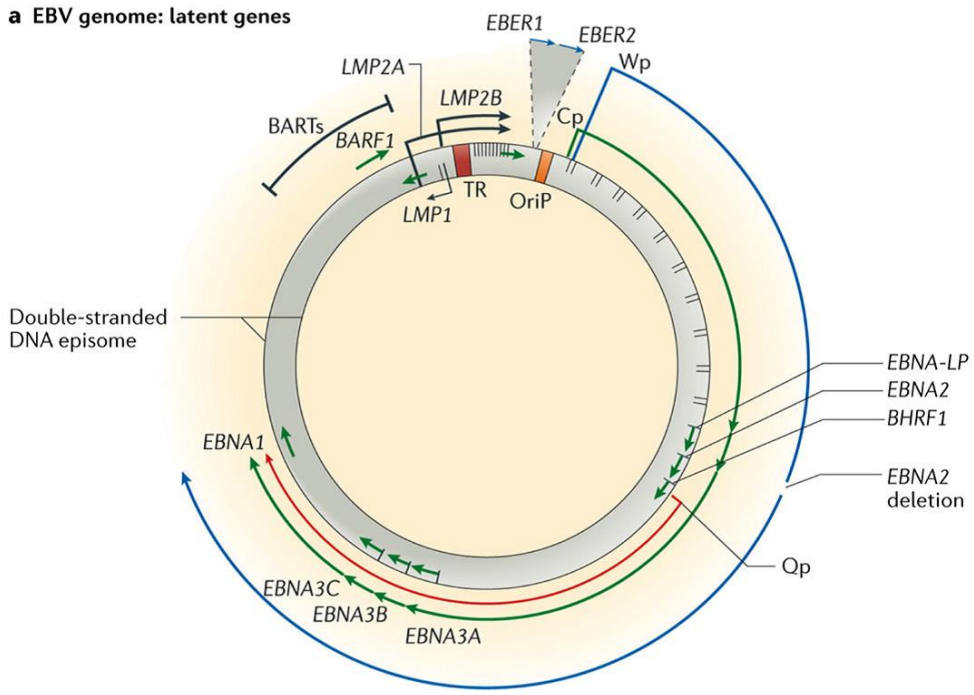

Fig.10 EBV and its latent genes. Location and transcription of Epstein-Barr virus latent genes on the double-stranded viral DNA episome**. (Young.,2020)**

IV.2.2.1.Epstein – Barr Virus Nuclear Antigens (EBNAs)

IV.2.2.1.1.Epstein – Barr Virus Nuclear Antigen-1 (EBNA-1)

Epstein – Barr Virus Nuclear Antigen-1 or EBNA-1 is definitely required for cHL oncogenesis. It has been shown that this key molecule is essential for the episome replication and segregation upon latent viral infection. It binds to specific sites of the viral latent origin of replication, OriP in order to initiate the viral genomic DNA replication. Besides, it manages the EBV episomes' segregation through mediating their attachment to host cell metaphase chromosomes. Furthermore, EBNA-1 acts as a transactivator of several latent genes and host genes; it is also involved in p53 degradation to decrease apoptosis, which leads to host cell survival. **(Kang & Kieff.,2015; Saridakis et *al.*,2005, Liu et *al.*,2020)**

IV. 2.2.1.2. Epstein – Barr Virus Nuclear Antigen-2 (EBNA-2) and EBV Nuclear Antigen-Leader Protein (EBNA-LP)

Activated by the action of EBNA-LP, EBNA-2 acts as a transcriptional activator of cellular and viral gene expression where it preferentially activates the major viral protein LMP1; likewise, for certain cellular components such as Cyclin D2 and MYC that are activated by EBNA-2 to speed up cellular proliferation, cell- survival and alter cell cycle progression. These damages caused by EBNA-2 resulted from EBNA-LP activity, which is reported to be the co-activator of EBNA-2; it is the first EBV latent protein to be produced after EBV infection of resting B- cells. A study by Szymula and colleagues **(2018)** demonstrated that EBNA-LP did not simply co-operate with EBNA-2 in activating gene expression, but rather facilitates the recruitment of several transcription factors to the viral genome, to enable transcription of virus latency genes, they also suggested that EBNA-LP is essential for the survival of EBV-infected naïve B cells. **(Yin et *al*.,2018; Kang & Kieff. 2015; Szymula et *al*.,2018)**

IV.2.2.1.3. Epstein – Barr Virus Nuclear Antigen 3 family (EBNA-3A,3B,3C)

- **EBNA-3A and EBNA-3B**

EBNA-3A and EBNA-3B are also believed to be coactivators for EBNA-2. Anyways, they play a key role for the activation and immortalization of EBV infected B-cells so as B-cell transformation. It has been shown that EBNA-3A interacts with the C-terminal-Binding Protein (CtBP) which is a corepressor known to be essential in B- cell transformation through a mechanism that binds these two molecules, with EBNA-3C to induce expression of $p16^{INK4A}$ for an epigenetic repression that is compulsory for EBV-infected B-cells proliferation. In vitro experiments showed that only EBNA3-B is unessential for EBV-mediated B-cell growth transformation. Instead, Yin and colleagues **(2018)** reported that EBNA-3B inhibits EBV-transformed B-cell proliferation to ensure long-time survival of the persistently infected host. **(Yin et *al*., 2018; Kang & Kieff.,2015, Bhattacharjee et *al*.,2016)**

- **EBNA-3C**

Epstein - Barr virus Nuclear Antigen 3C is also included to license B-cells transformation. Phenotypically, EBNA-3C enhances CD21 expression on B-cell surface. However, EBNA-3C has not been detected in Hodgkin Lymphomas according to Saha & Robertson **(2013)** since its high expression in EBV infected-B-cells was only observed upon latency III stage. **(Yin et *al*., 2018, Saha & Robertson.,2013; Bhattacharjee et *al*.,2016)**

IV.2.2.2 Latent Membrane Proteins (LMP1, LMP2A/B)

- **Latent Membrane Protein 1 (LMP1)**

More than 35 years ago and 20 years just after the EBV discovery; LMP1 (Latent Membrane Protein 1) has been discovered and identified as an Epstein - Barr virus encoded oncoprotein that belongs to the TNF (Tumor Necrosis Factor) receptor superfamily and acts as a key molecule to ensure the EBV-infected B cells transformation, immortalization and proliferation in cHL. **(Vrzalikova et *al*.,2018. Yin et *al*.,2018, Herbert & Pimienta.,2016).**

Studies demonstrated that LMP1 is the functional homolog of the tumor necrosis factor receptor superfamily (TNFR) CD40; which is known to be expressed on B cells, dendritic cells, and macrophages; besides, it functions as a transmembrane receptor charged of multiple cell-signaling pathways. **(Arcipowski et *al*.,2011).** In contrast; and as mentioned above, the case in classical Hodgkin Lymphoma has a different ending; where the LMP1 aids HRS cells to evade apoptosis and promotes their proliferation; **(Bentz et *al*,2012)**. LMP1 has a specific structure with a specialized cytoplasmic arrangement that mediates these functions. As a transmembrane protein of 386 amino acids (aa), it is comprised of a short cytoplasmic N-terminal region (1-24 aa); responsible of the protein integration into the HRS cell membrane. Six transmembrane domains TM1-6 (25-186 aa), directly bound to a Cytoplasmic C-terminal Tail (CCT) a.k.a carboxy-terminal activating region sites (CTARs) containing: CTAR1 (194-232 aa) and CTAR2 (351-386 aa) **(Fig.11)**. **(Yin et *al*.,2018; Kieser & Sterz .,2015, Wu et *al*.,2005, Uniprot Database)**. The most common feature observed in CD40 and LMP1 is their binding to the TRAFs (Tumor necrosis factor Receptor -Associated Factors) TRAF3 & TRAF5 precisely. Since a structural similarity of the recognition motifs in LMP1 and CD40 was revealed by Wu and colleagues **(2005)**. They could show that LMP1 carries a "PQQAT" motif that matches the CD40 motif "PVQET", by demonstrating their binding to the same binding crevice on TRAF3. **(Fig.12)**; which consequently qualifies LMP1 to recruit 80% of cellular TRAF3. Thus, the LMP1-TRAF3 complex will unsurprisingly induce a dysregulated signaling within infected B-cells **(Wu et *al*.,2005. KEGG Database).** CTAR2 in its turn acts as a key site. It has been shown that it harbors a "PYQLSYY" motif to bind to TNFR-Associated Death Domain proteins (TRADD) and Receptor Interacting Protein (RIP) to fit the NF-κB signaling pathway requirement and activate it in HRS cells. **(Wu et *al*.,2005; Yin et *al* .,2018)**

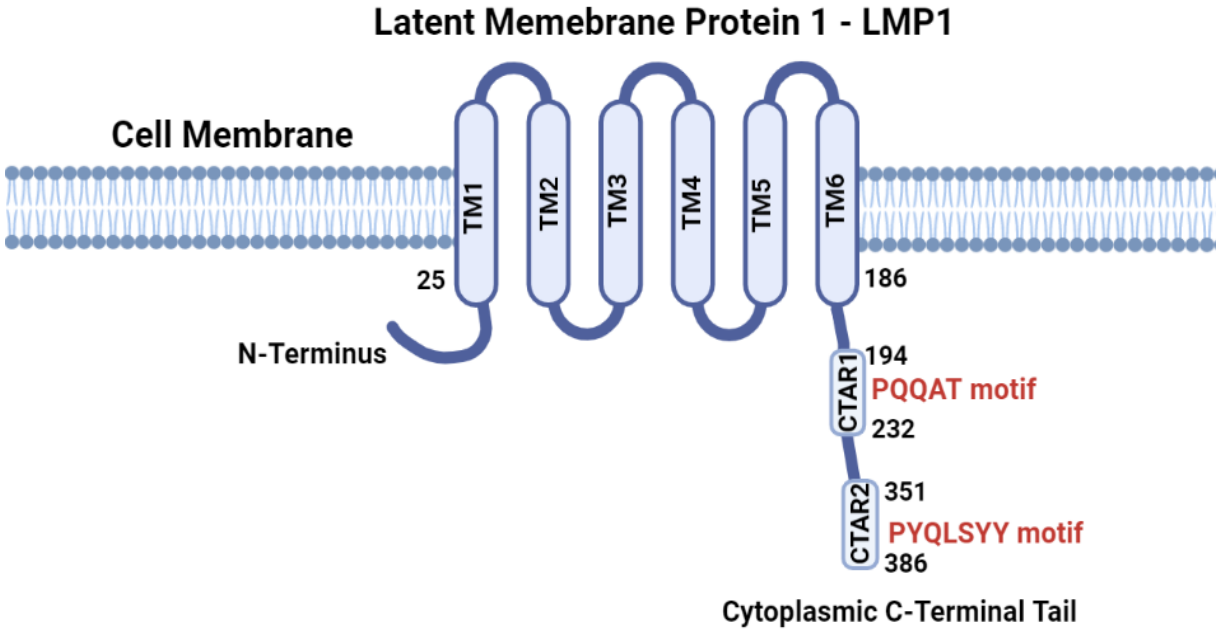

Fig.11. Latent Membrane Protein 1 - LMP1 structure. An N-terminal region directly bound to six transmembrane domains (TM1-6) connected to a short Cytoplasmic C-terminal Tail (CCT), this CCT comprises two C-Terminal Activating Regions CTAR1 and CTAR2 that aim to interact with cytoplasmic proteins to induce deregulating signaling pathways within HRS cells. **(Original illustration)** Reproduced from **(Kieser & Sterz.,2015)**

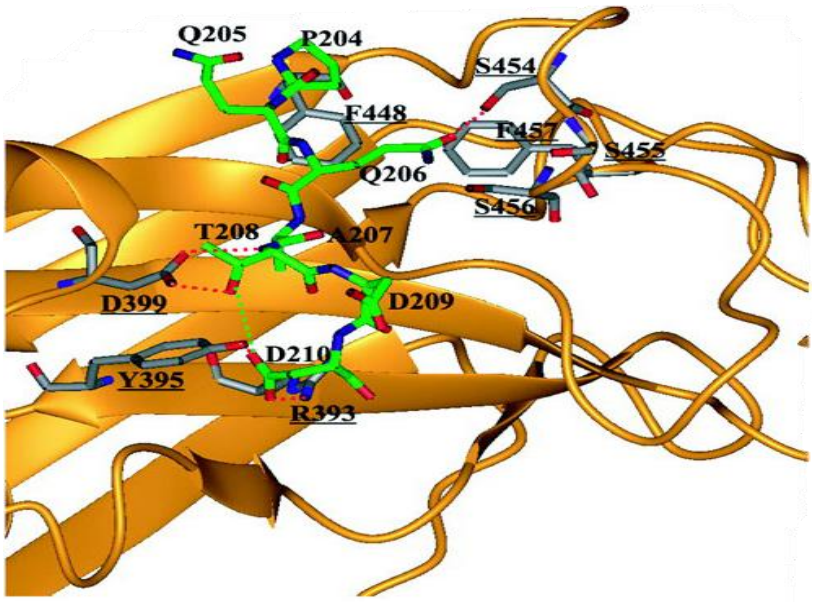

Fig.12. The contacts for LMP1-TRAF3 recognition are shown. This is a close-up view of the intermolecular contacts in the LMP1-TRAF3 complex, with TRAF3 shown as an orange ribbon and contact residues shown as gray ball-and-stick models. LMP1 is shown as a green ball-and-stick model. Critical contact residues are labeled, and the labels are underlined for residues from TRAF3. Intermolecular and intramolecular hydrogen bonds are drawn as red and green dotted lines, respectively. **(Wu et *al.*,2005)**

- **Latent Membrane Protein 2 (LMP2A/B)**

Latent Membrane Protein 2 is divided into two isoforms known as LMP2A and LMP2B, which share 8 common coding exons **(Murray and Bell.,2015);** both are expressed in cHL-HRS cells where LMP2A is known to maintain EBV latent infection by preventing the virus from lytic reactivation **(Uniprot Databas**e**).** While LMP2B is thought to negatively regulate the activity of LMP2A. In fact, LMP2A has several functions throughout malignant progression for being a BCR homolog expressed in infected B-cells, this mimic, permits B-cells development since BCR signaling is no longer available due to that change in cell fate, which is also triggered by LMP2A. Besides, LMP2A activates a number of signaling pathways that are important for B-cell survival, but not B-cell proliferation such as RAS/PI3K/AKT and mTOR pathways. **(Vrzalikova et *al*.,2018., Herbert & Pimienta.,2016).**

IV.2.2.3. Epstein- Barr Virus – Encoded small RNAs 1&2 (EBER1 et EBER2)

EBERs 1&2 were first discovered in 1981 as the most abundant EBV products in latently infected B – cells with approximately 106 copies per cell, making them reliable markers for EBV detection in cHL using *In Situ* Hybridization techniques. They are transcribed by RNA polymerase III into a non-coding RNAs (ncRNAs) of 167 nucleotides for EBER1 and 172 for EBER2. From a structural view, they have a highly conserved secondary structure albeit their sequences share only 54% homology, this secondary structure comprises several stem-loops formed by intramolecular base-pairing. **(Fig.13)**. Previous studies showed that EBERs are confined to the nucleus but recently, Ahmed and colleagues **(2018)** tracked the journey of EBERs from the nucleus to the excretory exosomes of EBV immortalized B-lymphocytes so they could demonstrate that the presence of EBERs is not only in the nucleus, but also in the cytoplasm of EBV infected B-cell lines. This evidence may contribute to a better understanding of EBERs interactions in EBV-infected B-cells and their microenvironment. Studies demonstrated that EBERs, when released in exosomes are associated to the Lupus antigen (La) which is a cellular protein that binds to all precursor RNA polymerase III transcripts such as EBERs as mentioned above; this complex may induce pro-inflammatory cytokines through TLR3 pathway. In contrast, for B-cell lines; Ahmed and colleagues observed low levels of La signals suggesting that EBERs are excreted in exosomes via alternative routes other than involving La. **(Yin et *al*.,2018, Iwakiri.,2014, Ahmed et *al.*,2018).**

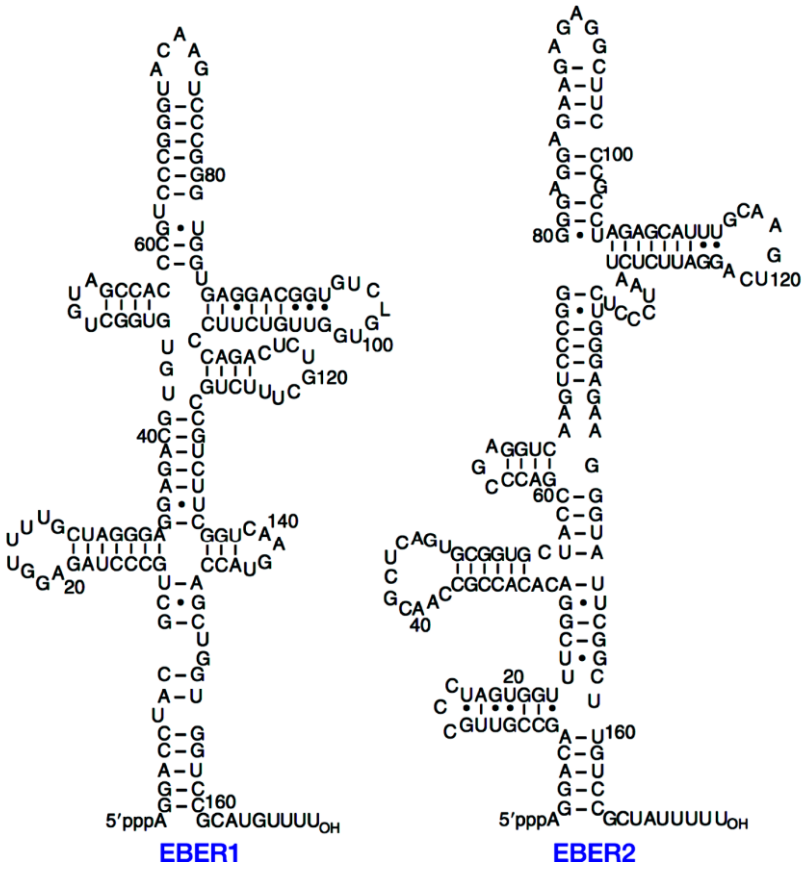

Fig.13. Secondary structures of EBERs. Reproduced from Rosa et al. EBER, Epstein – Barr Virus-Encoded RNA. **(Iwakiri.,2014)**

IV .2.2.4. Epstein – Barr Virus- encoded microRNAs (EBV miRNAs)

EBV can encode approximately 23 precursors 44 mature MicroRNAs (miRNAs). **(Yin et *al*.,2018)**. These precursors are grouped into two clusters, BamHI fragment H rightward open reading frame 1 (BHRF1) and the BamHI fragment A rightward transcript (BART). In classical Hodgkin Lymphoma, BARTs are considered deleterious when released in exosomes; for example, BART13-3p is one of the most highly expressed viral miRNA in cHL, and have the ability induce changes in the phenotype of macrophages leading to increased production the pro-inflammatory cytokine TNFα and the immunosuppressive cytokine, IL-10; which makes miR-BART13-3p a potential module of tumor-associated macrophages. MiR-BART2-5p has also been reported to play a role in maintaining EBV latency in cHL, by reducing B-Cell Receptor (BCR) signaling. **(Notarte et *al*.,2021; De Re et *al*.,2020)**

IV .2.3 EBV latency gene expression stages

Pre-latent phase of newly infected B-cells is followed by four latency stages (III.II.I.0) **(Fig.14)**. Each latency stage is characterized by its distinctive viral genes; Initiating with

latency III « growth program » where multiple copies of the EBV episomes express all viral genes (all EBNAs, LMPs and miRNAs) leading to the infected B-cell proliferation and expansion of the infected B cell pool. This growth program favors the viral transformation, which provides a high immunogenicity; the activation of the host's immune surveillance pathways is then demanded, although it cannot be reached due to the presence of viral genes responsible of immune escape. Once the viral transformation is successfully reached; Infected B cells enter the germinal center to express the latency II genes; a.k.a « default program », (EBNA1; LMP1 and LMP2A/B). This latency stage is less immunogenic due to a reduced production of viral proteins; on the other hand, it promotes the establishment of a memory B cell phenotype. Cells then exit the germinal center and progress to the memory B cell pool for a latency 0 stage; here EBV latent genes expression is silenced. At this level, cells engage normal signaling pathways to proliferate; this stage is a sort of preparation for latency I stage where proliferating memory B cells start expressing EBNA1 for viral episome segregation. Finally, memory B-cells can differentiate into plasma cells for the EBV replication, this process is thought to be driven by LMP2A. Young presumed that infected germinal center B-cells might also differentiate into plasma cells (indicated with a dashed arrow). Many studies based on identification of cHL-HRS cells surface molecules and latency II viral genes tracking could back-up the hypothesis of HRS cells' germinal center origin. **(Young.,2020; Herbet & Pimienta.,2016. Yin et *al*.,2018).**

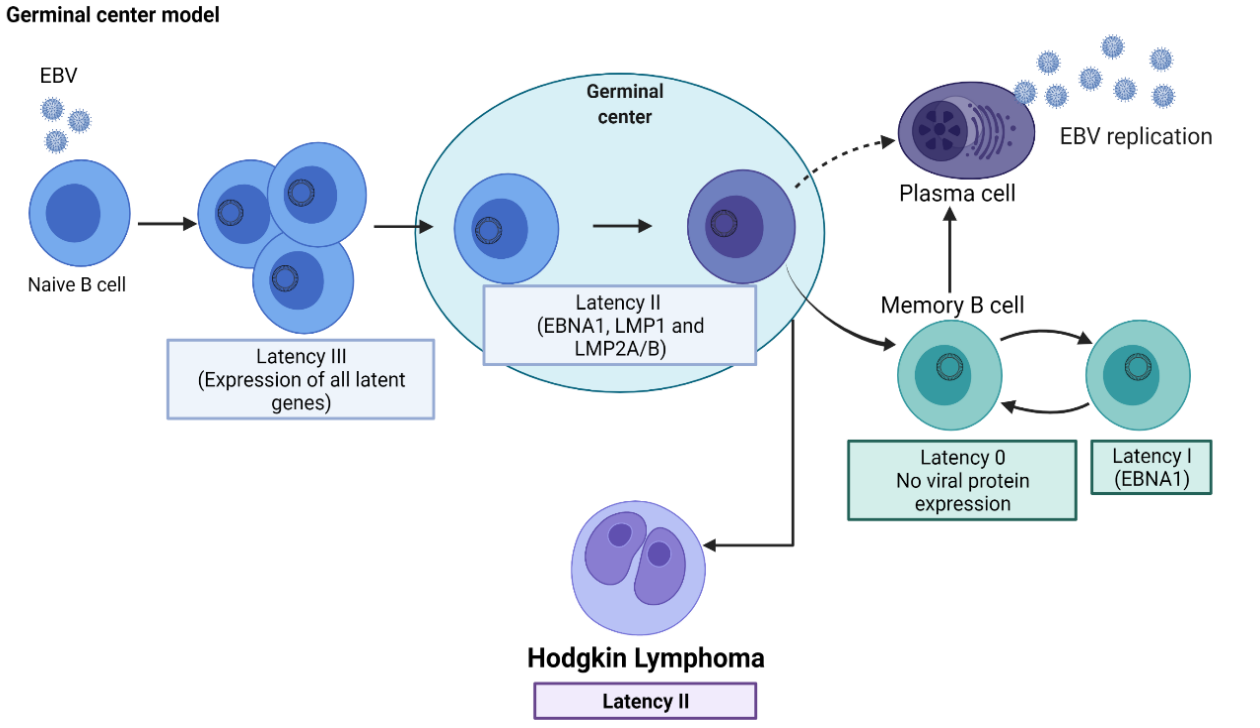

Fig.14. Schematic representation of EBV latency stages and cHL-HRS cells origin. **(Original illustration).** Reproduced from **(Young.,2020.)**

IV. 2.4. Molecular mechanism of EBV-encoded Latent Membrane Protein 1 in cHL-HRS cells:

IV.2.4.1. Latent Membrane Protein 1 (LMP1) expression in cHL

As previously mentioned; for being an oncogenic protein with a transmembrane receptor function. LMP1 is known to be involved in cHL through multiple manners, by activating several cell-signaling pathways for cell survival and by inducing overexpression of expert proteins that aim to protect malignant cells from apoptosis and immune evasion. **(Murray and Bell.,2015; Vrzalikova et *al*.,2018)**. NF-κB, JAK/STAT with AP-1/C-JUN/JUN-B, and PI3K/AKT/mTOR have been demonstrated to be active when LMP1 is expressed in HRS cells **(Murray and Bell.,2015; Vrzalikova et *al*.,2018; Yin et *al*.,2018)**. Other signaling pathways are implicated such as The Mitogen-activated protein kinases signaling pathway; these are induced to promote cell proliferation **(Luo et *al*.,2021; Kieser and Sterz.,2015)**

IV.2.4.2. LMP1 induced signaling pathways in cHL

IV .2.4.2.1. NF-κB signaling pathway

The Nuclear Factor κB (NF-κB) is a conserved transcription factor family, composed of five transcription factors i.e. RelA (p65), RelB, p50 (NF-κB1), p52 (NF-κB2) and c-Rel. The NF-κB signaling pathway is a process which is commonly known to be involved in cell survival, proliferation; differentiation and cell adhesion through two types of NF-κB signaling that lead to the activation of the NF-κB transcription factors; Canonical (classical) and non-canonical (alternative) pathways. Where c-Rel, RelA and p50 (NF-κB1) were found in the canonical pathway and the p52 (NF-κB2) with RelB in the non-canonical pathway. **(Luo et *al*.,2021; Weniger, & Küppers.,2016).** Through its CTARs, LMP1 binds to TRAF3 and mediates an NF-κB activity in HRS cells, at this level, and with several mutations in the NF-κB components; all five-transcription factors are involved. de Oliveira and colleagues **(2016)** demonstrated that HL cells are predominantly controlled by the non-canonical NF-κB signaling pathway; it is reported to be driven by the kinase NIK (MAP3K14), which therefore promotes abundant activities in the nucleus of HRS cells via p50 and p52. The classical NF-κB signaling pathway in HRS cells is associated to the IKK complex to promote p52 and RelB in the nucleus **(See Fig.15)**. **(Weniger, & Küppers.,2016; de Oliveira et *al*.,2016)**

IV.2.4.2.2. JAK/STAT and AP-1/C-JUN/JUN-B signaling pathways

A study by Green and colleagues **(2012)** demonstrated that PD-L1 (Programmed death-Ligand 1) is expressed on HRS cells where LMP1 indirectly upregulates the AP-1 activity to increase PD-L1 expression levels in EBV-positive classical Hodgkin Lymphoma cells. JAK/STAT pathway appears to be fundamental for this mission. The Molecular process starts with JAK3 activation, then related STAT dimer is activated, which promotes a transcriptional regulation in the nucleus; this mechanism enables LMP1 to provide a feedback and enhance its own expression **(Luo et *al*.,2021).** Furthermore, Green and colleagues **(2012)** confirmed that the PD-L1 enhancer was bound by cJUN and JUN-B. cJUN and JUN-B, bound the predicted PD-L1 AP-1-responsive enhancer element and the enhancer augmented PD-L1 promoter driven luciferase activity in an AP-1 dependent manner, engaging a signal that ends with a PD-L1 expression on HRS cells to enable it escape immune surveillance. **(See Fig.15) (Luo et *al* .,2021; Gravelle et al.,2017; Green et *al*.,2012).**

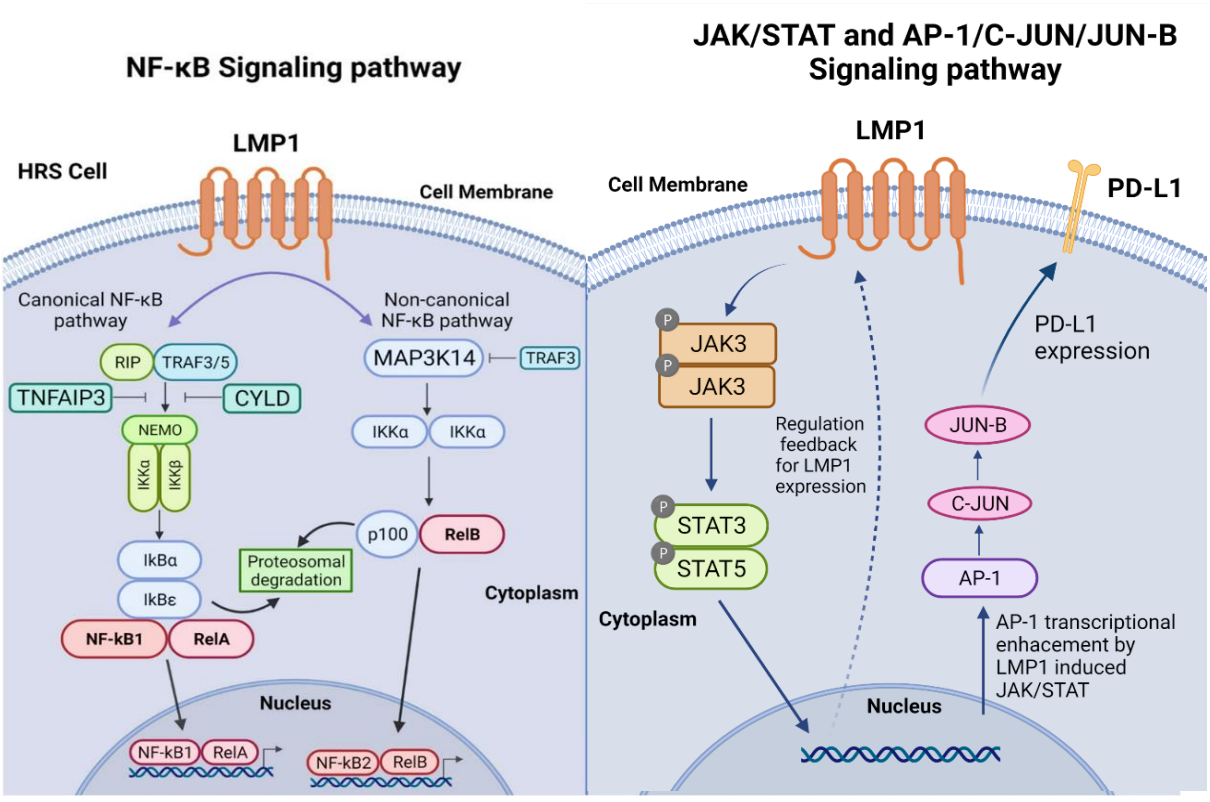

Fig.15 Schematic representation of the LMP1- induced NF-κB, JAK/STAT and AP-1/C-JUN/JUN-B signaling pathways in cHL-HRS cells. **(Original Illustration)** Reproduced from **(Weniger, & Küppers.,2016. Luo et *al*.,2021 ; Gravelle et *al*.,2017 ; Green et *al*.,2012.)**

IV.2.4.2.3. PI3K/AKT-mTOR signaling pathway

The cytokine receptor CD137 and its ligand CD137L are expressed on activated T cells and antigen-presenting cells (APC), respectively; to guarantee a strong anti-tumor response. **(Rajendran et al.,2016)**. In 86% of cHL cases, in order to eliminate the immune costimulatory activity of CD137/CD137L; CD137 expression was observed on HRS cells to disrupt this activity and evade the immune system. **(Ho et *al.*,2013; Aravinth et *al.*,2019)** Through EBV induced-cHL, Aravinth and colleagues **(2019)** showed that the Epstein - Barr virus encoded LMP1 utilizes the PI3K/AKT/mTOR signaling pathway to induce ectopic CD137 expression on HRS cells so they can escape immune surveillance. They demonstrated that LMP1 constitutively activates PI3K pathway leading to higher pAKT, activation of mTOR and pS6K, resulting in increased CD137 surface expression **(Aravinth et *al.*,2019)**, thus an IL13 secretion to decrease IFNγ levels occur to evade the anti-tumor response, and a stimulation of HRS cell growth follows next. The mechanism by which they do so is via the cytokine IL13 that has been reported to be secreted by HRS cells in cHL; additionally, it works as a powerful growth factor for these cells. Rajendran and colleagues **(2016)** demonstrated that HRS cells expressing CD137 would evidently communicate with APC expressing CD137L to engage a signaling to trigger IL13 secretion, which consequently reduce the cytokine INFγ levels, crucial for the type 1, cell-mediated immune response. **(See Fig.16) (Rajendran et *al.*,2016)**

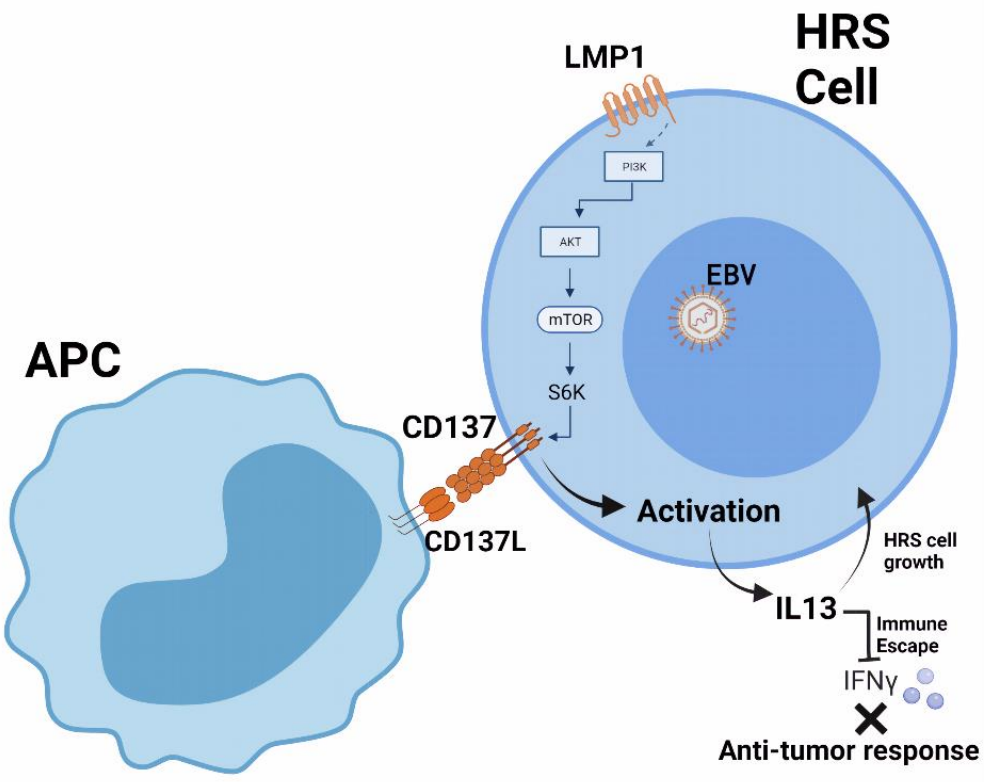

Fig.16. Schematic representation of the LMP1-induced PI3K/AKT/mTOR signaling pathway for CD137 ectopic expression on HRS cells. **(Original illustration)** Reproduced from (**Aravinth et *al.*,2019; Rajendran et *al.*,2016)**

IV.3. Epstein - Barr virus and the cHL microenvironment

In classical Hodgkin Lymphoma, malignant HRS cells are surrounded by a microenvironment with a destructive influence all over the tissue. HRS cells expressing their viral latent proteins; most importantly, Latent Membrane Protein 1 (LMP1), allow various interactions with their surrounding immune system and stromal components **(Dolcetti.,2015)**; these interactions contribute to a highly suppressive immune environment of Chl. The oncogenic activity of LMP1 that is mediated by cHL microenvironment was revealed in a set of experiments. It was in 2013 when Cader and colleagues demonstrated that LMP1 protects HRS cells from cell death and promotes survival of lymphoma cells by inducing expression of the tyrosine kinase receptor Discoidin Domain Receptor 1 (DDR1), which is activated by collagen interference; a subsequent NF-κB signaling is then triggered to warrant HRS cells immortalization. This evidence shows that collagen is an essential element in mediating LMP1 activity. As previously reported, LMP1 activates NF-κB signaling; this activity aims to boost the expression of numerous chemokines such as CCL5, CCL17 and CCL22, which recruit regulatory T cells (Treg) in order to reduce CD8+ T cell activity. As LMP1 upregulates the PD-L1 expression on HRS cells surface, it thus, interacts with a PD-1 receptor to induce T cell anergy and therefore increases the production of IL-10, Galectin-1 and TGFβ, which are immunosuppressive regulators. Furthermore, MAPK and PI3K signaling pathways are activated by LMP1 to induce cytokines secretion, including IL6, IL8 and IL10 for an autocrine activation of JAK/STAT signaling, where stimulated STAT6 is the key element charged of LMP1 transcriptional stimulation in the absence of EBNA2 expression. **(Cader et *al*.,2013; Murray and Bell.,2015).**

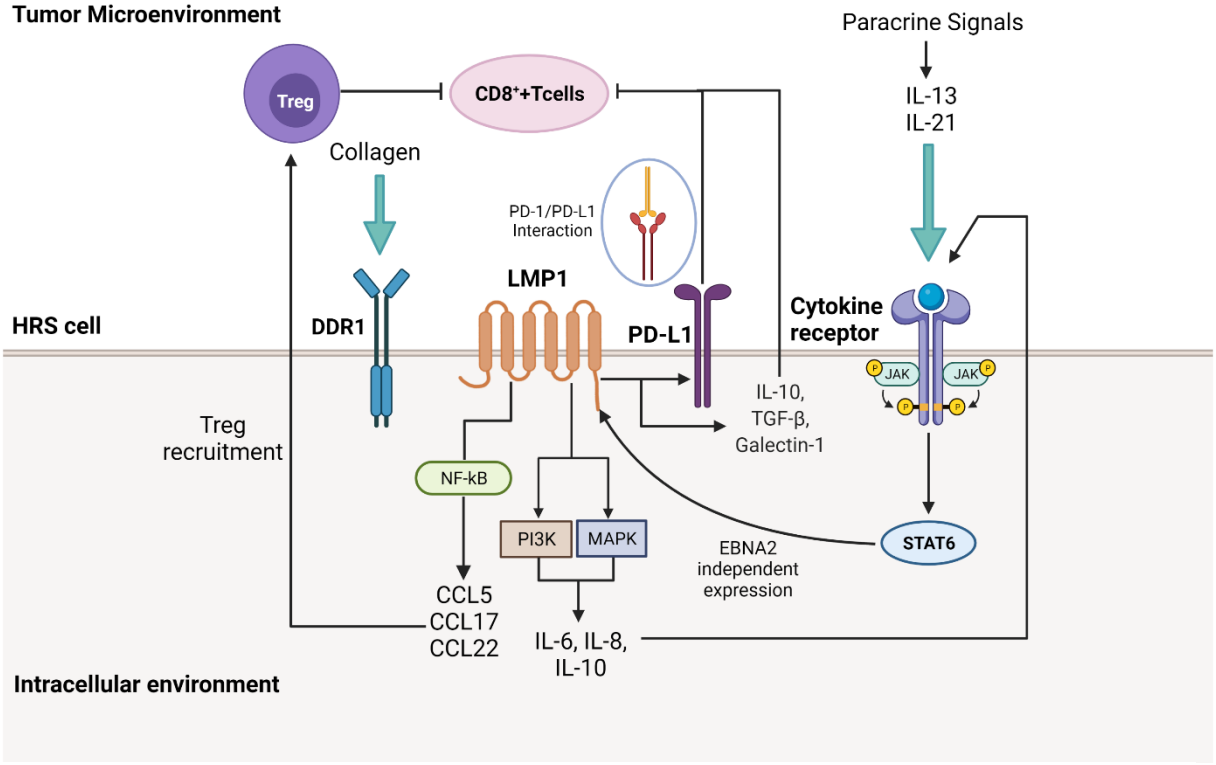

Fig.17 Interactions between EBV products and tumor microenvironment. **(Original illustration).** Reproduced from **(Murray and Bell.,2015.)**

CHAPTER II
Materials and Methods

I. Location of the experimental work

Our work was performed in Anatomy Cytopathology unit of DOUERA hospital, based on a retrospective-prospective study that has been realized in three laboratories: Histology laboratory, Immunohistochemistry laboratory and Molecular Biology laboratory in collaboration with the Archives service.

II. Materials

II.1. Patients selection

A group of 21 cHL diagnosed patients of the year 2020 at DOUERA hospital were selected from the archives distributed between males and females with variable age groups. Clinical informations were accessible for all the chosen cases: Patient's ID (last name, first name, age, sex, etc.), the place of care, the established diagnosis of certainty "morphological and immunohistochemical" Among these cases, there were cases first diagnosed in other hospitals and private clinics then sent for a second opinion to the Anatomy Cytopathology unit of DOUERA hospital. The collected samples were a prepared formalin fixed paraffin embedded (FFPE) tissue specimens ready for a study to investigate the expression of routine clinical markers including, CD15, CD30, CD20, CD3 and PAX5 and the expression of EBV markers, LMP1 and EBERs, for all age groups.

II.2. Biological material

Paraffin-embedded tissue blocks for histochemistry, immunohistochemistry and Chromogenic *In Situ* Hybridization.

Immunohistochemistry:

Antibodies:

- Anti-Epstein- Barr Virus, LMP
- Anti-Human CD30
- Anti-Human CD3
- Anti-Human CD20cy
- Anti-CD15/FUT4
- Anti-Human B-Cell-Specific Activator Protein (PAX5)
- Secondary Antibody (HRP-Polymer)

Chromogenic *In situ* Hybridization (CISH):

- Anti-DIG/DNP-MIX
- Secondary Antibody HRP/AP-POLYMER-MIX

(See Appendix.II)

II.3. Non-biological materials: (See Appendix.II)

II. Methods

Samples received at the Anatomy Cytopathology unit of DOUERA hospital passed by several procedures, among these samples there were, lymphadenopathies; lymph node biopsies, while others were a communicated paraffin blocks. These lymphadenopathies and lymph node biopsies were pre-treated for a sequential use. Grossing was the first step to be applied on these samples with the aim to select the regions of interest for a microscopic examination. Once determined, excisional biopsies and biopsy cores were measured and immediately placed in cassettes with the patient's ID; then immersed in a large volume of 10% formalin (at least 5X the volume of the sample) **(See Appendix. II)**. The next process consists of dehydration and embedding. The aim of dehydration is to remove the intracellular water and obtain a rigidity to the sample, while embedding is carried out using an "embedding center" utilizing molten paraffin to form paraffin blocks ready for lab use **(See Appendix. II).** Before each technique, Sectioning is the first step the paraffin block passes by, this step is achieved by using an apparatus carrying precision knives, called microtome in order to cut the Paraffin embedded tissue into sections of 1 to 5 μm, always depending on the use.

Our study has based on three lab techniques at the Anatomy Cytopathology unit of DOUERA hospital, which are the histochemical based Hematoxylin & Eosin staining (H&E), Immunohistochemistry (IHC) and Chromogenic *In Situ* Hybridization (CISH)

II.1. Histochemical based Hematoxylin & Eosin (H&E) staining:

H&E staining combines a basic nuclear staining with hematoxylin and an acidic cytoplasmic staining with eosin, which allows satisfactory visualization of cellular components and makes it easier to distinguish malignant cells from other surrounding cells by observing their morphology under light microscopy and therefore give a primary opinion about the nature of the tumor.

II.1.1. Sample preparation

In the microtomy, the obtained ribbons of 1-3 µm are transferred to a water bath of 37°C then picked up using a clean histological slide.

Dewaxing consists of removing the paraffin, before staining; where the obtained tissue sections mounted on slides are placed in the oven (90°C). In order to liquefy and thus remove peripheral paraffin, as well as impurities and water.

Deparaffinization allows the elimination of the intracellular paraffin by immersing the slide in 3 baths of xylene (3 × 5 min); then Rehydration with decreased concentrations of alcohol (at 95°,80°,70°) (1×3min) is done at room temperature.

II.1.2. Staining and mounting

Staining begins by immersing the slides in Harris hematoxylin for 6 to 10 min. For differentiation, the tissue sections are immersed in a 1% of acid alcohol for 30 seconds. Bluing is a crucial step that follows next, it allows to get a basophilic nucleus by using 0.2% ammonia water.

Counterstain in eosin solution is done for 4 to 6 minutes. Dehydration is done right after through 3 baths of ethanol with increased concentrations (70°; 95°; 100°). Clearing is the final step of this procedure with 2 changes of xylene, 5 minutes each.

The stained slides must be protected to allow microscopic examination and preservation without risk of deterioration: for this purpose: the slides are covered with EUKITT (resin) then cover slips.

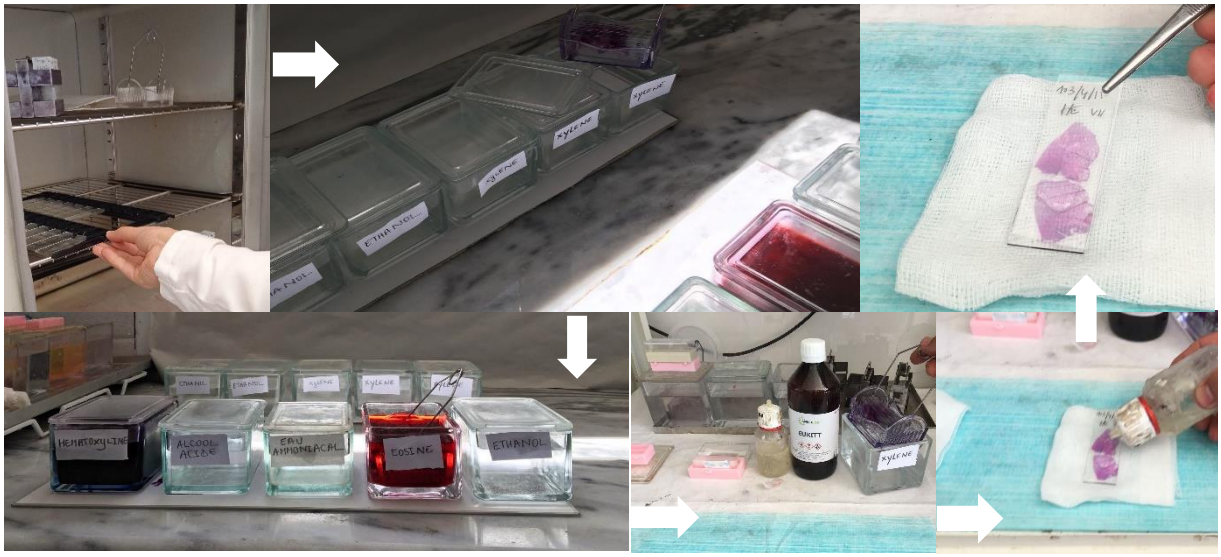

Fig.18. Protocol of dewaxing, hydration, staining, dehydration and mounting. **(Original photos)**

For routinely H&E staining. A specialized H&E automate "CoverStainer" is utilized at the Histochemistry laboratory of the Anatomy Cytopathology unit. **(See Appendix. II)**

II.2. Immunohistochemical staining

Each cancer can be phenotypically distinguished by its specific molecular markers that are present on the surface of its atypical malignant cells. For that purpose, a widely used technique for diagnosis of cancers was performed in order reveal some specific markers in cHL. Immunohistochemistry (IHC) is the that employs monoclonal so as polyclonal antibodies to uncover the distribution of the antigen of interest in the affected tissue.

Retrospectively, Immunohistochemistry was performed on formalin-fixed paraffin-embedded tissue sections of approximately 3 µm depth. The antibodies, AB Anti-CD15, AB Anti-CD30, AB Anti-CD20 were utilized as cHL-HRS cells markers, while AB Anti-LMP was utilized as an EBV cHL-HRS cells marker and an AB Anti-CD3 as a T cell marker. **Fig.19** bellow shows the IHC staining basics

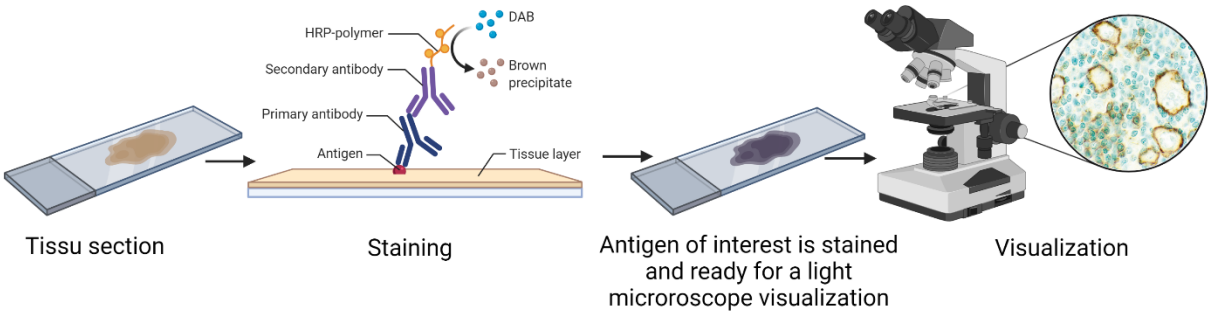

Fig.19 Basics of the Immunohistochemistry experiment. **(Original illustration)**

II.2.1. Samples preparation

Tissue sections of 1-3 µm are obtained by microtomy and transferred to a water bath of 37°C then deposed on a silanized slides, the next preparation procedure is based on the same steps followed in the H&E staining. (Dewaxing, Deparaffinization and Rehydration).

Dako EnVision™ FLEX material, reagents and antibodies were employed in our study for an optimal immunohistochemical staining for the markers CD30, CD20, CD3, PAX5 and LMP1.

For CD15, the primary antibody utilized was from Histo-Line Laboratories

II.2.2. Antigen retrieval: Heat Induced Epitope Retrieval (HIER)

The majority of formalin-fixed tissues require an antigen retrieval step that aims to break methylene bridges, these have been formed during fixation, causing a cross-link between proteins which ends with masking antigenic sites. Antigen retrieval methods allow antibodies to bind by exposing antigenic sites.

Heat Induced Epitope Retrieval (HIER) is the most used method the tissue sections are subjected to, it comes after deparaffinization and hydration to buffer; in this study, the Dako PT Link procedure was performed.

- **PT Link procedure**

Tissue sections mounted on slides were immersed in a Dako PT Link, containing tanks filled (1.5 L) of diluted Target Retrieval Solution (1:50 with distilled water. pH (High/Low) depends on the biomarker **(See table.02. Appendix. II**) where it has already been pre-heated at 65°C. Incubation takes 20 minutes at 97 °C. Sections are then left to cool in the PT Link at 65°C, then pulled up and get transferred to a slide plastic staining jar containing diluted room temperature TBS wash buffer (diluted at 1:20 in distilled water) for 1-5 minutes.

II.2.3. Immunostaining procedure

II.2.3.1. Blocking Endogenous Peroxidase activity

At room temperature, slide tissue sections were circled with a hydrophobic marker to prevent the waste of valuable reagents by keeping liquid pooled in a small droplet then incubated in a Peroxidase-Blocking Reagent for 15 minutes, then rinsed in distilled water for 30 seconds. A 3 to 5 minutes' incubation in TBS wash buffer follows next. The area around the tissue have to get dried carefully.

Fig.20 Blocking Endogenous Peroxidase activity. **(Original photos)**

II.2.3.2. Application of primary Antibody and Peroxidase- conjugated polymer (HRP)

The primary antibody targets the antigen of interest, before its incubation. Some primary antibodies require dilution in an Antibody Diluent **(See table.03. Appendix. II).** Then the incubation is realized in a humidified chamber for 30 minutes. An incubation in TBS wash buffer for 3-5 minutes comes next. A straight linking with labeled polymer-HRP solution is accomplished for 30 minutes**.** After incubation with the secondary antibody, slides were washed two times in fresh TBS for 30 seconds each.

Fig.21 Primary Antibody application procedure. **(Original photos)**

II.2.3.3 Chromogenic labeling (Substrate system, DAB+ Chromogen)

The substrate system (DAB+ Chromogen) from EnVision FLEX produces a crisp brown end product at the site of the target antigen. Before applying, DAB+ Chromogen must be diluted in a Substrate Buffer **(See Appendix. II)**. A quantity of substrate-chromogen solution is first applied to cover the tissue with an incubation of 5–10 minutes. DAB enhancer was next applied for 2 minutes. After IHC, sections were counterstained with Mayer's hematoxylin solution for 60 seconds, rinsed with distilled water for 20 seconds, and a 30 seconds' bluing step follows next. Dehydration was performed as follows: 70° ethanol for 15 seconds, 80° ethanol for 20 seconds, 90° ethanol for 20 seconds, and xylenes for 20 seconds. The stained tissue sections were mounted with mounting medium and covered with coverslips.

For routinely immunohistochemical staining. Specialized automated instruments "Autostainer" are utilized at the Immunohistochemistry laboratory of the Anatomy Cytopathology unit. **(See Appendix. II)**

II.3. Chromogenic *In Situ* Hybridization

In order to detect EBV-infected cells in five cHL cases of different: sex, age, specimen nature, subtypes and immunohistochemical markers, we applied the CISH method using a

digoxigenin-labeled probe (oligonucleotides) which is complementary to two EBV-Encoded small RNAs 1 & 2 (EBER1 and EBER2). The probe visualized via peroxidase and DAB (Diaminobenzidine) through a chromogenic reaction after it has hybridized to its target. The reagent used is the ZytoFast EBV Probe (PF29).

II.3.1. Principle of the Chtomogenic *In Situ* Hybridization

Chromogenic *In situ* hybridization (CISH) is a form of ISH that uses a chromogenic reaction to highlight qualitatively a specific nucleic acid sequences in cell preparations. The detection achieved by a Hapten-labeled nucleotide fragments, which called CISH probe and their complementary target sequences in the preparations that then co-denature and can anneal during hybridization. In case which the unspecific and abound probe fragments formed will remove by stringency washing steps. Duplex formation of the labeled probe will be demonstrated by application of primary (unlabeled) antibody, which is detected by polymerized enzyme-conjugated secondary antibody. Colored precipitates are formed as a result of the enzymatic reaction with the chromogenic substrates. The nucleus is visualized with a nuclear dye after counterstaining. Finally, the hybridized probe fragments can be visualized by light microscopy **(ZYTOVISION, zyto*Fast;* EBV Probe (Digoxigenin-labeled)).**

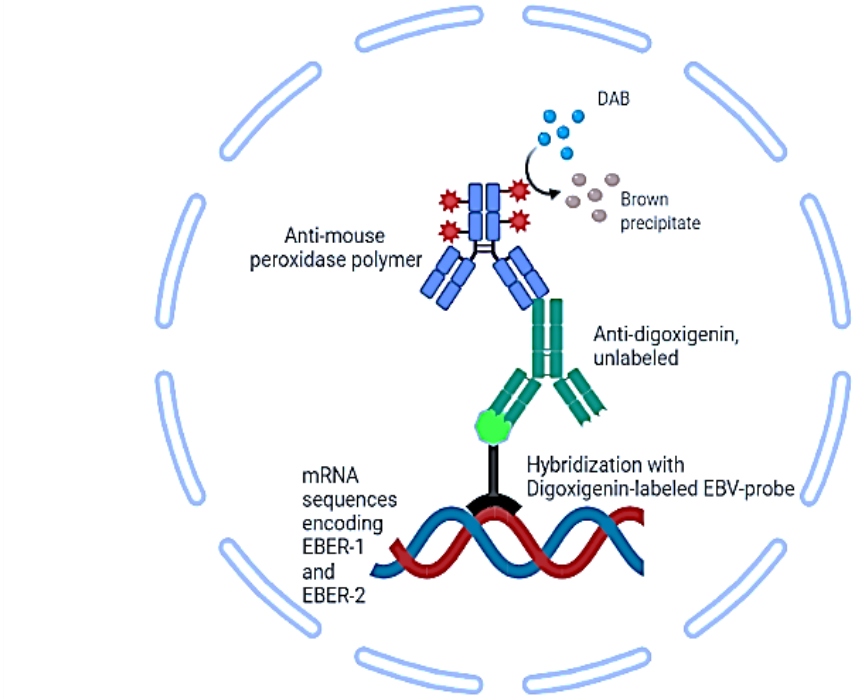

Fig.22.Principle of CISH; EBV Probe. **(Original illustration)** Reproduced from (**Isola and Tanner.,2004**)

II.3.2. Procedure (protocol "Appendix. II")

This histopathological diagnostic technique, which takes 4 hours, consists of six steps:

- Sections preparation
- Rehydration
- Tissue sections pretreatment
- Denaturation and Hybridization
- Rigorous washing
- Detection

II.3.2.1. Samples preparation

Sections of 4 microns were obtained from FFPT (Formalin-fixed Paraffin-embedded tissues) by a microtome with distilled water on silanized slides (silane prevents sections detachment), then incubate in the oven at 92°C (drying) and at 70°C in the hot plate which allows a better adhesion of the tissue sections on the slide as well as the melting of the paraffin. The following preparation procedures are based on the same steps followed in the H&E staining.

II.3.2.2. Tissues sections pretreatment

Before the use of any reagent, the tissue sections are wrapped with a retractable ballpoint pen to mark their positions delineating the reagents drops, the slides are placed in a humidity chamber to avoid any desiccation of sections then an endogenous peroxidase inhibition is performed in hydrogen peroxidase (H2O2) 30% (prepared by one volume of H2O2 30% + nine volume of pure methanol).

An enzymatic digestion is carried out with pepsin enzyme at 37% in a hybridizer to make the RNA accessible to the probe, followed by washing in tow distilled water baths.

For unmask the target antigen (EBER-1 and EBER-2) and removing excess formalin (formaldehyde bonds formed around the nucleus) the slides are incubate in pre-treatment solution (heat pretreatment solution EDTA “ZYTOVISION”) at 90°C (which has already been heated in a water bath at 98°C), a washing with distilled water is applied **(Fig.23).**

Finally, the slides are passed through a three increasing concentration ethanol baths (70%,90%,100%) and air-dried (to avoid dilution of the probe in the alcohols).

Fig.23.Sections pretreatment: endogenous peroxidase inhibition, proteolysis and unmasking of target antigens **(original photos)**

II.3.2.3. Denaturation and hybridization

1 to 2 drops of probe "Zyto*Fast* EBV probe" (hybridization solution) are applied (covering the entire section), then the slides are covered with coverslips (avoiding trapped bubbles), fixing it with Fixogum Rubber Cement to prevent the probe evaporation.

Under darkness, the slides are placed in hybridizer to be incubated for 2h: looking for first the denaturation step (5min at 75°C) followed by the hybridization step (1h at 55°C) which continue with automatic process **(Fig.24).**

Fig.24. Denaturation of mRNA and hybridization of EBV probe in automatic hybridizer **(Original photos)**

II.3.2.4. Rigorous washing

This washing consists of treating the tissue sections with a wash buffer in three successive passes.

After peel of the rubber cement carefully from the slides, the first wash is performed by immersing them in TBS wash buffer (ready to use) at AT (ambient temperature) to make easy the coverslips detachment without damaging sections. The second wash is performed by passing slides in TBS wash buffer preheated at 55°C to remove excess cement and probe. Finally, to avoid shocking the specimen a third wash effected in the TBS buffer at AT **(Fig.25).**

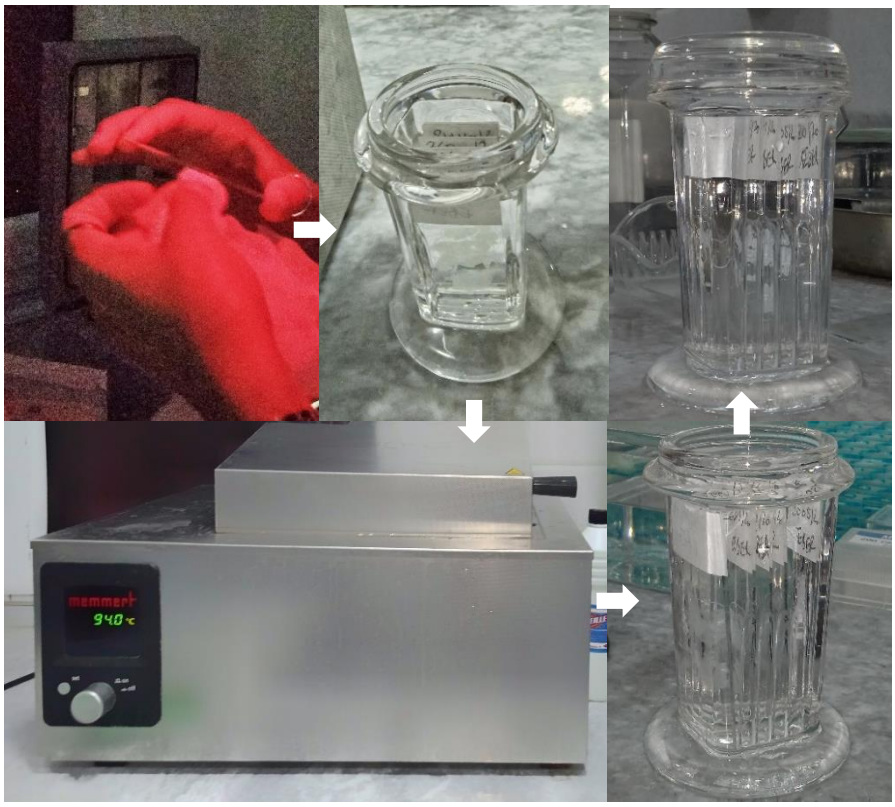

Fig.25. Slides rigorous washing with TBS buffer **(Originals photos)**

II.3.2.5. Detection

1 to 2 drops of Mouse anti-Dig (AB1) are added to each slide then incubated in hybridizer at 37°C (under darkness), excess of this antibody is removed by washing in the TBS buffer PH:7 three times at AT. After adding 1 to 2 drops of Mouse HRP-polymer (AB2) to the slides, an incubation in hybridizer is performed. Three washes in the TBS buffer at AT and DAB reagent are applied (mix 1 ml of AP-Red B solution with 1-2 drops of AP-Red A solution) then an incubation in hybridizer at 37°C is achieved. A final wash of slides is done in distilled water three times at AT, followed by Mayer's hematoxylin counterstaining, a wash under distilled

water, an immersing in increasing concentration ethanol (70%,90%,100%) then in xylene tow times end up by air drying.

The slides are mounted with a mounting solution (ZytoVision) **(Fig.26).** Light microscopic observation of positive reactivity for Epstein-Barr virus EBER RNA in the target cells is indicated by a brown stained nucleus.

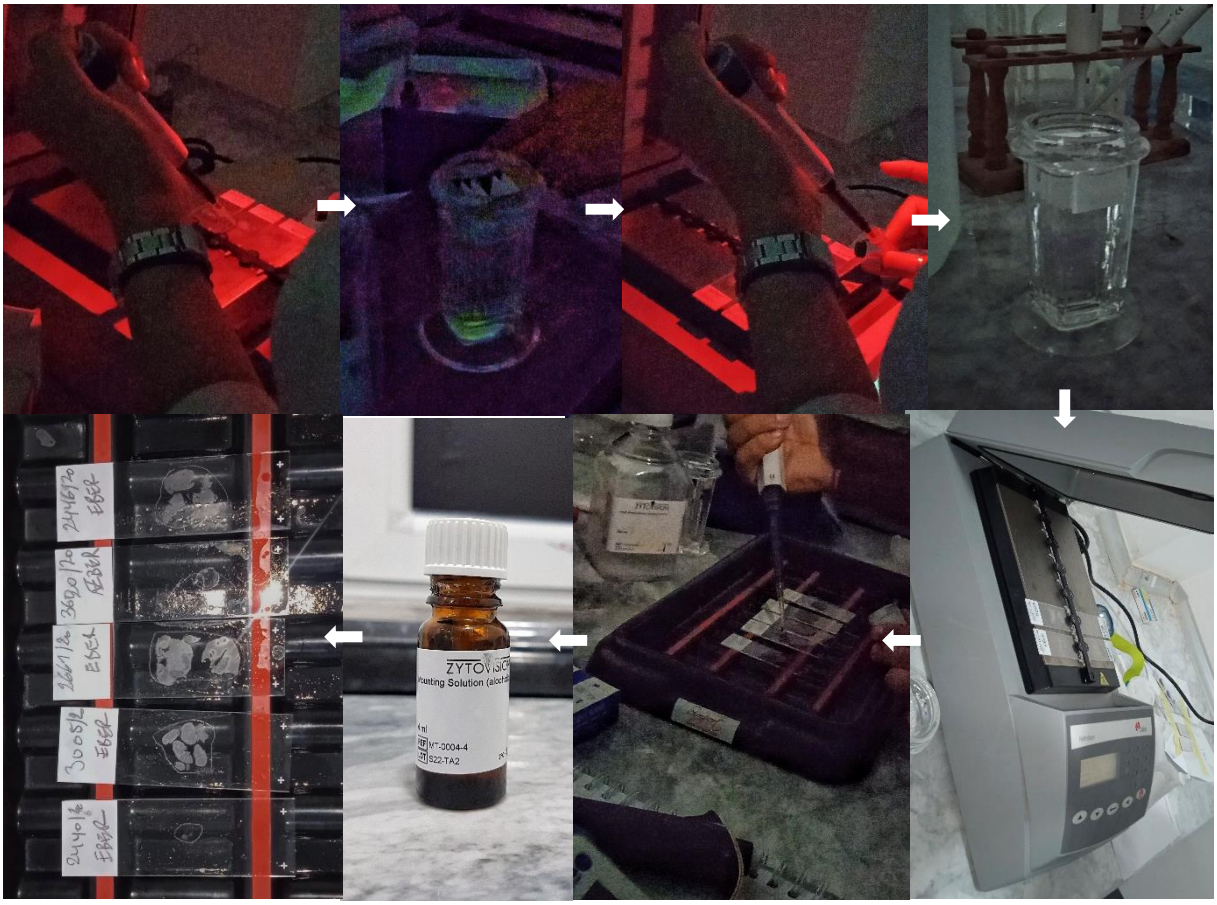

Fig.26. Post-hybridization processing main steps: detection, counterstaining and mounting **(Original photos)**

CISH NOTES:

- The **EBV probe** is intended to be used for the qualitative detection of human Epstein-Barr virus (EBV) EBER RNA in formalin-fixed, paraffin-embedded specimens, such as lymphomas, by chromogenic I*n Situ* hybridization.
- **Anti-DIG/DPN-Mix and HRP/AP-polymer-mix** mouse antibodies are intended to be used for detection steps in chromogenic *In Situ* hybridization applications.
- **AP-Red Solution B and AP-Red Solution A** are intended to be used as a substrate for an AP-conjugated antibody in chromogenic *In Situ* hybridization applications.

CHAPTER III
Results and Discussion

This chapter contains three parts: the first is targets the morphological study of tumor cell population in the first place and the microenvironment in the second place, while the second one deals with determination of immunohistochemical markers for neoplastic cells. Finally, the third one lies in the investigation of viral expression.

I. Analysis of clinical features

We have analyzed the clinical features of 21 cases diagnosed as cHL and presented them in the form of diagrams.

I.1. Result

I.1.1. Age of the patients

The bar graphs below show the age distribution of 21 cHL patients from archives data sources for the year 2020 of anatomopathology department Douera hospital. Horizontal bars represent the age of cases in each age group by which jostles between 3 and 71 years with a mean age recorded in the 36 years. The majority of cHL cases affected are people between ages 3 and 36 years old **(Fig.27).**

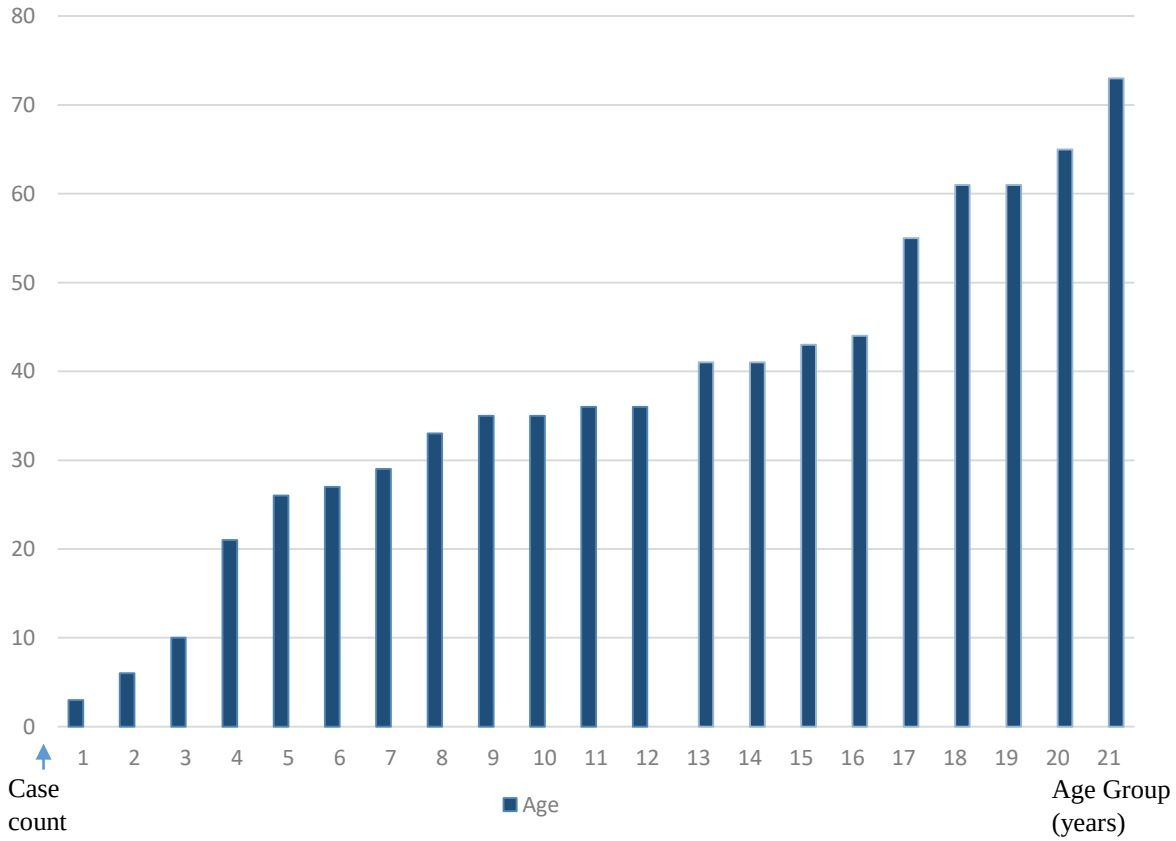

Fig.27. Bar graphs showing age distribution of 21 CHL patients

I.1.2. Gender of patients

Gender distribution of 21 cHL patients from archives data sources for the year 2020 of anatomopathology department Douera hospital. In our study, most cHL patients are females (57%) while only 42% are males, a female predilection with a male: female ratio of 0.75 **(Fig.28).**

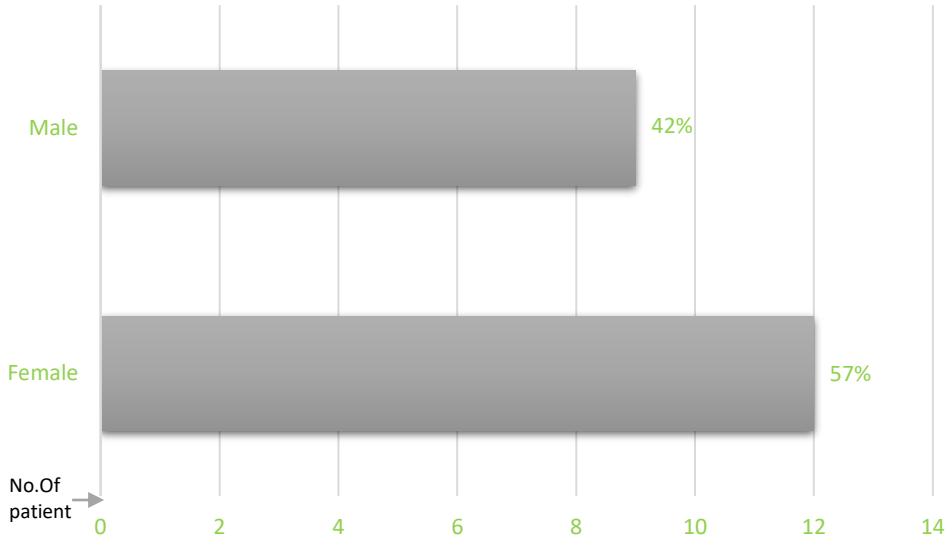

Fig.28. Bar chart showing gender distribution of CHL patients

I.1.3. Lymph node topography

The distribution of lymphadenopathy status according to clinical cases nature is shown in **Fig.29**. Lymphadenopathies located in peripheral cervical topography was significantly higher (24%) than that of patients who had lymphadenopathies located in axillary and mediastinal topography (5%,5%). 66% are unspecified lymphadenopathies.

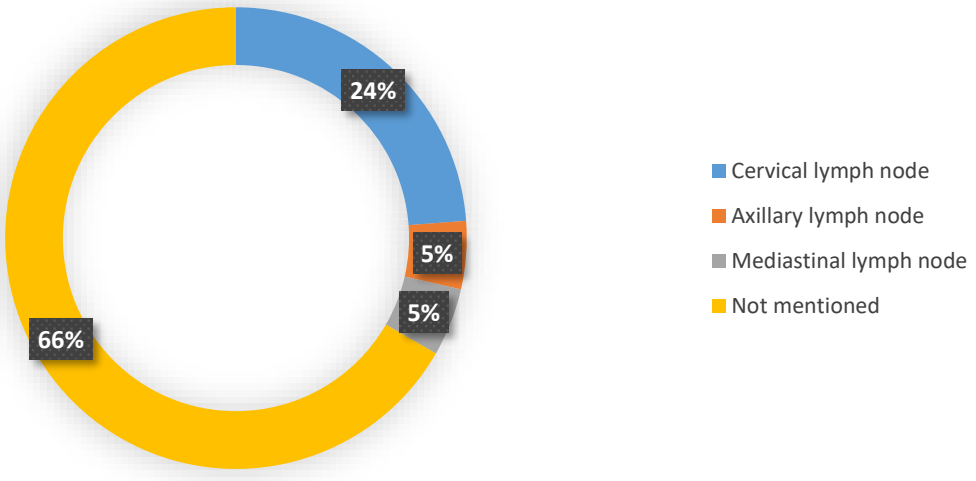

Fig.29. Pie chart showing lymph node topographic distribution of 21 CHL patients

I.2. Discussion

Although cHL is listed as a definitive pathological subgroup in the new WHO classification, the rarity and heterogeneous histological appearance of some subtypes such as lymphocyte-rich **(Younes et *al*.,2021)** make them difficult to diagnosis and identify their clinicopathological characteristics.

The analysis of clinical features cHL patients have revealed a progressive age evolution in terms of age group. Therefore, the small number of our cohort cases studied can contributing to a not really interpretable result. cHL is among the most common cancers in young adults and adolescent; the number of patients increases with age and the majority of people affected are between 3-36 years of age, with an estimated mean age of 36 years old.

Hodgkin lymphoma affects both sexes, with a slight female predominance observed recently in France (sex ratio: 0.92) quoted by **Morère et *al* (2011)**, which corresponds closely to what we have found for classical Hodgkin lymphoma as a whole (0.78 in favor of women). This female predominance suggests that there are possible gender-related changes in exposure to risk factors for cHL when we compare our result with what was quoted in the majority of studies such as **Ashley et *al* (2020)** and **Xin et *al* (2011**) which proved that cHL affect men more than women.

Epidemiologic studies conducted over the past few decades have identified several risk factors that are associated with HL disease, including infection with the mononucleosis associated Epstein–Barr virus (EBV), as well as socioeconomic status and having a family history. Other factors, including occupational exposure to chemicals and reproductive factors such as parity, have also been reported in some studies although these associations have not been consistent **(Cairong et *al*.,2014).**

Further factors that may directly or indirectly influence tumor development such as immunosuppression, physical constitution (age, weight, genetic disposition, sports activity or body mass index) have been discussed. An example is **Wolk et *al* (2001)**, who found a correlation between obesity and the risk of developing cancer according to gender. A threefold increased risk of developing cHL is reported for obese men, while for obese women there was no increased risk.

On the other hand, **Keegan et *al* (2006)** found a risk dependence in young women with lack of physical activity and an above average BMI, while there was no risk association in older

women. Physical activity reduces the risk in both cases. Certainly, high BMI is only a secondary and indirect risk factor. However, it is possible that there is an interaction between the immune system, hormonal balance and the development of tumors due to physical activity. It is interesting to note that in 5 cases (24%) there was a previous history of lymphoma. In 3 cases, it was a recurrent cHL **(Völker et *al.*,2020).**

Several studies have provided epidemiologic data on head and neck lymphoma. However, it seems that additional information from different regions of this disease could be useful to clinicians and further research. According to literature HL is commonly arises in cervical lymph nodes **(Kaseb and Babiker.,2021)**; our findings are similar. The majority of cHL patients present with superficial lymphadenopathy with predominant cervical lymph nodes (25%), while mediastinal involvement and axillary presentation are less common. In addition, extranodal presentations are considerably rare. Typically, HL presents with lymph node involvement **(Youngzhi et al.,2016).**

II. Histopathological study

The morphological study of cHL histopathological appearance was performed using histological technique based Hematoxylin & Eosin (H&E) staining.

II.1. Result

II.1.1. Histopathology presentation

Of our reviewed 21 CHL cases **(Table.01)**, most showed a nodular sclerosis (NC) subtype with 13 (62%) cases. Furthermore, 7 (33%) cases were mixed cellularity and the subtype that appeared rare in this cohort was lymphocyte-rich (1 case (5%)). The lymphocyte depleted subtype was not represented. **(Table 01)**.

Table.01. Histological subtypes of reviewed 21 classical Hodgkin lymphoma (cHL) cases

Histological diagnosis	Number	Percentage
Classical HL (CHL)	**21**	**100%**
Nodular Sclerosis (NS)	**13**	**62%**
Mixed Cellularity (MC)	**7**	**33%**
Lymphocyte Rich (LR)	**1**	**5%**
Lymphocyte Depleted (LD)	**0**	**0%**

II.1.2. Morphological features of classical Hodgkin lymphoma

II.1.2.1. Microscopic appearance of normal lymph node

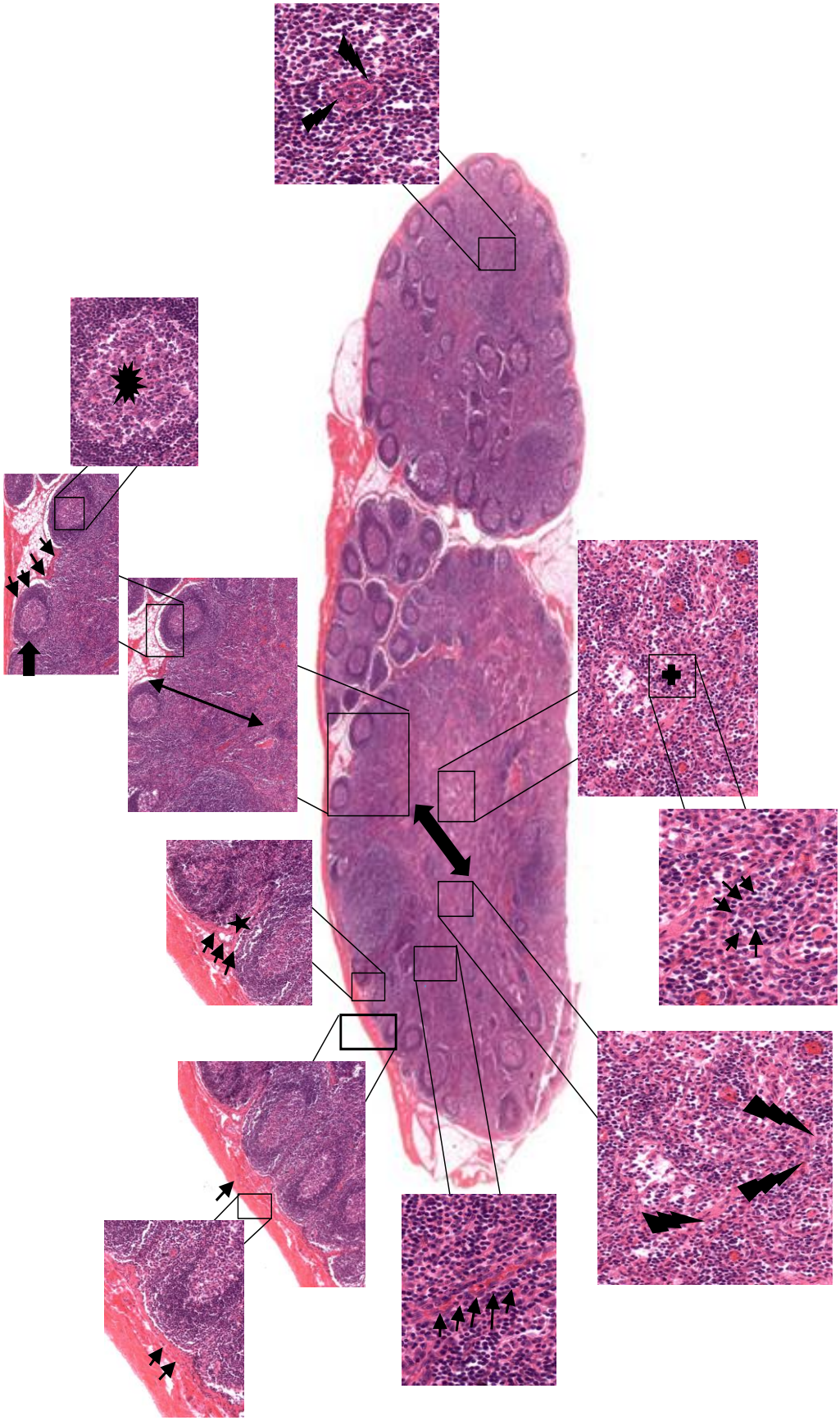

Fig.30 Microscopic aspect of a lymph node at different magnifications (virtual slide under light microscope, HE staining) **(Brelje and Sorenson; Atlas Histology Guide.,2005)**

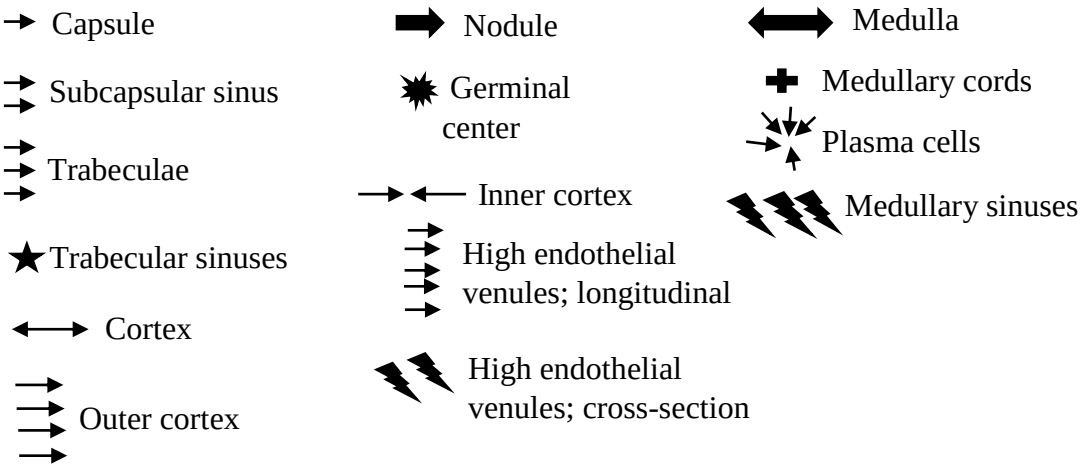

- **Capsule _ Subcapsular sinus:** The wall of the sinus is a discontinuous layer of flattened endothelial-like cells.
- **Cortex:** Dark, due to abundant basophilic lymphocytes.
- **Outer cortex_nodules:** Follicular lymphatic tissue with primary and secondary lymphatic follicles.
- **Inner cortex:** Diffuse lymphatic tissue. High endothelial venules (HEVs).
- **Medulla:** Light, due to fewer cells and abundant lymphatic sinuses.
- **Medullary cords:** rich of plasma cells, B lymphocytes, and macrophages.
- **Medullary sinuses:** the wall of the sinus is a discontinuous layer of flattened endothelial-like cells.

II.1.2.2. Nodular sclerosis classical Hodgkin lymphoma subtype

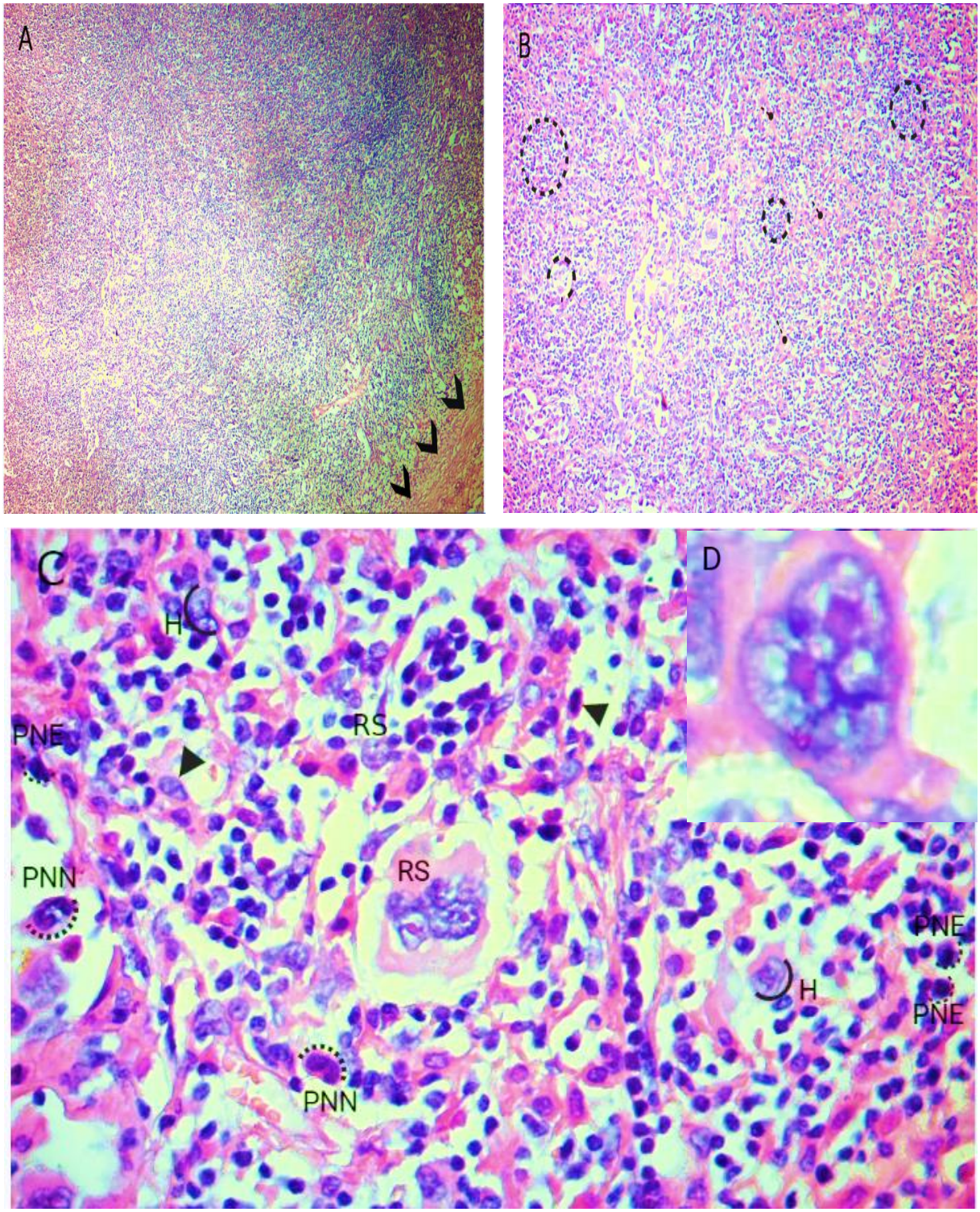

Board.I Photomicrographs of Nodular Sclerosis classical Hodgkin Lymphoma (lymphadenopathy tissue sections). Hematoxylin-Eosin staining **(Original photomicrographs. Adjusted with Upscale, Snapseed and Adobe Lightroom).**

Fig.A. Photomicrograph of lymphadenopathy shows a complete erasure of lymph node architecture. Hematoxylin-Eosin staining; **G4X.**

- Light pink color reflects fibrosis, dark pink color represents the rich cells regions and arrows indicate fibrous collagen.

Fig.B. Photomicrograph of lymphadenopathy presenting a nodular infiltrate surrounded by large fibrous bands of collagen. Hematoxylin-Eosin staining; **G10X.**

- This Fig shows a nodular infiltrate with the presence of fibrosis which is due to a malignant cellular infiltration of lymphoid nature that is made up of several large cells with vesicular nuclei, sometimes bi- or multi-nucleated corresponding to those of Reed Sternberg.
- Dashed circles demonstrate lymphoid cells, dashed dot: fibroblasts cells and dashed circles lines: granulomatous background.

Fig.C. Photomicrograph of Hodgkin and Reed Sternberg cells found on a polymorphic granulomatous background of plasma cells, neutrophils and eosinophils. Hematoxylin-Eosin staining; **G40X.**

- This Fig Present a malignant cellular infiltration: bi-nucleated Reed Sternberg(RS) and Hodgkin cells (H), scattered in a polymorphic inflammatory background: Polynuclear Eosinophils (PNE), Polynuclear Neutrophils(PNN) and plasma cells (arrows).

Fig.D. Photomicrograph of bi-nucleated Reed Sternberg cell. Hematoxylin-Eosin staining; **G40X.**

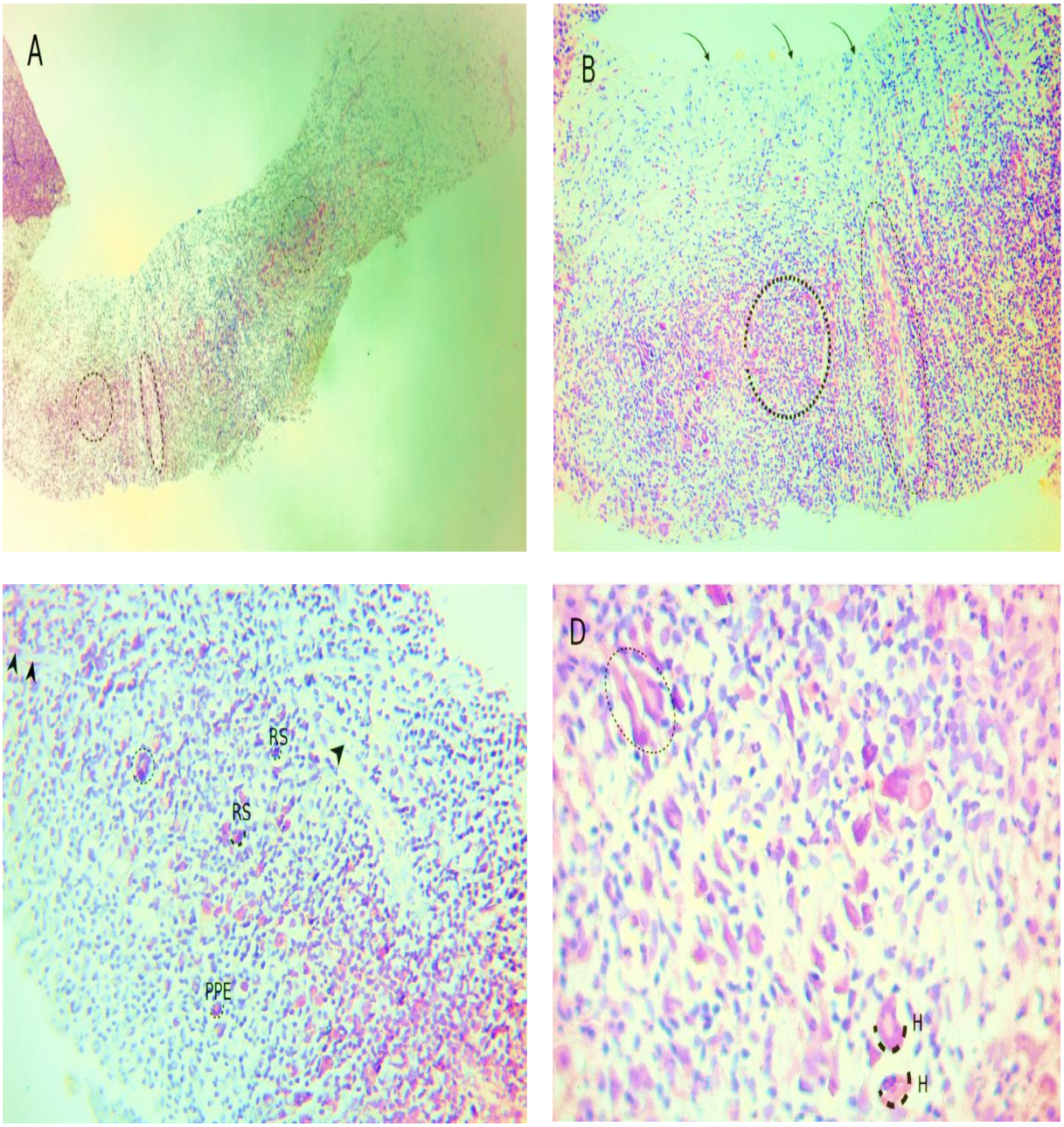

Board. II. Photomicrographs of Nodular Sclerosis classical Hodgkin Lymphoma (axillary (A ,B,C) and cervical (D) lymph node biopsies tissue sections .Hematoxylin-Eosin staining **(Original photomicrographs. Adjusted with Upscale, Snapseed and Adobe Lightroom)**

Fig. A.B. Photomicrographs of axillary lymph node biopsies demonstrating a lymphomatous proliferation arranged as nodules surrounded by variable thickness septa with the loss of capsule. Hematoxylin-Eosin staining; **G4X, G10X** respectively.

- Arrows indicate the loss of capsule
- Dotted circles indicate the nodules

Fig.C. Photomicrographs of axillary lymph node biopsies presenting some polymorphic inflammatory background rich in polynuclear eosinophils, on which are disposed tumor cells of Hodgkin **(H)** type and Reed Sternberg **(RS)** sometimes multinucleated. Hematoxylin-Eosin staining; **G20X.**

- Arrows indicate the fibrous septa

Fig.D. Photomicrographs of axillary lymph node biopsies show a tumor cell distribution of Hodgkin and Reed Sternberg and some lacunar cells with retracted cytoplasm. Hematoxylin-Eosin staining; **G40X.**

- Dotted circles: lacunar cells

II.1.2.3. Mixed Cellularity classical Hodgkin lymphoma subtype

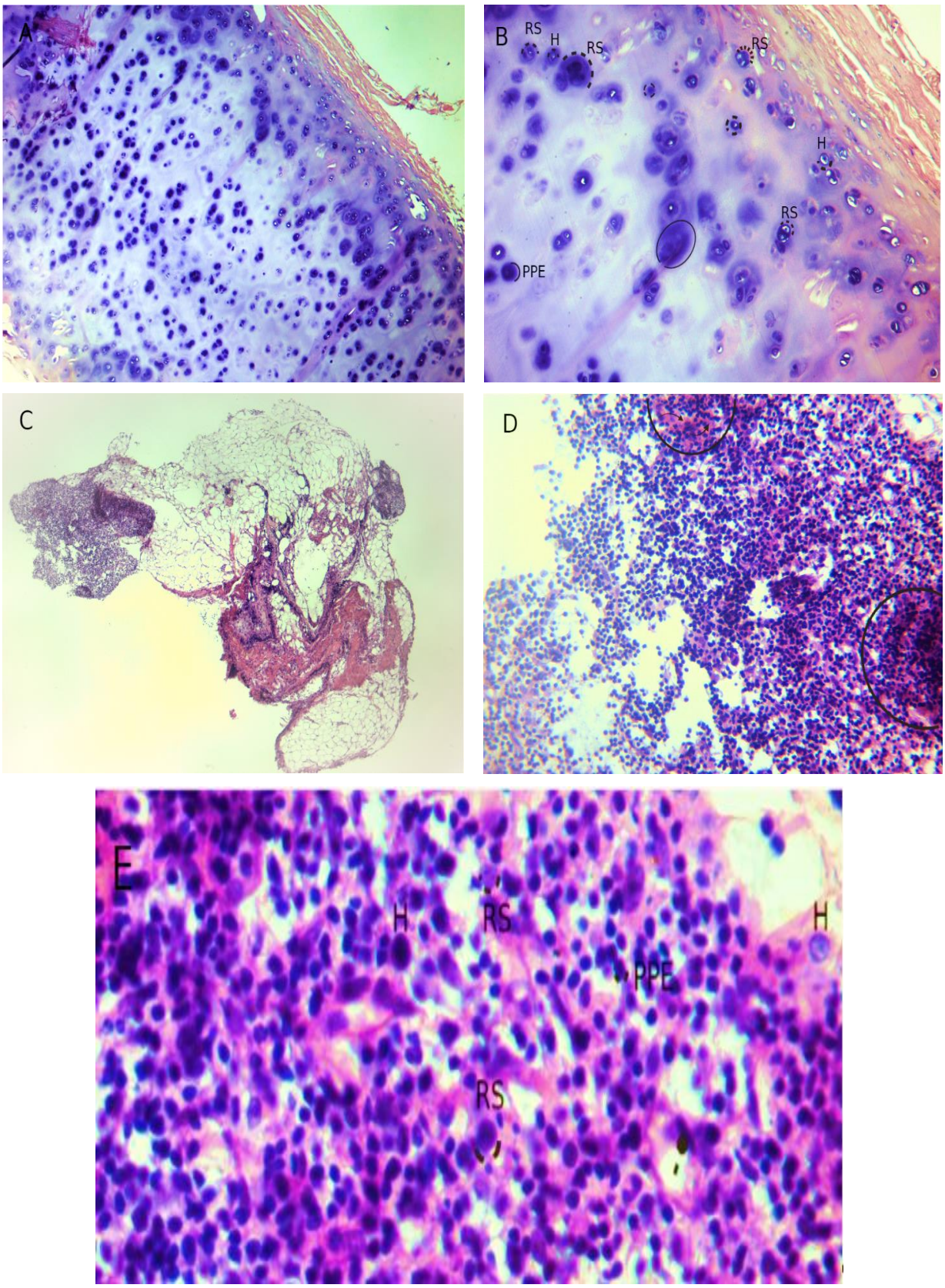

Board.III. Photomicrographs of Mixed Cellularity classical Hodgkin Lymphoma (tissue sections of lymph node biopsies (A, B) and lymphadenopathy (C, D ,E). Hematoxylin-Eosin staining **(Original photomicrographs. Adjusted with Upscale, Snapseed and Adobe Lightroom)**

Fig. A. Photomicrographs of lymph node biopsies show an appearance of lymph node parenchyma partly erased by a lymphomatous proliferation of diffuse architecture Hematoxylin-Eosin staining; **G20X.**

Fig. B. Photomicrographs of lymph node biopsies show a polymorphic lymphomatous background full of lymphocytes and polynuclear eosinophils. Hematoxylin-Eosin staining; **G40X.**

On this background, a number of large tumor cells with irregular nuclei and prominent eosinophilic nucleoli corresponding to Hodgkin cells are scattered.

Some cells with bilobed nucleus corresponding to RS and lacunar cells are present.

- PPE: polynuclear eosinophils.

Fig. C. Photomicrographs of lymphadenopathy show a lymph node parenchyma completely effaced by a lymphomatous neoplastic proliferation. Hematoxylin-Eosin staining; **G4X**.

Fig. D. Photomicrographs of lymphadenopathy presenting a lymphoplasmacytic and eosinophilic granulomatous background. Hematoxylin-Eosin staining; **G10X**.

- Circles indicate granulomatous background.

Fig. E. Photomicrographs of lymphadenopathy demonstrate a background in which the Hodgkin (H) and Reed Sternberg (RS) are found with presence of plasma cells. Hematoxylin-Eosin staining; **G40X.**

- Dashed dot indicate plasma cells

II .1. 2.4. Lymphocyte rich classical Hodgkin lymphoma subtype

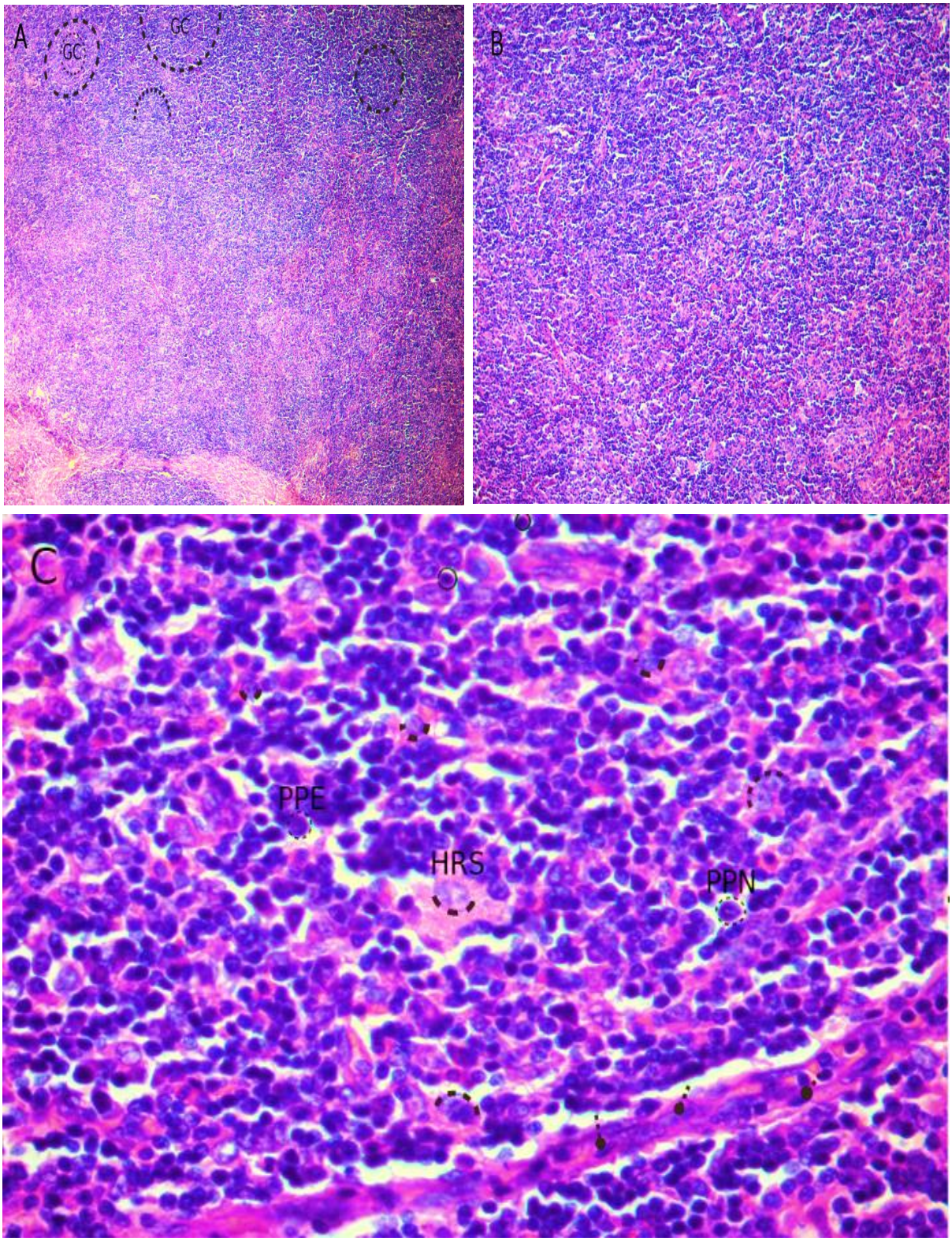

Board.IV. Photomicrographs of lymphocyte rich classical Hodgkin lymphoma (lymph node biopsy tissue section). Hematoxylin-Eosin stinging **(Original photomicrographs. Adjusted with Upscale, Snapseed and Adobe Lightroom)**

Fig. A. Photomicrograph of lymph node biopsy showing a partial effacement of the architecture. Hematoxylin-Eosin staining; **G4X**.

- The follicles (dashed circles) are partially preserved with detectable germinal center (GC).

Fig. B. Photomicrograph of a lymph node biopsy show the lymphocyte abundance in the infiltrate. Hematoxylin-Eosin staining; **G10X**.

- Blue areas indicate the zones which are rich in lymphocytes.

Fig. C. Photomicrograph of a lymph node biopsy show a lymph node parenchyma infiltrated by a few large neoplastic cells of Hodgkin type and others of Reed Sternberg type on a lymphocytic background with presence of rare polynuclear and some epithelioid cells. Hematoxylin-Eosin staining; **G40X**.

- Dashed dots indicate epithelioid cells.

II.2. Discussion

The literature existing on significance of different histological features in diagnosis and prognosis of HL disease is still insufficient **(Kaumudi et *al*.,2016).** HL cases in developed and developing countries differ in their histopathological features **(Saadettin et *al*.,2013).** This part of study analyzed the morphology as well as factor that have used to determine classical Hodgkin lymphoma variants**.**

As for subtypes obtained in this series, NS-CHL is the most frequent (62%), followed by MC-CHL (33%), while LR-CHL is less frequent (5%). As mentioned above, the NS-CHL histological sub-type accounts for more than half of all cases in developed parts of the world. On the other hand, the MC-CHL histological subtype is more common in developing or underdeveloped countries **(Saadettin et *al*.,2013)**. Overall, our histological distribution is similar to those reported in **Ashley et *al* (2020)** study**,** there are no cases in our sample representing lymphocyte depleted subtype which is in consistent with **Xin et *al* (2011)** in subtype distribution in Chinese. This is due to its rarity, accounting for 1% to 1.5% of classic Hodgkin lymphoma cases in western countries **(Thida and Tun.,2021).**

The prognosis of NS disease is slightly better than that of LD and MC disease which has a prognosis intermediate between the prognosis of LR and LD subtypes **(Shin-ichi and Katsuyuki.,2006)**, this may indicate that the majority of patients in our cohort presented a favorable prognosis.

This study analyzed histological parameters, such as thickness of capsule, nodular infiltration, effacement – whether complete or partial, fibrous bands, nodule formation, composition of background population of cells, type of RS cells, granulomas.

Nodular sclerosis cHL shows an effacement whether complete or partial with a partially nodular growth pattern, characterized by broad collagen bands separating the lymphoid tissue defined at least one nodule and some inflammatory background rich of polynuclear neutrophils, eosinophils, plasma cells, histocytes of which they are not spotted in our slides and fibroblasts which is in common with **Hatem and Hani (2021**). A granulomatous background is present. RS and mononuclear Hodgkin cells are present. The number of RS is highly variable which allows to participate together with the atypia of these cells, the degree of cellularity in the nodules and the amount of sclerosis in the separation of nodular sclerosis into grade 1 and grade 2 which is more aggressive with a lower outcome according to the British National Lymphoma Investigation (BNLI) **(Annarosa et *al*, 2014)**. Although, this grading in not required for clinical

purposes because it remains controversial whether this classification has a clinical significance or not **(Oviedo et *al*.,2020).**

Lacunar cells which are among RS variants appearance are more common, that is in consistent with what was quoted by **Hatem and Hani (2021).** These cells are characterized by abundant clear cytoplasm, possessing more complicated nuclei and less prominent nucleoli that often retracts during tissue fixation and sectioning, leaving the nucleus in what appears to be empty space (lacune-like space) than RS cells in other classical HL types. The lacunar cells sometimes aggregate and form cohesive sheets or nests around the necrotic areas of the nodules which we have not observed in our cases examined **(Shin-ichi and Katsuyuki.,2006)**.

Mixed cellularity cHL present usually an erased lymph node architecture with diffuse nodular growth pattern. Sclerosis bands absent in the inflammatory background. Fine interstitial fibrosis may be present, and typical RS cells are plentiful which are scattered in polymorphic lymphomatous background that includes some mononuclear Hodgkin cells, eosinophils, neutrophils, histocytes and some lacunar cells with some aggregation granulomatous clusters. Interstitial fibrosis may be present our result is similar to **Hatem and Hani (2021) and Shin-ichi and Katsuyuki (2006)**.

Lymphocyte-rich HL shows a nodular growth pattern in an inflammatory background that consists predominantly of lymphocytes among which RS and mononuclear Hodgkin cells are scattered, with rare polynuclear eosinophils and neutrophils. Some lymph node follicles are partially preserved with some detectable germinal centers. A granulomas formation has observed with some epithelioid spread cells. This is confirmed by **Hatem and Hani (2021) and Shin-ichi and Katsuyuki (2006)**.

Hodgkin and Reed-Sternberg cells appear large, with (biloped or multilobed) enlarged irregular nucleus bearing the eosinophilic appearance, surrounded by a clear halo (in the form of an owl's eye) with a prominent nuclear membrane and abundant amphiphilic cytoplasm. Some cells have large vacuoles. The morphology varies from the classical polynuclear RS to mononuclear Hodgkin cells. These pathognomonic signs indicate the presence of malignant cells and its activation in the lymphatic tissue (high protein production).

From this result, we conclude that classical Hodgkin's lymphoma is composed of two malignant cell populations: mononucleated Hodgkin's cells and bi- or multinucleated Reed-Sternberg cells, which leads us to ask an intriguing question about the relationship between these two cell types.

Studies have suggested that RS cells can be generated from Hodgkin's by fusion of two independent cells, and it has been discussed whether the HRS cell of a whole clone can be derived from a cell fusion, which has been argued by the mixed immunophenotype and the generally aneuploid karyotype of HRS cells, but later a molecular studies excluded this fusion hypothesis**(Küppers.,2018).**

Recent studies based on firm evidence on HL cell lines demonstrate that HRS cells derive from Hodgkin mononuclear cells by a process of incomplete cytokinesis **(Küppers.,2018).**

The division of Hodgkin cells often fails at the final separation of the daughter cells giving RS cells after going through a refusion phenomenon. However, the proliferative compartment of the HRS cell clone are the mononuclear Hodgkin cells so that the RS cells have little proliferative potential, which may explain the rarity of RS cells in the tumor tissue **(Küppers.,2018).**

Histologically, our result is convincing since our hematoxylin-eosin slides are clearly demonstrated neoplastic cells scattered in a lymphomatous background rich in reactive cells. Noting that non-Hodgkin's lymphoma and even non-hematopoietic malignancies may present cells that resemble HRS cells, also called HRS-like cells. Therefore, the identification of HRS cells in a given tumor does not necessarily designate that it is a cHL; to bring closer to the diagnosis, it is necessary that these cells need to be identified in an appropriate inflammatory context **(Gelvez and Smith.,2015)**. In another hand, the morphological detection of H and RS cells alone is not sufficient which requires the use of an appropriate panel of markers to strengthen and confirm the diagnosis.

III. Immunophenotypical profile

III.1. Results

III.1.1 Distribution according to immunohistochemical tests

In the selected 21 patients of the year 2020, the immunohistochemical profile of our study presented the following results:

The total of immunohistochemical staining tests for the markers CD15, CD30 and CD20 was done for the 21 patients; where 20/21 cases were positive for CD15 except one case where the antibody was not available for the test. The CD30, was positive for all cases, while the CD20 was positive in 17/21 cases and negative in 4/21 cases, the distribution of CD20 within the cellular environment is shown below**.** The total tests for the PAX5 were 8/21, where 7 patients with cHL presented a positive expression of this marker and 1 patient did not present any expression. The EBV-LMP1 immuhistochemical staining has been done for 4/21 cases, and the results showed a positivity in 3 patients whereas 1 patient did not show any expression. 18 patients were tested for the expression of the T cell marker CD3 and the results showed a positivity for all the 18 cases. **(See Fig.31)**. The total distribution of IHC results is shown in **(table.04)** of **Appendix.III**

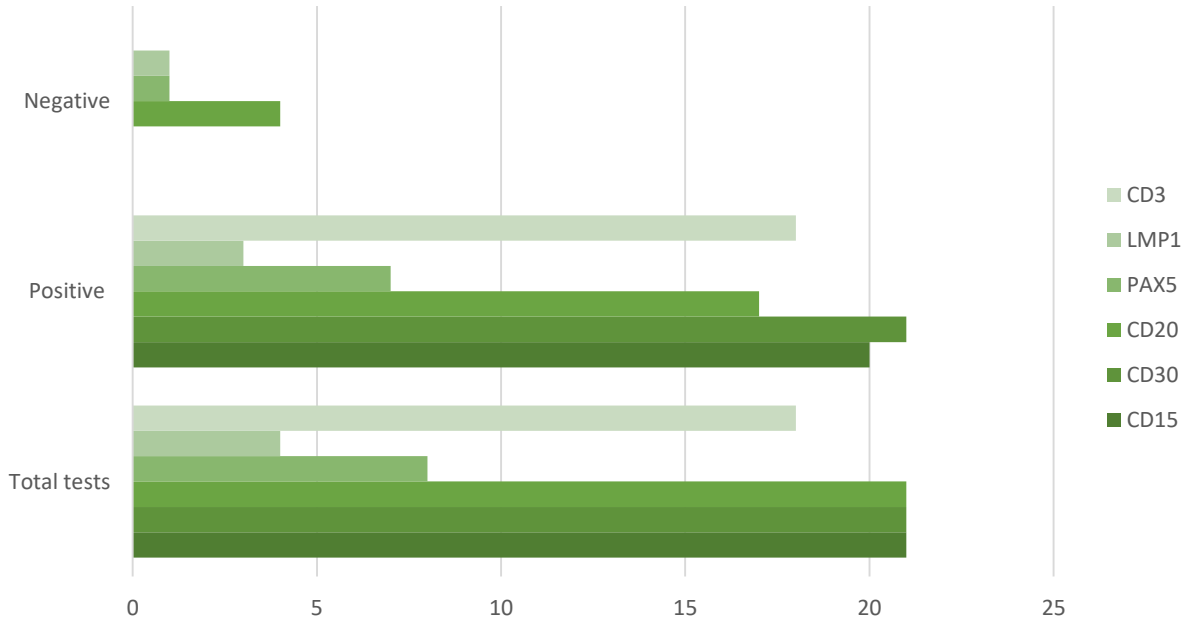

Fig.31 Immunohistochemistry results of the selected 21 patients of the year 2020.

III.1.2 CD20 distribution in the cellular environment

The positivity of the Immunohistochemical pattern CD20 in all cases is in fact distributed between HRS cells and the surrounding B-cells as it is shown in **Fig.32** bellow. Here, only 8/21 cases that expressed CD20 on HRS cells whereas 8/21 (38%) were positive for CD20-expressed B cells. 4 (19%) cases were negative for CD20 expression in the cellular environment.

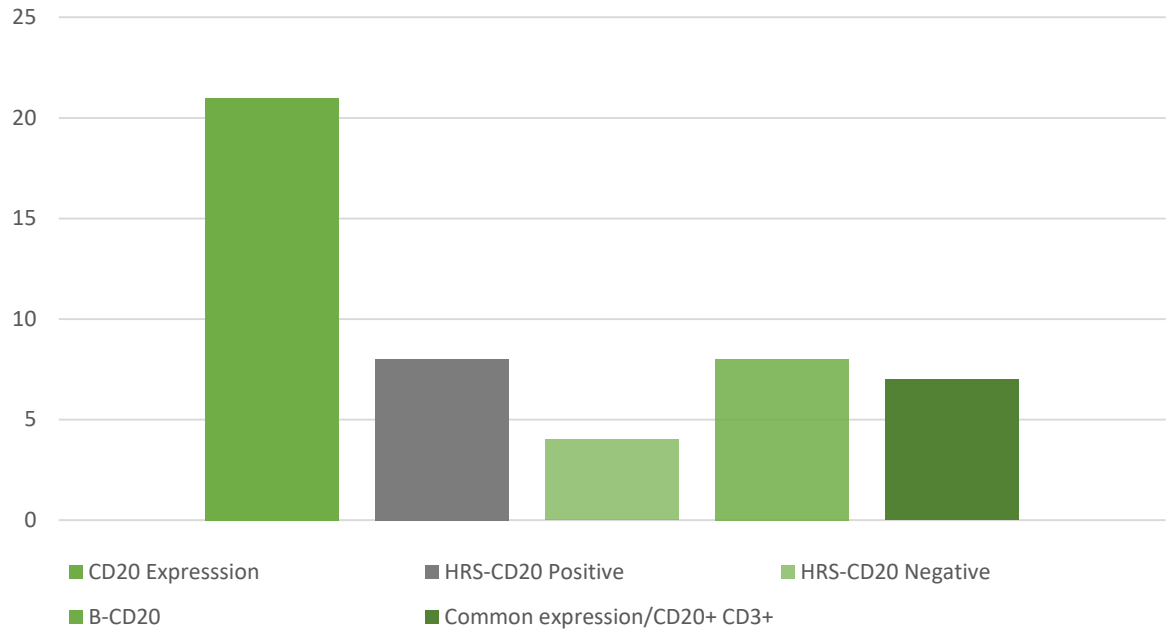

Fig.32 Distribution of CD20 expression in the cellular environment within the tested 21 patients.

III.1.3 Histological findings of cHL markers

In the present study, we reviewed all the immunohistochemical findings of the 21 patients diagnosed in 2020.

Here we show bellow the immunostaining results of the immunophenotypical patterns CD15, CD30, CD20, PAX5, CD3 and the EBV pattern LMP1.

III.1.3.1 CD15

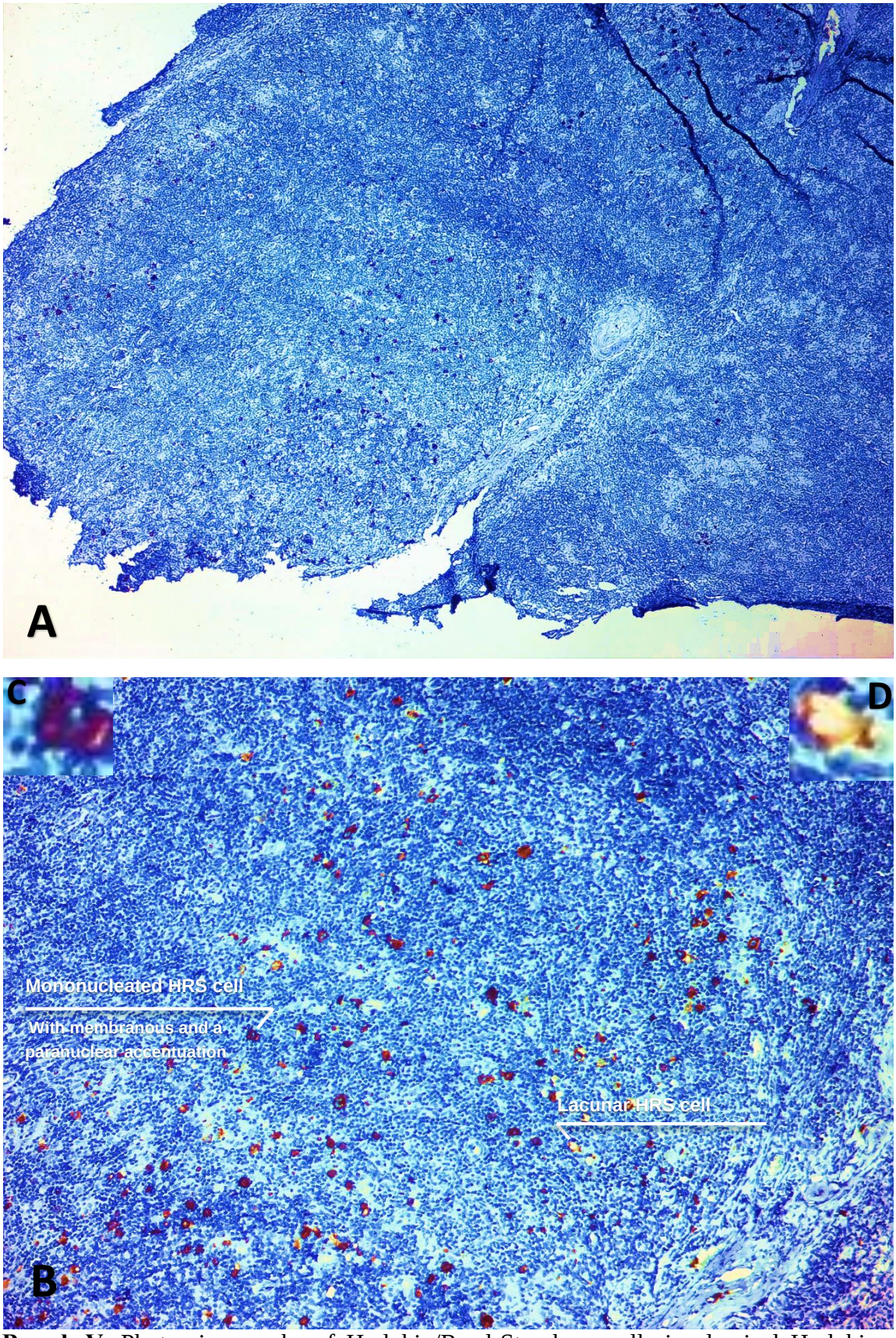

Board. V. Photomicrographs of Hodgkin/Reed-Sternberg cells in classical Hodgkin Lymphoma expressing CD15 detected by antibody LeuM1 **(Original photomicrographs. Adjusted with Upscale, Snapseed and Adobe Lightroom).**

Fig. A.B. Above show 2 different microphotographs of CD15 immunostaining results with the objectives **G4X**, **G10X** respectively of the same tissue section representing a MCcHL, revealing the distribution of CD15' signal within the tissue.

Fig. C. Demonstrating a mononucleated HRS cell with membranous and a paranuclear accentuation of CD15 expressing. **G10X.**

Fig. D. Demonstrating a lacunar HRS cell. **G10X**.

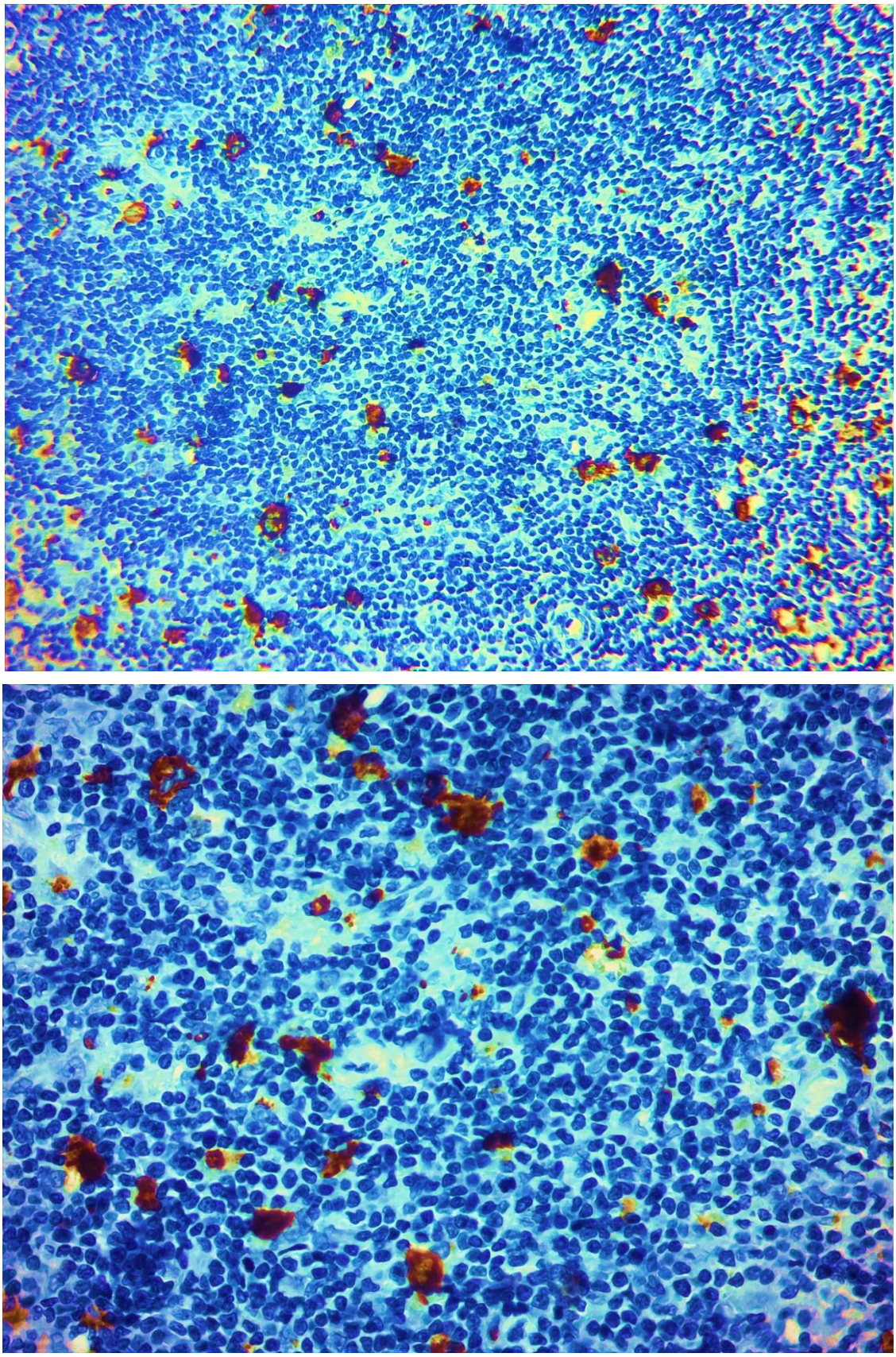

Board .VI. Photomicrographs of Hodgkin/Reed-Sternberg cells in classical Hodgkin Lymphoma expressing CD15 detected by antibody LeuM1. **(Original photomicrographs. Adjusted with Upscale, Snapseed and Adobe Lightroom).**

Fig. A.B. Photomicrographs show a CD15 immunostaining results with the objectives **G20X**, **G40X** respectively of the same tissue section representing a MCcHL, revealing the staining pattern in HRS cells.

A. Show some infiltrate rich of binucleated RS cell with a membranous and a paranuclear accentuation of CD15 expression, lacunar cell.

B. Show a background of which the bilobated RS cell with a cytoplasmic distribution of CD15 expression and mummified cells are scattered.

CD15 immunostaining resulted in brown dots within the malignant tissue and appears to be intensively expressed with a membranous localization and a Golgi accentuation (paranuclear), sometimes with a cytoplasmic distribution on the Hodgkin & Reed Sternberg variants including; binucleated RSs, mononucleated RSs, Lacunar RSs and some mummified RS cells as indicated in the microphotographs **(Boards.V.VI).**

III.1.3.2 CD30

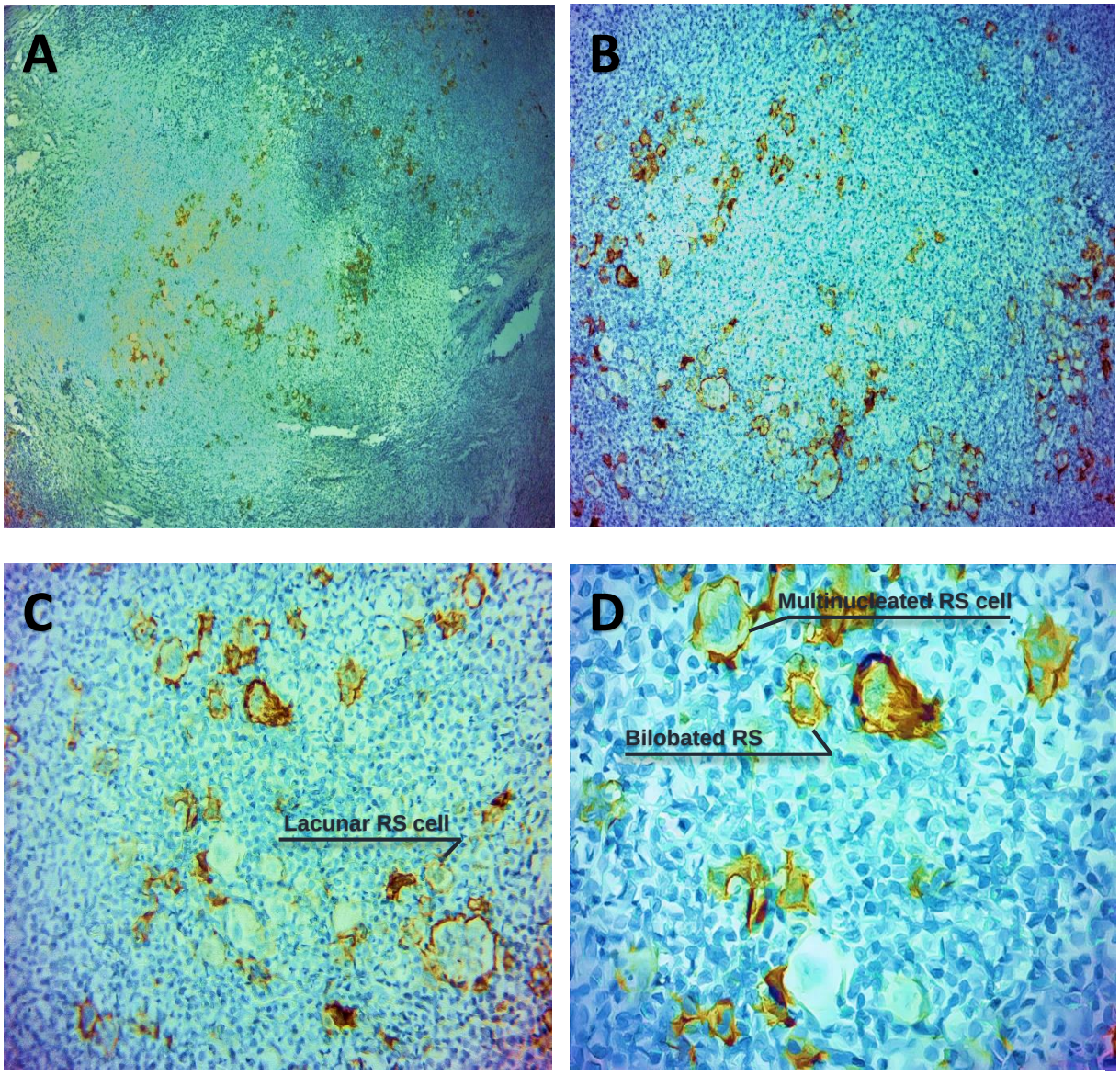

Board. VII. Photomicrographs show Hodgkin/Reed-Sternberg cells in classical Hodgkin Lymphoma expressing CD30 detected by antibody Ber-H2. **(Original photomicrographs. Adjusted with Upscale, Snapseed and Adobe Lightroom).**

Fig.A. Photomicrographs show Hodgkin/Reed-Sternberg cells in classical Hodgkin Lymphoma expressing CD30 detected by antibody Ber-H2. **G4X**.

Fig.B. Photomicrographs show Hodgkin/Reed-Sternberg cells in classical Hodgkin Lymphoma expressing CD30 detected by antibody Ber-H2**. G10X.**

Fig.C. Photomicrographs show Hodgkin/Reed-Sternberg cells in classical Hodgkin Lymphoma expressing CD30 detected by antibody Ber-H2. **G20X.**

Fig.D. Photomicrographs show Hodgkin/Reed-Sternberg cells in classical Hodgkin Lymphoma expressing CD30 detected by antibody Ber-H2**. G40X.**

Figures **(Fig.A, B, C, D)** above show 4 different microphotographs of CD30 immunostaining results with the objectives **(G4X, G10X, G20X, G40X)** of the same tissue section representing a NScHL. Where **(Fig.A)** shows the signal distribution within the malignant tissue referring to HRS cells, while **(Fig.B,C,D)** show the staining pattern of CD30 in HRS cells.

The reviewed slide showed brown staining referring to CD30 antigen that is visibly expressed on HRS cells membrane so as on the Golgi region. The staining appears on the RSs variants including: Multinucleated RSs, Lacunar RSs and the bilobated RSs as it is indicated in the microphotographs above.

III.1.3.3 CD20 expression on HRS cells

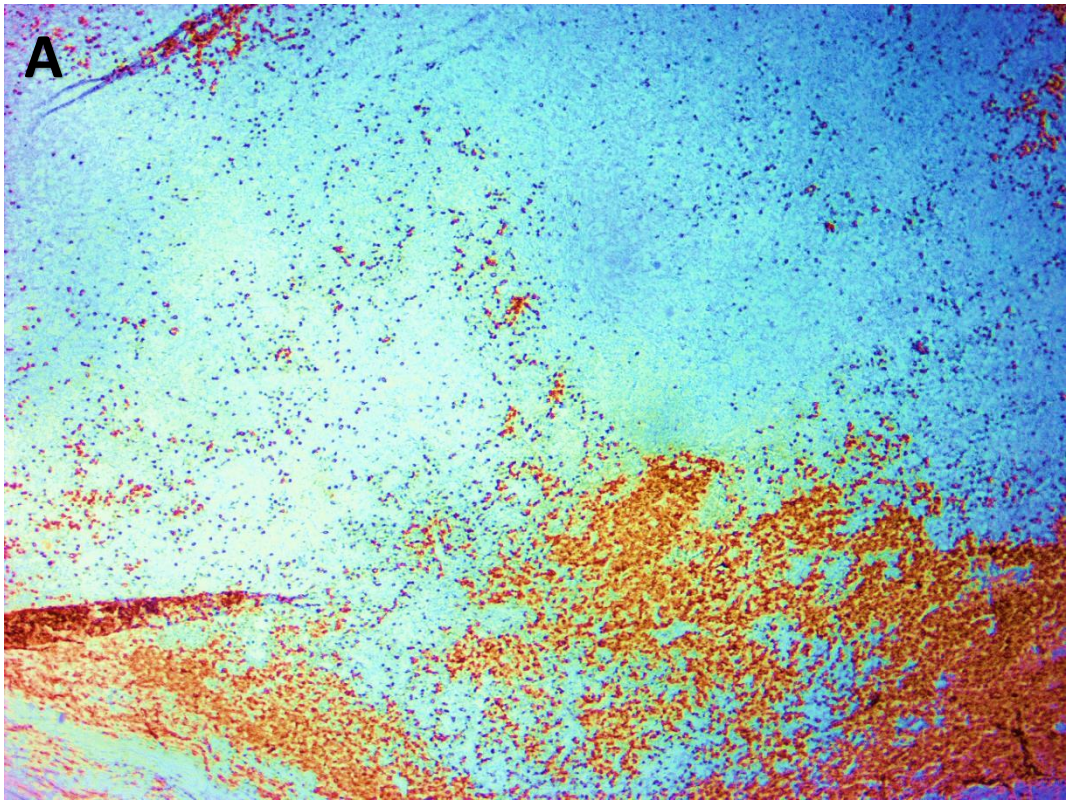

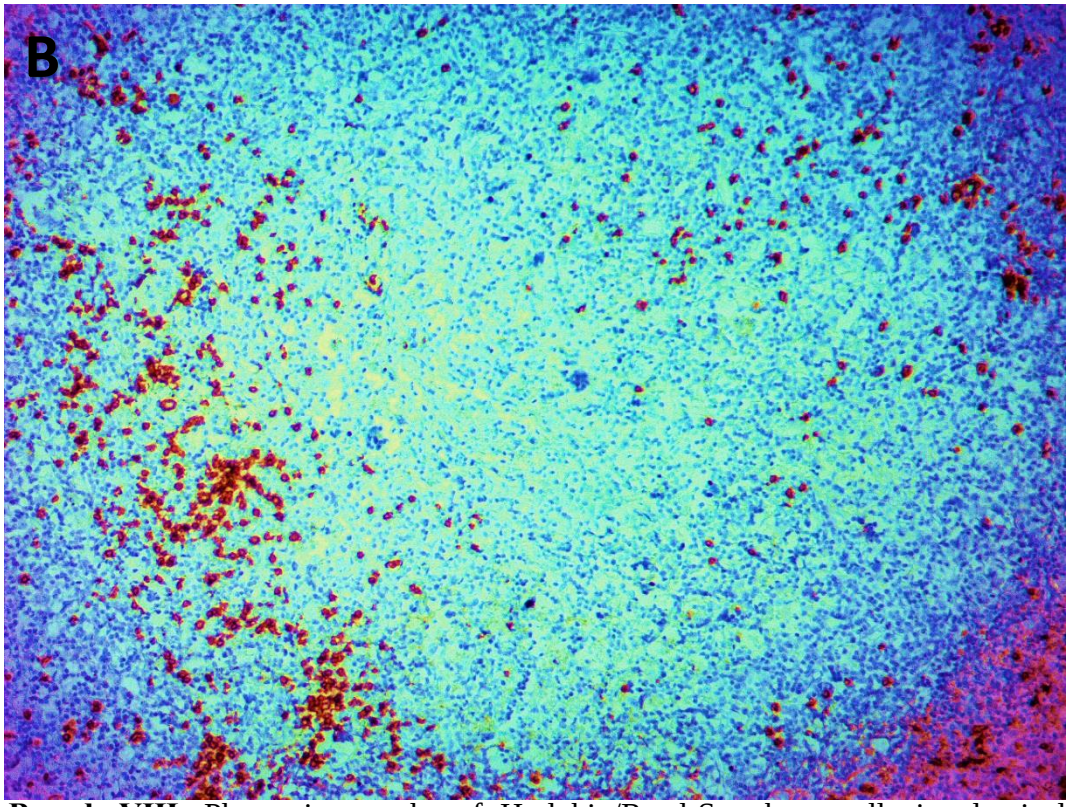

Board. VIII. Photomicrographs of Hodgkin/Reed-Sternberg cells in classical Hodgkin Lymphoma expressing CD20 detected by antibody L26. **(Original photomicrographs. Adjusted with Upscale, Snapseed and Adobe Lightroom).**

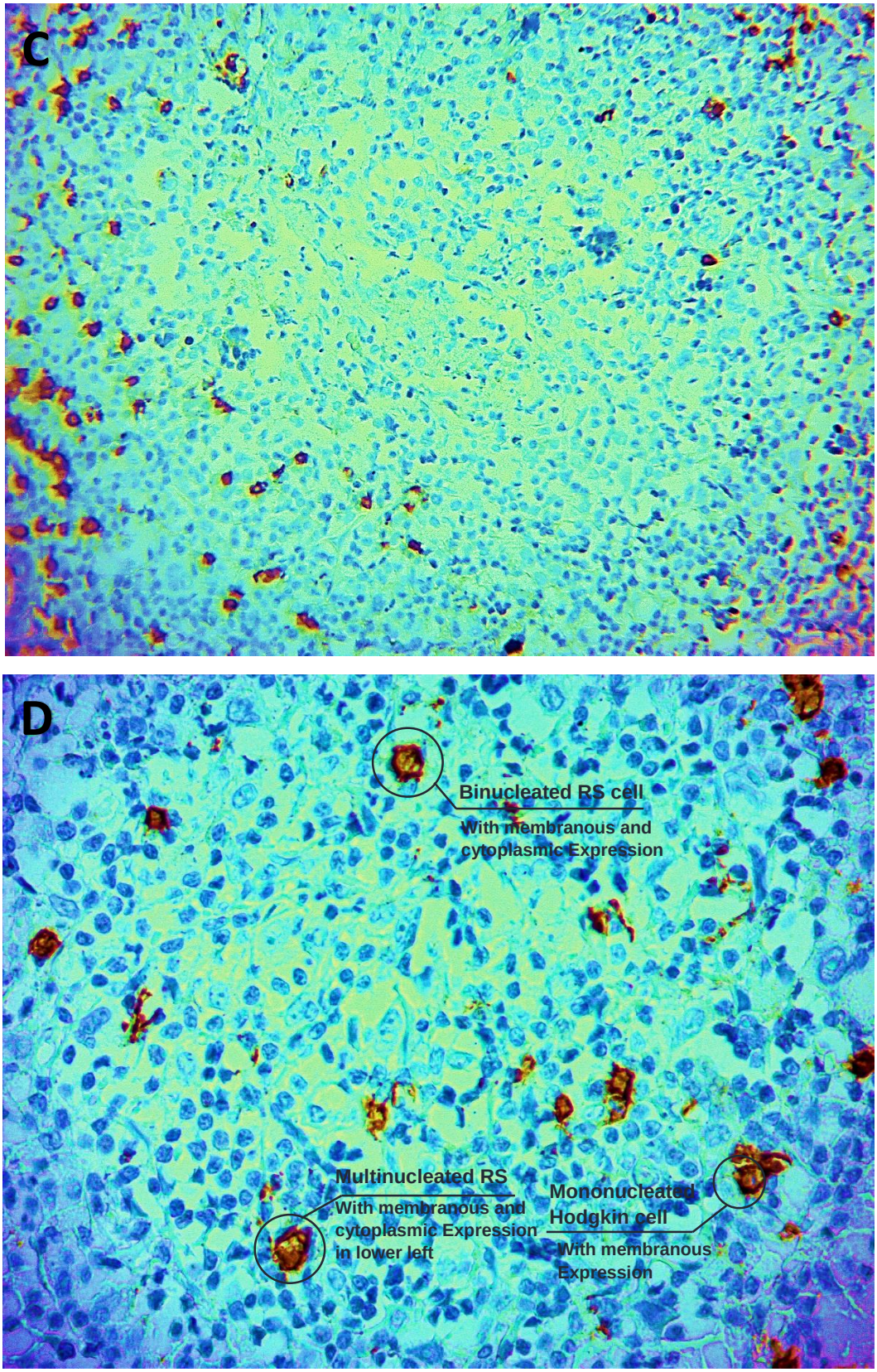

Board. IX. Photomicrographs of Hodgkin/Reed-Sternberg cells in classical Hodgkin Lymphoma expressing CD20 detected by antibody L26. **(Original photomicrographs. Adjusted with Upscale, Snapseed and Adobe Lightroom).**

Board. VIII.IX.

Fig.A.B.C.D. Above show 4 different microphotographs of HRS/CD20 immunostaining results with the objectives **G4X, G10X, G20X, G40X** respectively of the same tissue section representing a NScHL.

The objectives **G4X**, **G10X** reveal CD20' distribution within the tissue, whereas **G20X**, **G40X** in **Fig.D** shows the staining pattern of CD20.

The slide showed a brown signal indicating CD20 expression on HRS variants including, mononucleated Hodgkin cells, Multinucleated RS cells and Binucleated RS cells. The staining pattern appeared on the membrane and in the cytoplasm near the membrane of HRS cells.

III.1.3.4 Reactive CD20 and CD3 on the inflammatory background in cHL cases

- **CD20**

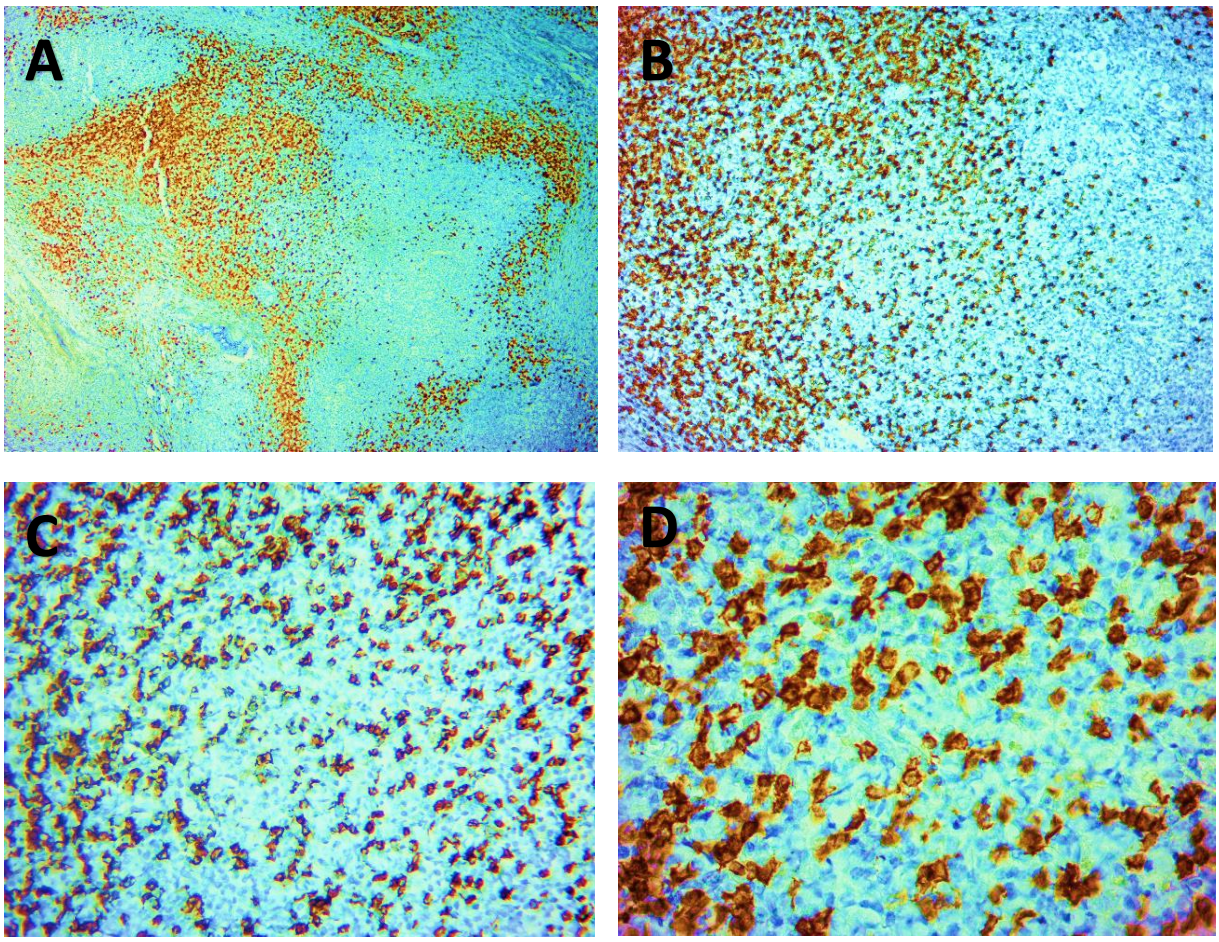

Board. X. Photomicrographs B cells in classical Hodgkin Lymphoma expressing CD20 detected by antibody L26. **(Original photomicrographs. Adjusted with Upscale, Snapseed and Adobe Lightroom).**

Figure **A.B.C.D.** Above shows a tissue section with NScHL expressing CD20 on B cells of the inflammatory background. The staining resulted in brown signals showing the B immunoblasts distribution in the affected tissue. **G4X, G10X, G20X, G40X** respectively**.**

- **CD3**

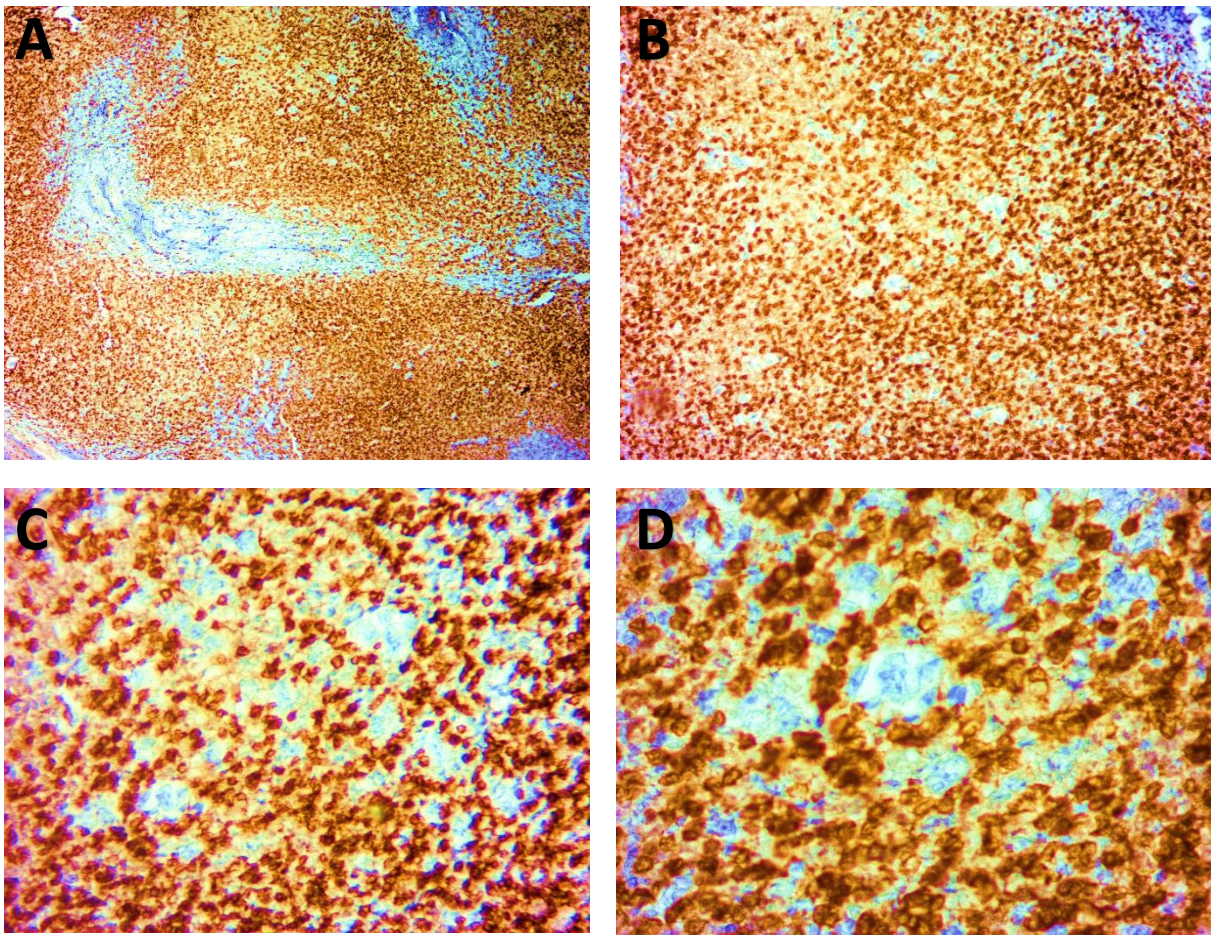

Board. XI. Photomicrographs of T cells in classical Hodgkin Lymphoma expressing CD3 detected by antibody UCHT1. **(Original photomicrographs. Adjusted with Upscale, Snapseed and Adobe Lightroom).**

CD3 immunostaining resulted in brown signals showing the distribution of reactive T cells in the inflammatory background of cHL **(Fig. A, B, G4x, G10x** respectively**),** CD3+ T cells staining appears on the membrane as it is shown in **(Fig. C, D, G20X, G40X)** above, the reviewed slide is from the same tissue section of a patient presenting a NScHL.

III.1.3.5 PAX5

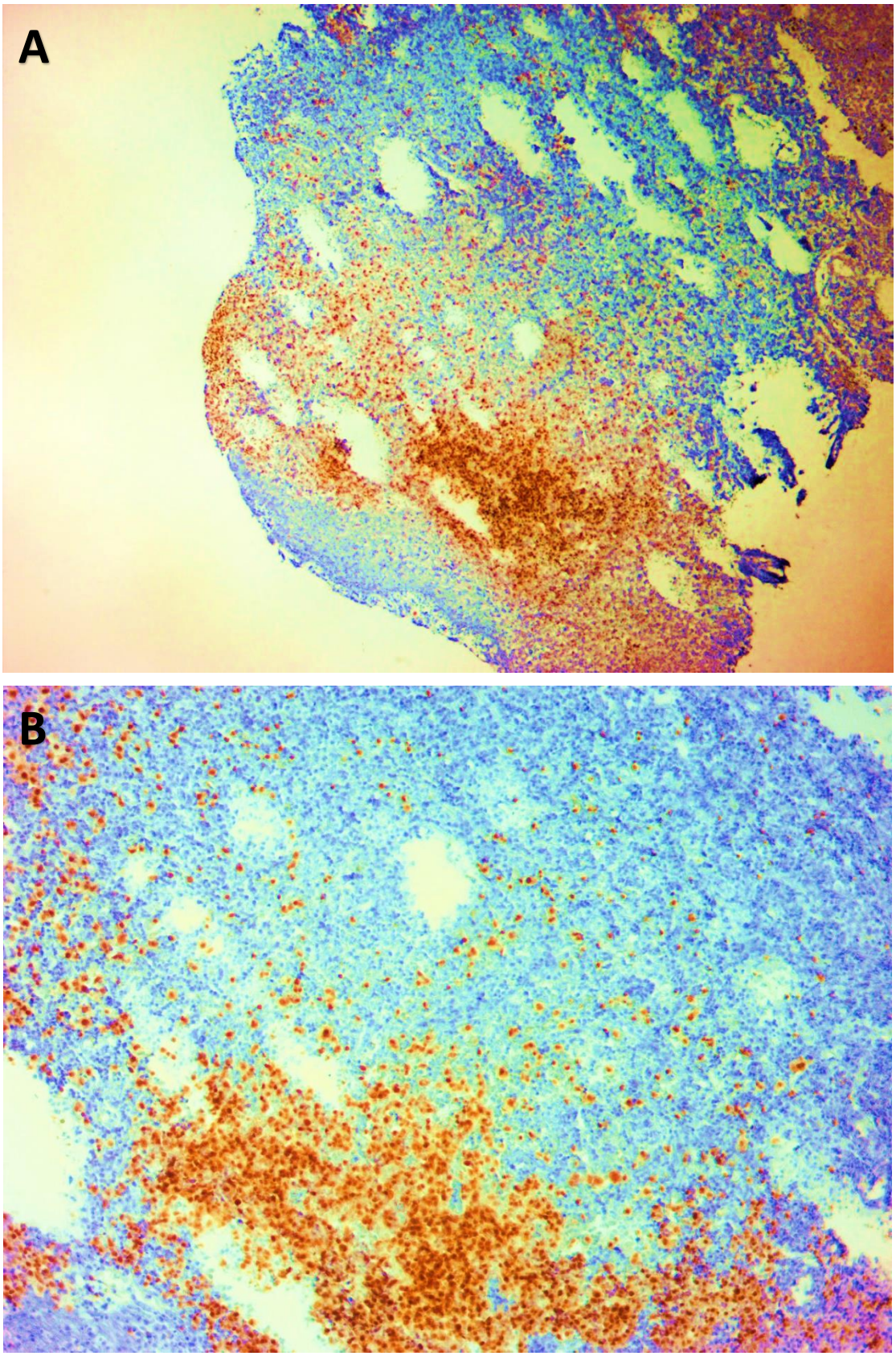

Board. XII. Photomicrographs of HRS cells in classical Hodgkin Lymphoma expressing PAX5 detected by antibody DAK-Pax5. **(Original photomicrographs. Adjusted with Upscale, Snapseed and Adobe Lightroom).**

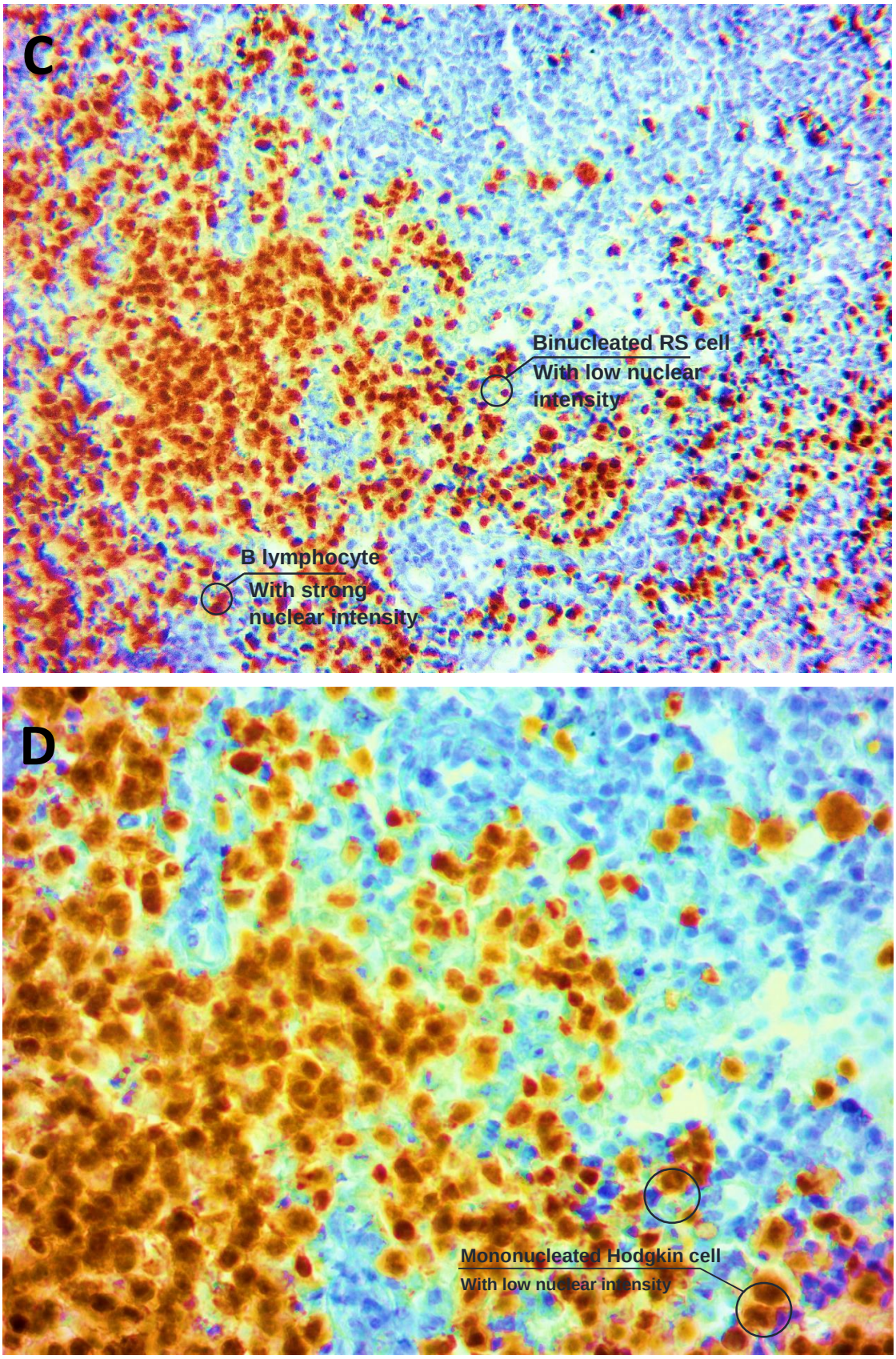

Board. XIII. Photomicrographs of HRS cells in classical Hodgkin Lymphoma expressing PAX5 detected by antibody DAK-Pax5. **(Original photomicrographs. Adjusted with Upscale, Snapseed and Adobe Lightroom).**

Fig. A, B, C, D above show the distribution of PAX5 signal in the affected tissue (**G4X**, **G10X** respectively) with a weak nuclear brown signal **(G20X, G40X** respectively**)** indicating PAX5 expression pattern on HRS and a strong signal on B lymphocytes in the same tissue section of a patient presenting a LRcHL.

III.1.3.6 EBV-LMP1

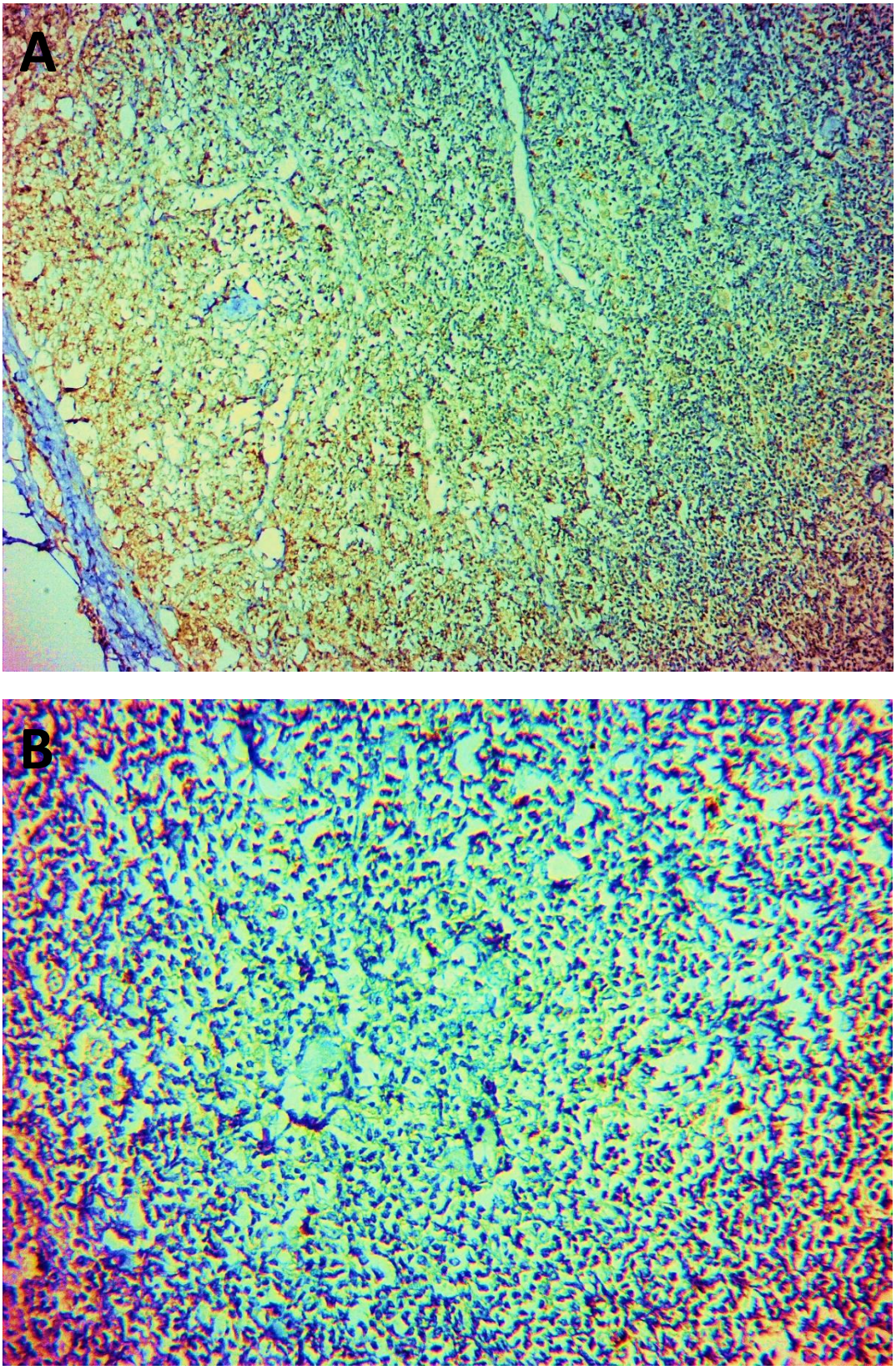

Board. XIV. Photomicrographs of HRS cells in classical Hodgkin Lymphoma expressing LMP1 detected by antibody. CS.1-4 **(Original photomicrographs. Adjusted with Upscale, Snapseed and Adobe Lightroom).**

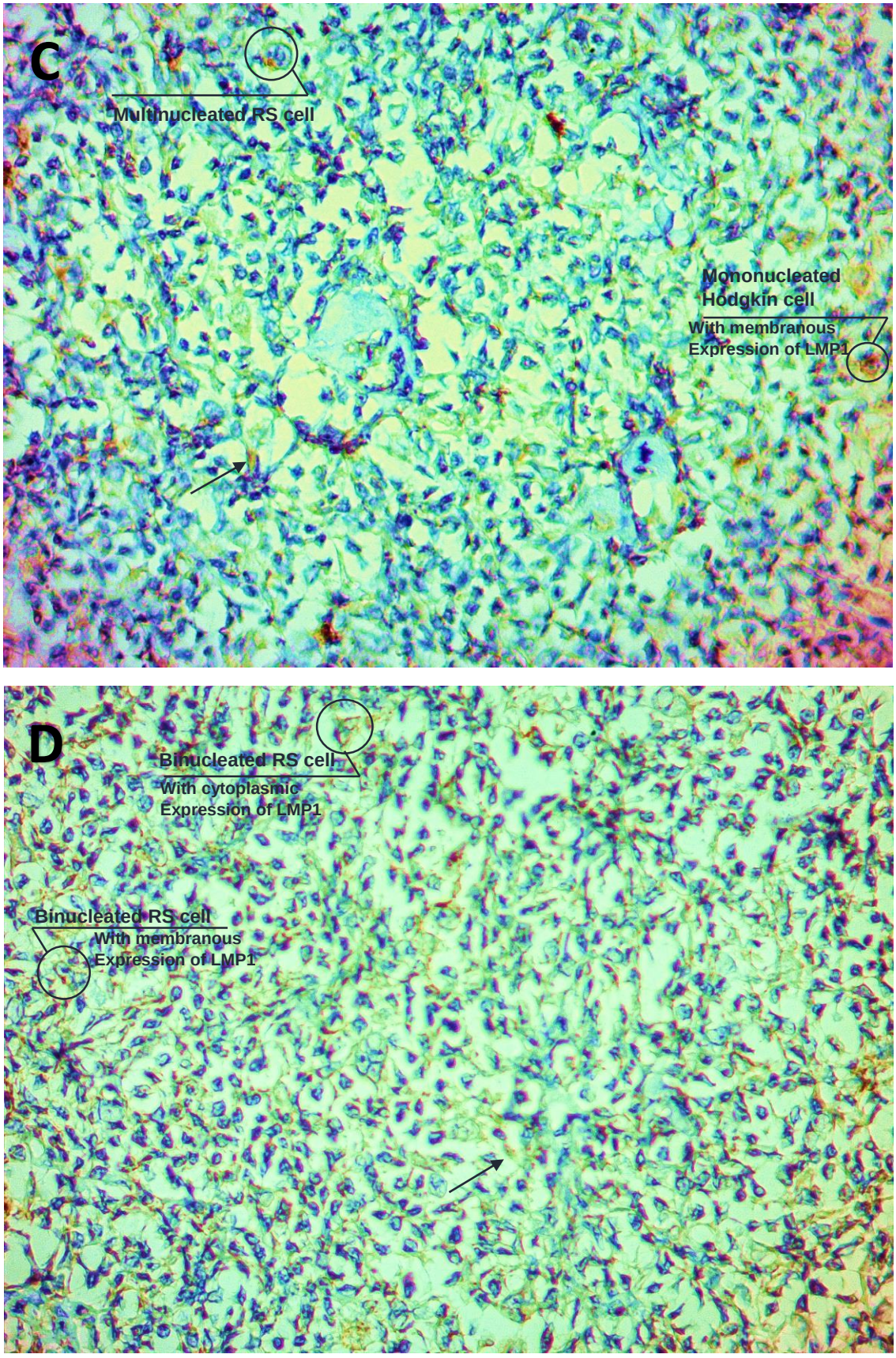

Board. XV. Photomicrographs of HRS cells in classical Hodgkin Lymphoma expressing LMP1 detected by antibody. CS.1-4 **(Original photomicrographs. Adjusted with Upscale, Snapseed and Adobe Lightroom).**

The photomicrographs **A, B, C, D** above are for a patient with a MCcHL. The results of EBV-LMP1 immunostaining showed a positivity for LMP1 expression on HRS cells, the staining pattern appeared in a brown signal (**G4x, G10x** respectively) with variable intensity on the membrane of HRS cells, sometimes in the cytoplasm as indicated in the photomicrographs (**G20X, G40X** respectively). The multinucleated RS cell in a circle (**Fig.C**, **G20X**) showed a light expression of LMP1 on the membrane with a strong intensity in one segment forming a "cap".

A Cytoplasmic pale staining was also observed on nonspecific cells such as fibroblasts (Indicated with dark blue arrows)

III.2 Discussion

III.2.1 cHL clinical markers and the EBV-LMP1 pattern

According to the American Registry of Pathology Expert Opinions, the immunohistochemical examination of classical Hodgkin Lymphoma lays on displaying a group of markers consisting of CD15, CD30, CD20, CD3 and PAX5 to provide a confident diagnosis. Each marker is extant in a series of patients with a precise average of positivity.

Starting with CD15 that has been reported to be positive in 26% to 90% of cHL cases **(O'Malley et *al*., 2019).** In our study, CD15 was positive for the 20 tested patients which means 100% of tested cases were positive for CD15, this result is higher than reported by other authors since our series comprised 21 case, a total with which we cannot fully relate the immunohistochemistry distribution results (the correlation study is confirmed starting from 37 sample and above)

CD30 expression on HRS cells is reported to be positive in 92% to 100% of cHL cases **(O'Malley et *al*.,2019).** Our results can confirm the reported immunoreactivity of this marker with 100% of positive CD30-cases.

The CD20 expression among the 21 patients was positive in all cases but distributed between HRS cells and immunoblasts (B cells). As reported by O'Malley and colleagues, CD20 is expressed on HRS cells with an average between 7% and 44%. In our study CD20 was expressed in HRS cells with an average of 38% (8/21) which therefore confirms the immunoreactivity report of CD20 in cHL. The observed B cells expressing CD20 in 8/21 of cases will be discussed below.

CD3 reactivity in the tumor microenvironment is commonly reported to be seen in all the peripheral backgrounds of cHL cases but rarely expected to be positive in the HRS cells **(O'Malley et *al*.,2019)**, which is the case in our study as it is shown in the distribution results above. However, this T reactivity of the peripheral background has an important contribution in cHL, which is discussed below.

PAX5 should be expressed by HRS cells in up to 95% (80-98) of cHL cases **(O'Malley et *al*.,2019)** which is seen in the 8/21 tested patients for PAX5, 7/8 (86%) were positive for PAX5. This result cannot be correlated since the total of the tested patients for this marker is insufficient to confirm.

The EBV_LMP1 pattern is known to be variably positive with an average between 19% and 36% in a large series of cHL patients **(O'Malley et *al*., 2019)**. However; EBV's positivity depends on many factors such as age, gender, histological subtype, ethnicity and geographical local **(Vrzalikova et *al*., 2018).** In the present study EBV-LMP1was positive in 3/4 of the tested MCcHL (86%) cases and negative in 1/4 tested patient presenting a NScHL, additionally, positive EBV-LMP1 patients were under 10 years old (3and 6 years old) and above 60 years old (61 year). Studies have confirmed that MCcHL is the most histological subtype to be EBV positive; in contrast, NScHL is less associated with EBV infection **(Oviedo et *al*., 2020; Oviedo and Moran, 2016)** which is observed for the EBV-LMP1 tested patients in our study. As mentioned above, age is a related to EBV infection; it has been shown that EBV+ HL patients were frequently under 10 years old and over 60 years old **(Engert and Younes., 2020),** which was also seen in the positive EBV-LMP1 tested patients. Our clinical and immunohistochemical distribution results regardless the average of immunoreactivity within this series can in some way confirm that the age and the histological subtype are major factors for EBV's positivity. Nonetheless, the positivity distribution of 86% in our series vis-à-vis LMP1 immunoreactivity cannot be correlated, as long as the total of the tested patients for EBV-LMP1was too small for affirmation.

III.2.2 CD20 distribution in the cellular environment: Reactive CD20 and CD3 in cHL microenvironment

In our study, there were cases that expressed CD20 on the reactive B cells instead of HRS cells, 7 cases commonly demonstrated a mixture of B and T immunoblasts expressing CD20 and CD3, respectively; giving rise to a mixed inflammatory background. Further report will be added in the histological findings of cHL.

III.2.3 cHL markers

CD15 antigen (a.k.a Lewis X antigen or X-hapten), a trisaccharide, 3-fucosyl-N-acetyllactosamine, which is formed by the 1-3 fucosylation of a type 2 blood group backbone chain (Gal1-4GlcNAc) **(Bhargava, & Kadin., 2011).** With CD30, this molecular marker of 220Kda is known for being a key pattern to recognize HRS cells in order to confirm cHL diagnosis. Its expression on HRS cell membrane with a paranuclear/Golgi accentuation (corresponding to the Golgi region) or cytoplasmic distribution is a strong evidence to confirm diagnosis **(Cozzolino et *al*., 2019).** With the obtained results we could

confirm the expression features of this clinical marker as it is indicated in the histological photomicrographs above.

Often expressed with CD15, CD30 is a cell surface cytokine receptor that is present in cHL malignant cells. **(Pierce et *al*. 2016.)**. Since a membranous strong expression and a Golgi accentuation in HRS cells are quite evidence to affirm cHL diagnosis. **(O'Malley et *al.*2019)**. CD30 immunohistochemical staining is then mandatory in the histopathological study. In our results we confirmed the staining characteristics of CD30 as it is shown above. CD30 was found to essential in several signaling pathways such as MAPK/ERK1/ERK2 and NF-kB canonical pathway to guarantee an anti-apoptotic and pro-survival effect for HRS cells **(van der Weyden et *al*., 2017)**. CD30 is known to be an important therapeutic target for treatment of HL by using monoclonal antibodies that aim to attract immune cells and thus; promote an anti-tumor activity, which thereby makes CD30 examination very helpful to select the adequate therapy. **(Ranuhardy et *al*.2018).**

B-lymphocyte antigen CD20 is a transmembrane glycosylated phosphoprotein of 35 kDa **(Payandeh et *al*.2018**, **Portlock et *al.*2004***)*** that is produced by the MS4A1 gene, is known to be expressed on the surface of mature B-cells. This molecule functions as a regulator of human B-cell growth and differentiation **(Rassidakis et *al*.2002; Santos & Lima.2017).** Its presence in cHL cases somehow confirms that HRS cells descend from germinal-center B cells at the centroblast stage **(Santos & Lima.2017)**.CD20 has a key importance in: suppression of Th1 antitumoral immune responses through IL-10 production; stimulation of non-malignant B lymphocytes through cytokine liberation, which supports HRS cell survival; proliferation of HRS cells by direct stimuli on Hodgkin stem cells **(Santos & Lima.2017)**.With Immunohistochemistry, HRS cells weakly and/or variably express CD20 compared to the surrounding B cells in activate state. **(O'Malley et *al*., 2019).**

The wide expression of the antigens CD20 and CD3 on reactive B and T lymphocytes, respectively; originates from the immunoblastic proliferation which is the result of the affected lymphoid tissue enlargement. The profound expansion of reactive immunoblasts in the interfollicular areas leads to the effacement of the normal architecture by forming a polymorphous infiltrate **(Treetipsatitet *al*., 2014)** which is demonstrated in a subset of cases (38%) of our study. These Reactive lymphocytes in fact are believed to promote the proliferation of HRS cells through cytokines and chemokines behaving as paracrine factors. **(Chetaille et *al.*,2009)**

PAX5 (Paired Box Gene 5); a nuclear transcription factor, where the protein produced is called B-cell Lineage Specific Activator Protein (BSAP), playing a major role in cell differentiation and proliferation, which explains its increased expression throughout B-cell maturation **(Desouki et *al*.2010)**. PAX5 expression is nuclear but less intense in HRS cells than normal B cells **(O'Malley et *al.*2019)**, which we could see in our results. In cHL, Hodgkin and Reed-Sternberg cells usually express BSAP, which therefore; confirms the B-cell origin of HRS cells **(O'Malley et *al.*2019)***;*** As long as HRS cells do not usually display the B-cell antigen CD20, that makes PAX5 an additional marker that helps to diagnose cHL when it lacks CD20 expression **(Jensen et al.2007; Morgan.2014)**. In our results PAX5 was immunostained in patients that already expressed CD20 on HRS cells, we suggest that PAX5 was tested to eliminate the doubt of other mimickers of cHL because a uniform strong expression or a complete lack of PAX5 will raise the possibility of other diagnosis **(O'Malley et *al.*2019)**. Desouki and colleagues **(2010)** found faint PAX-5 nuclear staining in the Hodgkin's and Reed-Sternberg cells in the majority of cHL cases. Similarly to our result, our histological findings showed a nuclear staining in the majority of tested patients for PAX5. PAX5 plays a role in B cells malignancies caused by EBV. When EBV persists and gives rise to a lymphoma, PAX5 has the ability to recruit p300 HAT to support EBNA1-Driven Transcription since they colocalize in the nucleus. **(Liu et *al*.,2020)**

A previous study by Gulley and colleagues **(2002)** reported that EBV-LMP1 examination may aid in developing treatment and finding an exact prognosis for EBV-associated diseases **(Gulley et *al*.2002)**, which makes EBV detection extremely important in cHL. Qi and colleagues **(2012)**, similarly to other authors; found that LMP1 expression on HRS cells is localized on the membrane and in the plasma, which is confirmed in our findings. Latent Membrane protein 1 is a major functional transmembrane molecule that highly contributes to the progression of cHL by inducing several deregulating signaling pathways in HRS cells leading to their immortalization and their continuous proliferation, furthermore; LMP1 provide an advantageous but deleterious microenvironment by communicating directly or indirectly with the extracellular components to guarantee malignant progression whether throughout the tissue or for the HRS cell itself.

IV. Chromogenic *In Situ* Hybridization

IV.1 Results

IV.1.1 Distribution results

The selected patients were diagnosed with different subtypes of cHL (NScHL= 2, MCcHL = 2, LRcHL = 1). Regarding to age range, the age of the selected patients was as following, NScHL: 36, 41; MCcHL: 3,61; LRcHL: 73.

The tested 5 patients for EBERs positivity through CISH technique came with the following results:

In total 3/5 cases were positive for EBERs expression and 2/5 were negative. The positive results were in the patients presenting MCcHL with 2 positive results and a LRcHL with 1 positive result. The two NScHL tested cases for EBERs expression were negative.

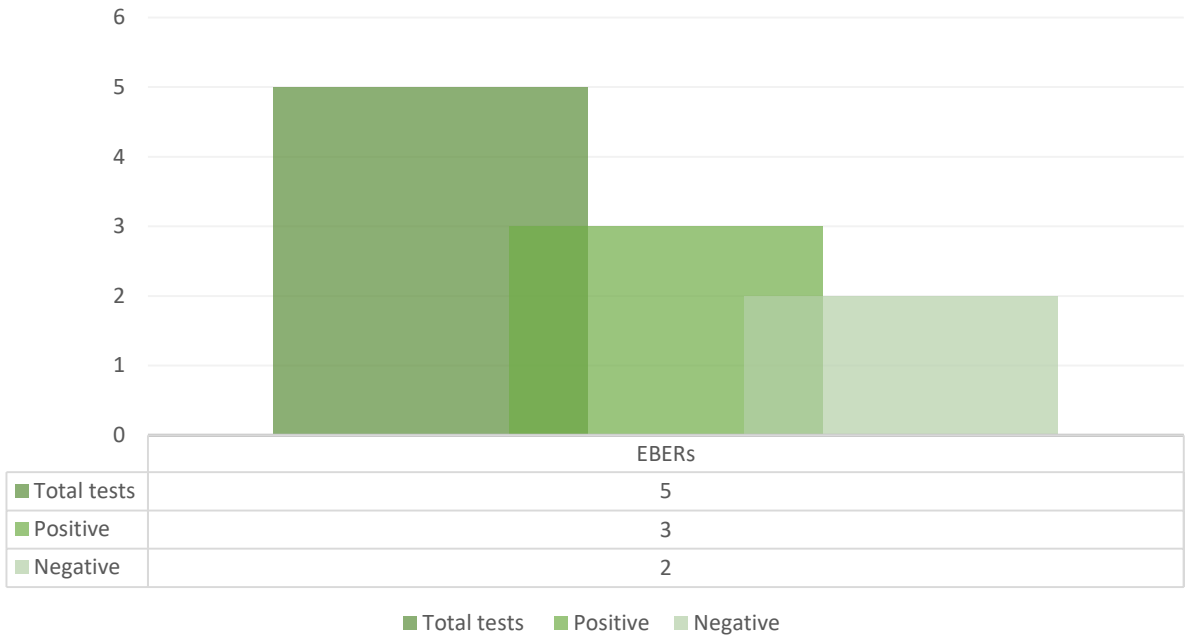

Fig.33. Chromogenic *In Situ* Hybridization results of the selected 5/21 patients for a prospective study.

IV.1.2 Histological findings

The histological findings of our study presented the following results

- **CISH results on a NScHL patient**

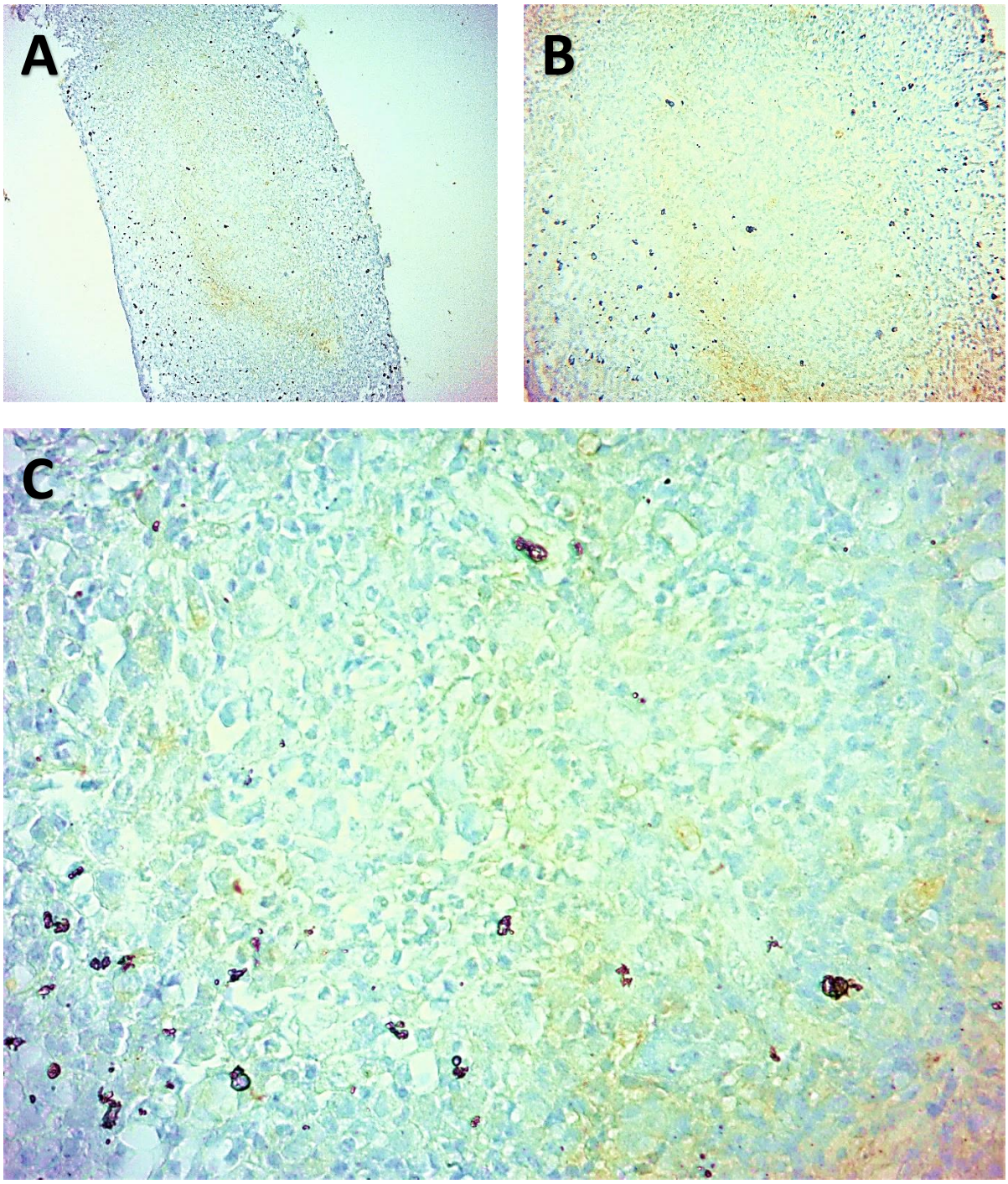

Board. XVI. Photomicrographs of Chromogenic *In Situ* Hybridization histological result of a patient with NScHL. **(A; G4X, B; G10X, C; G20X). (Original photomicrographs. Adjusted with Upscale, Snapseed and Adobe Lightroom).**

- **CISH results on a MCcHL patient**

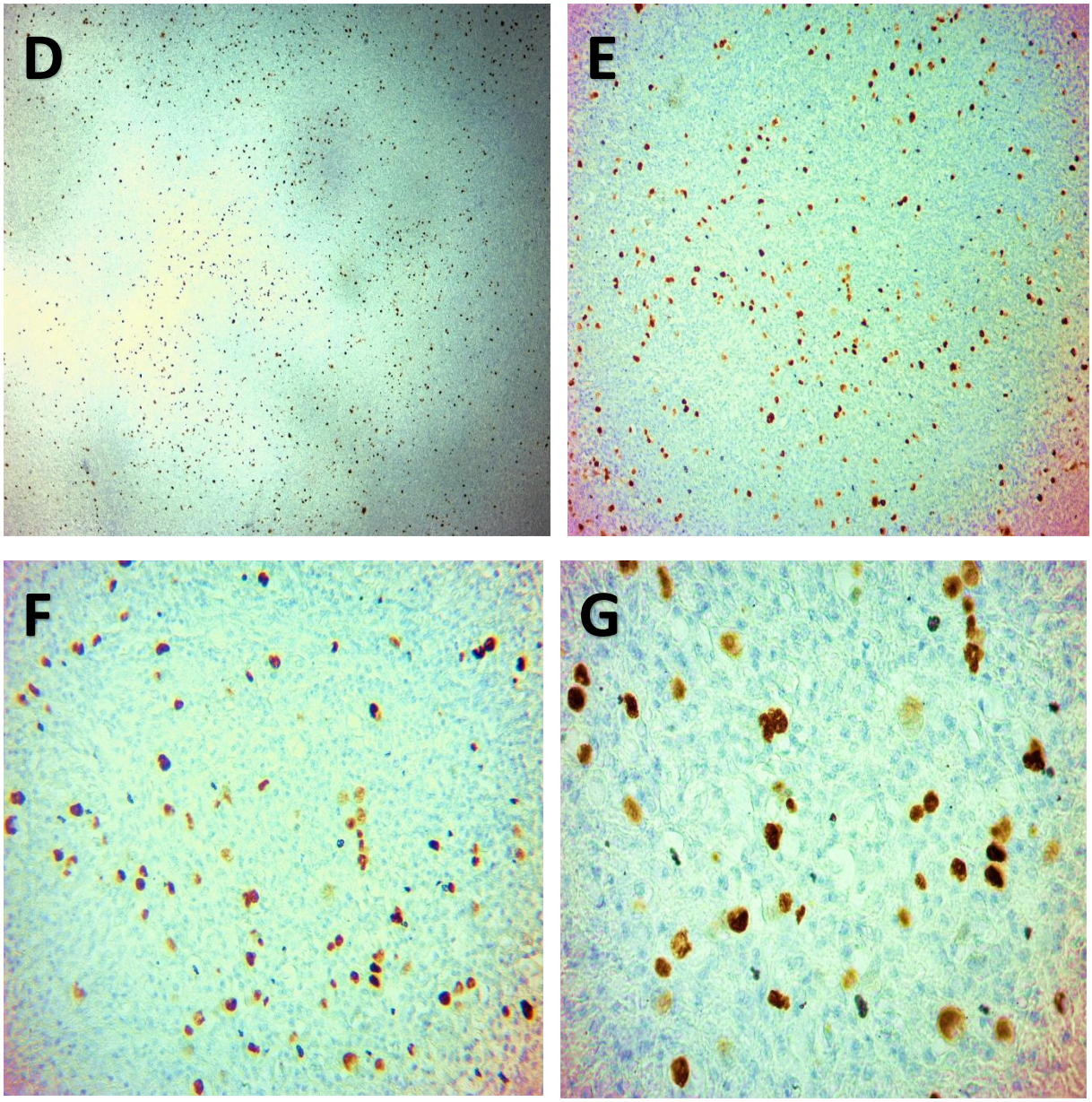

Board. XVII. Photomicrographs of Chromogenic *In Situ* Hybridization histological result of a patient with MCcHL. **(D; G4X, E; G10X, F; G20X, G; G40X). (Original photomicrographs. Adjusted with Upscale, Snapseed and Adobe Lightroom).**

- **CISH results on a LRcHL patient**

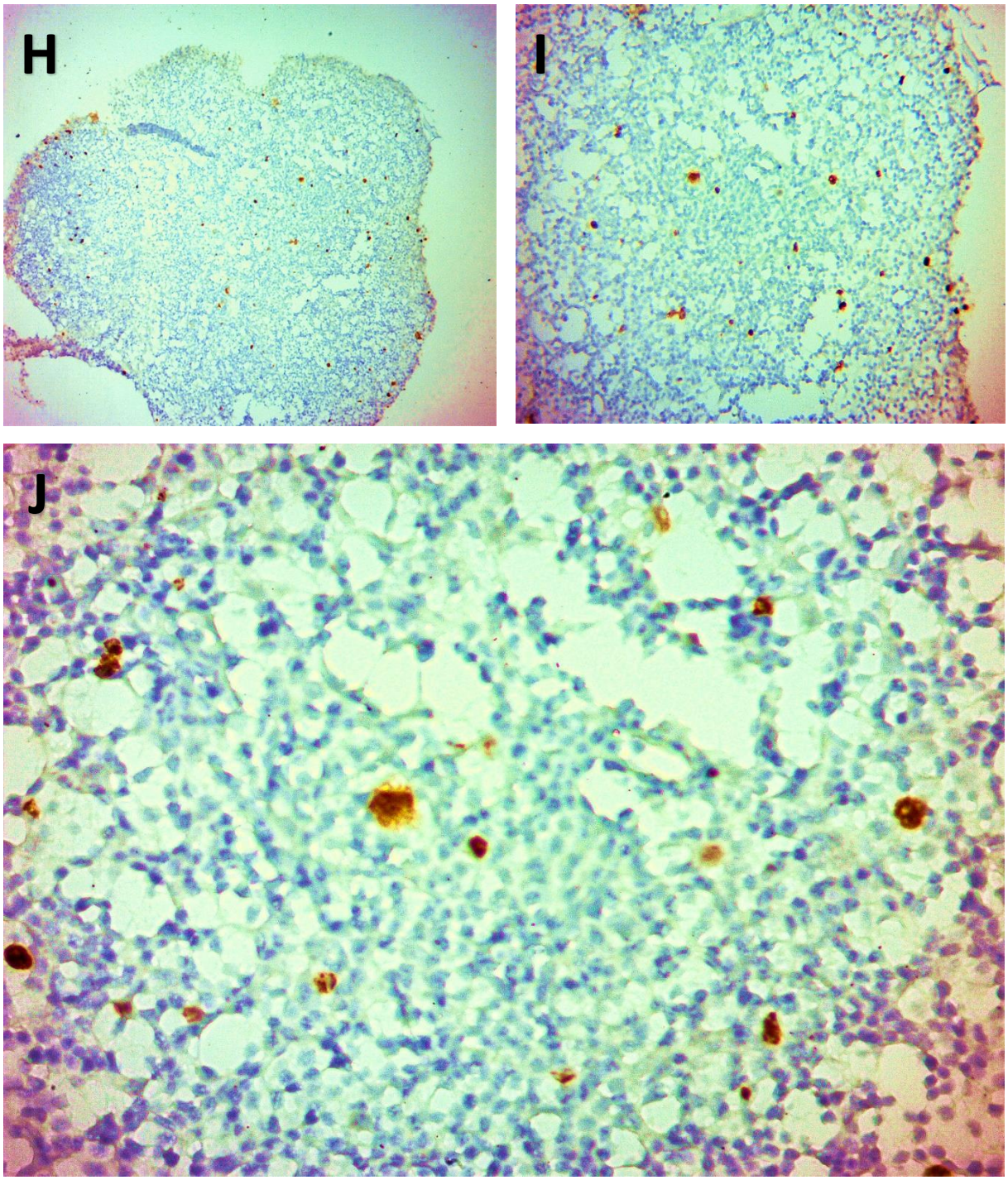

Board. XVIII. Photomicrographs of Chromogenic *In Situ* Hybridization histological result of a patient with LRcHL. **(H; G20X, I; G4X, J; G10X). (Original photomicrographs. Adjusted with Upscale, Snapseed and Adobe Lightroom).**

The first result representing an NScHL didn't show any brown signal giving a negative result for EBERs expression **(Board. XVI.)**, while the second and the third histological findings **(Board. XVII and Board. XVIII)** of patients presenting MCcHL and LRcHL, respectively showed brown signals with variable intensity indicating EBERs distribution in the tissue (**G4X, G10X**). EBERs signal was localized in the nucleus.

VI.2 Discussion

As previously discussed in the immunohistochemical distribution, EBV's positivity depends on several factors, in our results are mostly dependent to age and histological subtype. In the present study, EBERs were positive in 2/5 of the tested MCcHL, the only tested patient with LRcHL was positive for EBERs test. 2/5 cases presenting a NScHL were negative for EBERs expression. Positive EBERs patients were under 10 years old (3 years old) and above 60 years old (61 year and 73 years old). According to Oviedo and colleagues **(2020)** MCcHL is the most histological subtype to be EBV positive with 75% then LRcHL with 50%. In contrast to the other cHL subtypes, NScHL is less associated with EBV infection **(Oviedo and Moran, 2016, Faramarz.,2018)** which is observed for the EBERs tested patients in our study. Regarding to age groups, it has been shown that EBV+ HL patients were frequently under 10 years old and over 60 years old **(Engert and Younes., 2020),** which was also seen in the positive EBERs tested patients. Nevertheless, these quantitative results cannot be correlated due to the few number of tested patients for EBERs.

As reported by Gulley and colleagues **(2002),** EBERs localization is commonly seen in the nucleus with variable intensity, which we could observe in the positive cases. Currently, there is no evidence of EBERs interactions with the cellular components in HRS cells compared to BJAB cells, where EBER1 and EBER2 were considered as functional backup of LMP1 to induce PI3K/Akt signaling pathway **(Herbert & Pimienta 2016).**

CHAPTER IV Bioinformatics analysis

This chapter was based on the analysis of a published data in order to reveal genes and pathways that might be involved in cHL microenvironment. The aim of establishing this independent part of our work is to show how bioinformatics can contribute in giving new perspectives and understandings of the involved processes in a given malignancy.

I. Materials and methods

I.1 Microarray data

The raw data of GSE13996 based on the GPL571 platform contributed by Chetaille et al **(2008)** accessible on Gene Expression Omnibus database was the data of our interest (https://www.ncbi.nlm.nih.gov/geo/query/acc.cgi?acc=GSE13996) for further bioinformatics analysis. The GSE13996 dataset comprises 73 sample with 63 cHL patients presenting the following histological subtypes: Nodular Sclerosis (NS; n = 42), Mixed Cellularity (MC; n = 17), and Lymphocyte Depleted (n = 1). 10 patients where considered as unclassified. EBV status of cHL samples was assigned according to the IHC detection of latent membrane protein-1 (LMP1) and/or *In Situ* hybridization of EBER as negative (n = 35), positive (n = 18), or undetermined due to technical reasons (n = 10). cHL patients were treated with relatively uniform and standard first-line anthracyclin-based chemotherapy regimens and presented a variable outcome as following: Forty-one patients (31 adults and 10 children) had a favorable outcome defined as durable complete remission during a minimum follow-up of 50 months, and 21 adult patients had an unfavorable outcome, characterized by either failure of complete remission, disease progression, or relapse during follow-up **(Chetaille et *al*.,2009)**.

I.2 GEO2R web tool analysis

In the present study, GSE13996 dataset was analyzed with different bioinformatics tools. For GEO2R web tool, 53 samples were selected according to EBV status and divided into 4 groups for DEGs analyzing as following:

- **HL-P**: Hodgkin's Lymphoma--Adult/EBV—Positive.
- **HL-N**: Hodgkin's Lymphoma--Adult/EBV—Negative.
- **HL-CHILD-N**: Hodgkin's Lymphoma--Child/EBV—Negative.
- **HL-CHILD-P**: Hodgkin's Lymphoma--Child/EBV—

Positive. The analysis was performed with the following

options:

- P-values adjustment: Benjamini & Hochberg (False discovery rate)
- Category of Platform annotation: NCBI generated
- Limma, P.adj<0.05

I.2.1 Results and discussion

I. 2.1.1 Visualization of the distribution of selected samples values

The box plot below, generated by R boxplot, allows to visualize the distribution of the values of the selected samples. The x-axis shows the different samples and the y-axis shows the expression value. The black line in each box represents the median of the expression for each sample. The expression medians were similar for all samples.

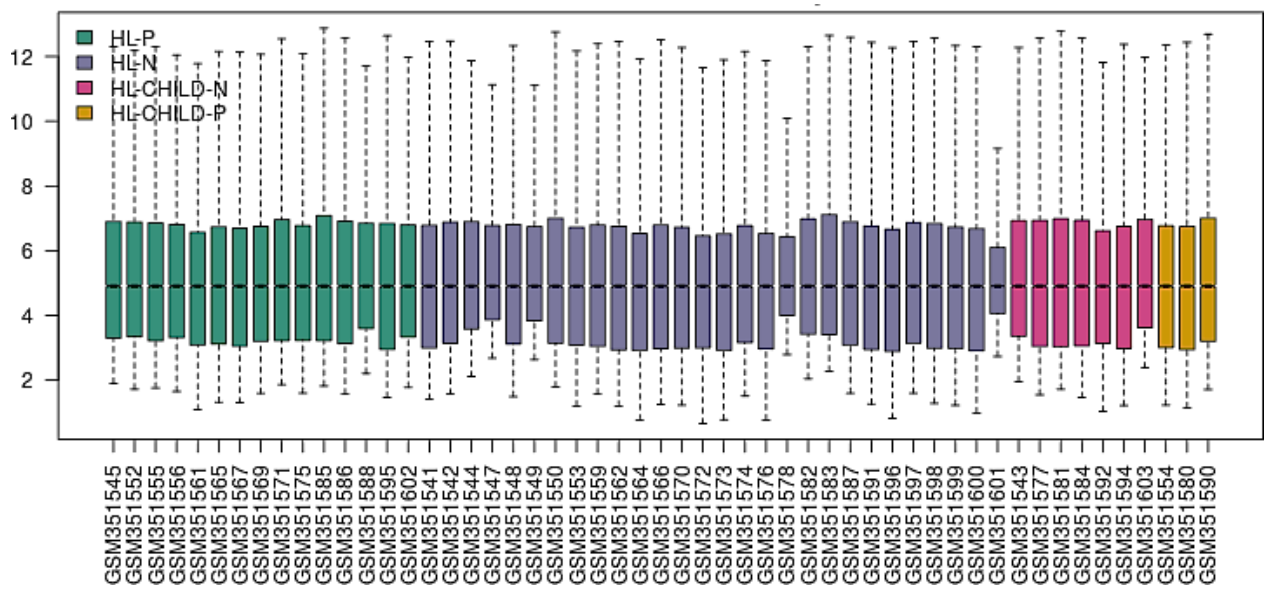

Fig.34.Box plot of samples expression data.

I. 2.1.2 Exploration of the overlap in significant genes between EBV-positive and EBV- negative cHL patients in adults and children

To determine the downregulated and upregulated genes in our series selected GSE13996 and compare them in adults and children patients diagnosed as EBV-positive and EBV-negative classical Hodgkin lymphoma, a Venn diagram generated with limma was obtained. In total, 22163 genes were detected and analyzed, only 114 genes were shown to be differentially expressed in one compared group, which is the **HL-P vs HL-N**

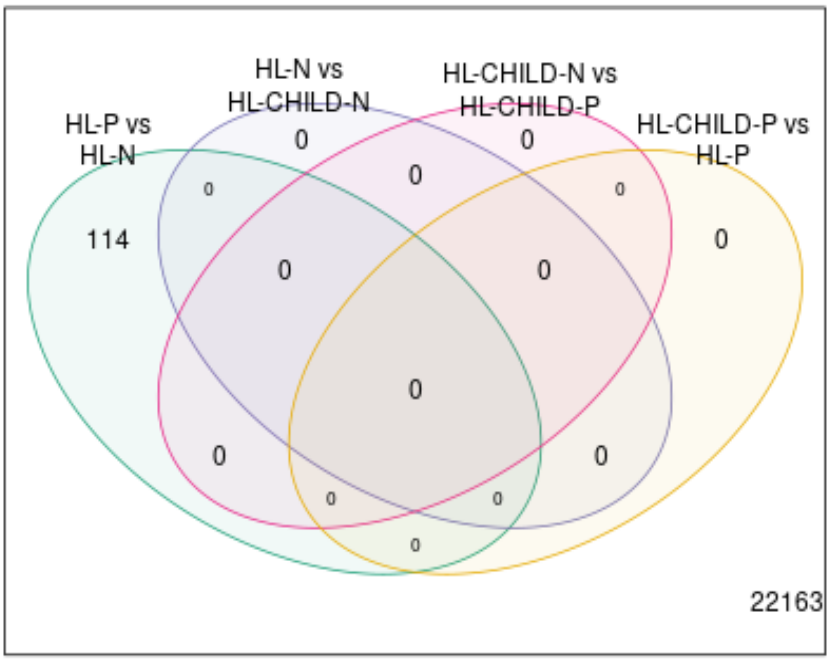

Fig.35. Venn diagram showing the overlap of significant genes within two study groups **HL-P vs HL-N** with 114 DEGs. Padj<0.05

I. 2.1.3 Highlighting of upregulated and downregulated genes in classical Hodgkin lymphoma study groups

The volcano plot generated with limma tool **(Fig.36)** shows the statistical significance (-log10

P. Value) versus magnitude of change (log2 fold change) for visualization of differentially expressed genes in the study groups where HL-P vs HL-N was the group of interest since it's the only group to be presenting DEGs. The highlighted genes are significantly differentially expressed at a default adjusted p-value threshold of 0.05 (red = upregulated, blue = downregulated). The top DEGs of GSE13996 dataset were saved for selection. Our selection of DEGs was basically based on fold changes (log2(fold change)), where 14 genes (7 Up Reg / 7 Down Reg) that are differentially expressed were selected. **(See Appendix IV. Table.04)**

The Top Differentially Expressed Genes were reviewed in the GEO2R web tool to visualize the expression profile graphs of our selected genes.

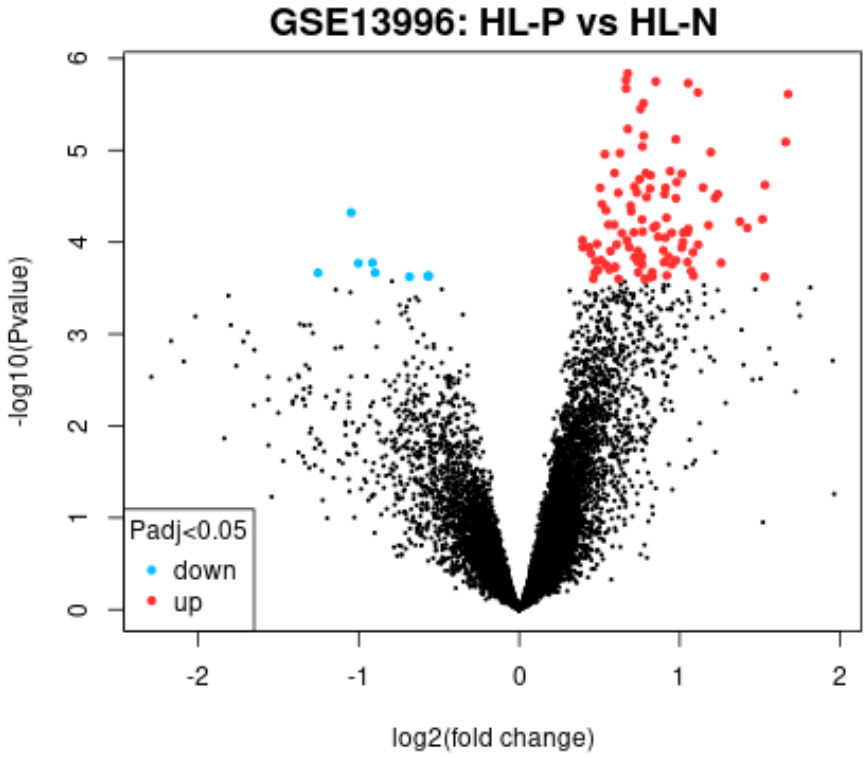

Fig.36. Volcano plot of differentially expressed genes in classical Hodgkin lymphoma. Red dots indicate significantly upregulated genes; blue dots indicate significantly downregulated genes. FC, fold change. GSE13996: molecular profiling of classical Hodgkin's lymphoma tissues HL-NS vs HL-P, Padj<0.05

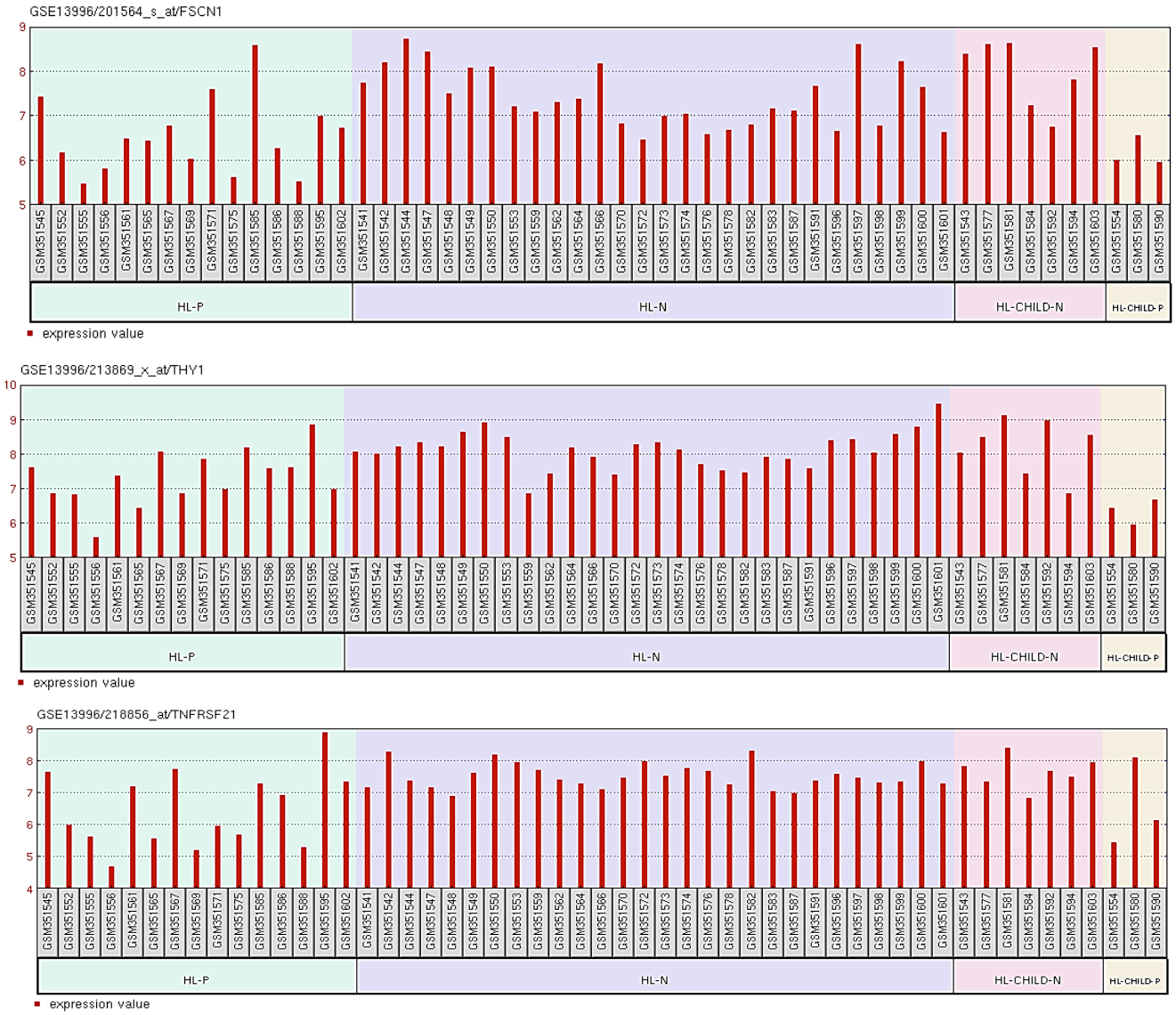

Fig37.expression profile graphs of FASCIN, THY1 and TNFRSF21 genes. Genes with the smallest P-value are the mo st significant. Generated by NCBI GEO2R.

- **Fascin-1**

The actin-bundling protein Fascin (FSCN1) is a tumor marker that is highly expressed in Reed Sternberg cells of classical Hodgkin's lymphoma **(Romana et *al*.,2010).** It is important for migration and metastasis of tumor cells, by which can promote mechanically cancer cell migration and invasion during metastasis dissemination **(Shengchen et *al*.,2020).** According to our findings, FASCN1 gene was among the seven downregulated genes (log2(fold change) = -0.897) in classical Hodgkin lymphoma EBV+ and EBV-, adult and child groups. A study by Mohr et *al* **(2014)** suggested that the EBV- encoded oncoprotein latent membrane protein 1 (LMP1) is sufficient to induce both Fascin mRNA and the Fascin protein in B lymphocytes which is mainly regulated by LMP1 via the C-terminal activation region 2 (CTAR2) depending on NF-κB signaling pathways (canonical and non-canonical NF-κB pathways), which makes canonical NF-κB signaling and Fascin expression contribute to the invasive migration of LMP1-expressing B lymphocytes through the extracellular matrix. Correlated to our result, the smallest P-values shown in the expression profile of FASCIN1 (indicating the upregulation of this gene) represented in EBV+HL patients which may assessed the suggesting that EBV can induce the expression of FASCIN. Subsequently, they found that Hodgkin's lymphoma (HL)-derived cells used in their study were LMP1-negative with high expression of Fascin-1. Despite this; the canonical and non- canonical NF-κB pathways are constitutively activated in HL disease due to genetic damages, auto- and paracrine signalings, and expression of members of the TNF receptor (TNFR) family. On the other hand, constitutive activation of the NF-kB pathway is of advantage for the survival of HL tumor cells which might explain the overexpression of Fascin-1 in the absence of LMP1.In contrast, it cannot be ruled out that FASCIN-1 can be induced by EBV latent proteins without further investigations.

Fascin-1 was discussed as a prognostic marker of cHL based on our results in the profile of expression, in which; FASCIN1 (downregulation) in the samples: GSM351555 and GSM351588 were with favorable outcome compared to samples with the GSM351585, GSM151544, GSM351597, GSM153577, GSM153581, GSM351603 were with unfavorable outcome, we can be in agreement deducing that the overexpression of FASCIN related to an unfavorable outcome. Therefore, we can assess that the understanding of this mechanism will be advantageous for the development of anti-metastasis therapeutics targeting Fascin-1 **(Shengchen et *al*.,2020).**

- **THY1**

Thy-1 membrane glycoprotein known as CD90 is a receptor on endothelial cell (EC), belonging to the Ig superfamily. In humans, its expression is restricted to activated EC, fibroblasts, neuronal cells, and subset of peripheral CD34 stem cells **(Elke et *al*.,2012)**. Thy-1 is an important regulator of cell–cell and cell–matrix interactions in several biological events, including axon regeneration, apoptosis, adhesion, migration, and fibrosis. The anti-CD20 monoclonal antibody (Ab) rituximab has been considered as a standard therapy for being an effective therapeutic Ab for CD20-positive malignant B-cell lymphoma including Hodgkin's lymphoma, but recently some recurrent lymphoma patients; approximately 60% have developed a resistance to rituximab **(Maloney et *al*.,1994)**. For the improvement of therapeutic outcome of antibody medicine finding a way to develop a new therapeutic antibody against B- cell lymphoma; Yoshihito and colleagues **(2010)** assessed the issue of whether anti-Thy1 antibody treatment has cytotoxic effects on B cell lymphoma. First; they analyzed the different glycogens expression in terms of Epstein–Barr virus (EBV) infection of a Burkitt's lymphoma cell line Akata, subsequently in other B-cell lymphoma using a model B cell lines. Consequently, Thy1 was highly expressed in EBV-positive Akata cells and other B-cell lymphoma lines independent to EBV infection. These cells have been treated with an anti-Thy1 monoclonal antibody and therapeutic Ab rituximab; 0subsequently the proliferation inhibitory effect of anti-Thy1 Ab was strongly than that of rituximab. Correlating with our finding the low expression value of Thy1 **(Fig.37)** which reflect the upregulation of this gene in the EBV+ HL patients with an unfavorable outcome may strengthen the suggestion that the inhibition of Thy1 could be an effaces therapeutic way in terms of cell proliferation inhibition for the treatment of EBV+ Hodgkin lymphoma.

- **TNFRSF21**

The expression value of TNFRSF21 was variable in HL-P group compared to HL-N group. However, our results from Limma Volcano plot highlighted TNFRSF21 as a downregulated gene (log2(fold change) = -1.047). According to GO process, this gene negatively regulates B cell proliferation, it is also involved in B cell apoptotic process. Its downregulation within the patients is related to their outcome and their EBV status since patients with favorable outcome showed a favorable expression value of this gene compared to those with EBV+, we suggest that its high expression in the tumor

microenvironment can be related to the malignant progression of cHL and influenced by EBV.

Tumor necrosis factor receptor superfamily member 21 a.k.a Death Receptor 6 (DR6) is known to be highly expressed in lymphoid organs including spleen, thymus, lymph nodes and bone marrow **(Benschop, et *al.*,2009)**. Its high expression in the EBV-positive and EBV-negative groups may support a recent study by Gebauer et al **(2021)** reporting that TNFRSF21/DR6 is implicated in increased cellular division and reduced apoptosis rates in B-cells and T-cell malignancies and EBV-driven type of cancer. Another study by Gewurz and colleagues **(2011)** demonstrated that canonical NF-κB activation is essential for Epstein-Barr Virus Latent Membrane Protein 1 TES2/CTAR2 gene regulation, they showed with gene set enrichment analyses that LMP1 TES2-upregulated genes are significantly enriched for pathways in cancer such as EBV lymphoproliferative diseases, TNFRSF21 was included. This insight enhances our result regarding TNFRSF21 as shown in the expression profile. Benschop, et al **(2009)** suggested that tumor cells may provide an immune evasion mechanism by recruiting MMP-14 to release the extracellular domain of DR6, which is responsible of cell death. According to Uniprot database, TNFRSF21 interacts with TRADD that interacts with LMP1/TES2 to promote an NF-κB signaling. Based on this information we suggest that TNFRSF21 is a secondary key protein to be related to LMP1, thus, to promote malignant progression of HRS cells.

I.3 R programming, KEGG pathways and Phantasus application

R is one of the most widely-used and powerful programming languages in bioinformatics. Our use for this tool was to explore signaling pathways that might be involved in cHL depending on the Differentially Expressed Genes from GSE13996 dataset.

Several packages have been installed for raw microarray data processing, including "BiocManager, GEOquery, annotationDbi, limma, dplyr, pathview and gage". With GEOquery we could call for GSE13996 dataset to R environment. AnnotationDbi was utilized to annotate the Top Differentially Expressed Genes. Pathview and gage are essential to explore the possible signaling pathways in cHL basing on the Top Differentially expressed genes. The R script from GEO2R was introduced to R in order to skip programming of the already obtained results from GEO2R and move forward to pathways analysis. Kyoto Encyclopedia of Genes and Genomes (KEGG) was helpful to view the components of the explored pathways. To view whether the implicated genes of a chosen

pathway were up or down regulated within the samples considering the EBV status, the histological subtype and the outcome, Phantasus application was utilized for a better view and interpretation.

I.3.1 Results and discussion

Programming with R enabled to see a list of signaling pathways that might be involved in cHL microenvironment. **Table.02** below shows the top 20 signaling pathways obtained list from R.

Table.02 Pathway enrichment analysis of DEGs (Top 20 KEGG pathways explored with R)

KEGG ID	Signaling pathway	p.val
hsa00232	Caffeine metabolism	*NA*
hsa00983	Drug metabolism - other enzymes	*NA*
hsa00230	Purine metabolism	*NA*
hsa04514	Cell adhesion molecules (CAMs)	*NA*
hsa04010	MAPK signaling pathway	*NA*
hsa04012	ErbB signaling pathway	*NA*
hsa04062	Chemokine signaling pathway	*NA*
hsa04150	mTOR signaling pathway	*NA*
hsa04210	Apoptosis	*NA*
hsa04370	VEGF signaling pathway	*NA*
hsa04380	Osteoclast differentiation	*NA*
hsa04510	Focal adhesion	*NA*
hsa04530	Tight junction	*NA*
hsa04620	Toll-like receptor signaling pathway	*NA*
hsa04630	Jak-STAT signaling pathway	*NA*
hsa04660	T cell receptor signaling pathway	*NA*
hsa04662	B cell receptor signaling pathway	*NA*
hsa04664	Fc epsilon RI signaling pathway	*NA*
hsa04666	Fc gamma R-mediated phagocytosis	*NA*
hsa04722	Neurotrophin signaling pathway	*NA*

From the obtained signaling pathways, chemokines signaling pathway can be discussed as an example. Chemokines are cytokines with chemoattractant properties, these molecules play an important role in recruitment of different subsets of cells and, therefore, in formation and maintenance of the specific background present in HL. CXCL-10 is an important component in chemokine signaling pathway by promoting CCL20 production in order to attract Treg cells ***(*Baumforth et *al.*,2008*)***. Studies showed that IP-10 (CXCL-10) is highly expressed in EBV positive HL, which is what we observed in the heat map bellow within the patients with unfavorable outcome. Conversely to CCL20; unexpectedly was downregulated within cHL patients with an EBV infection. This may raise the question, why is CCL20 downregulated as long as the outcome is not favorable. These elements in EBV positive cHL patients might be investigated in the future .

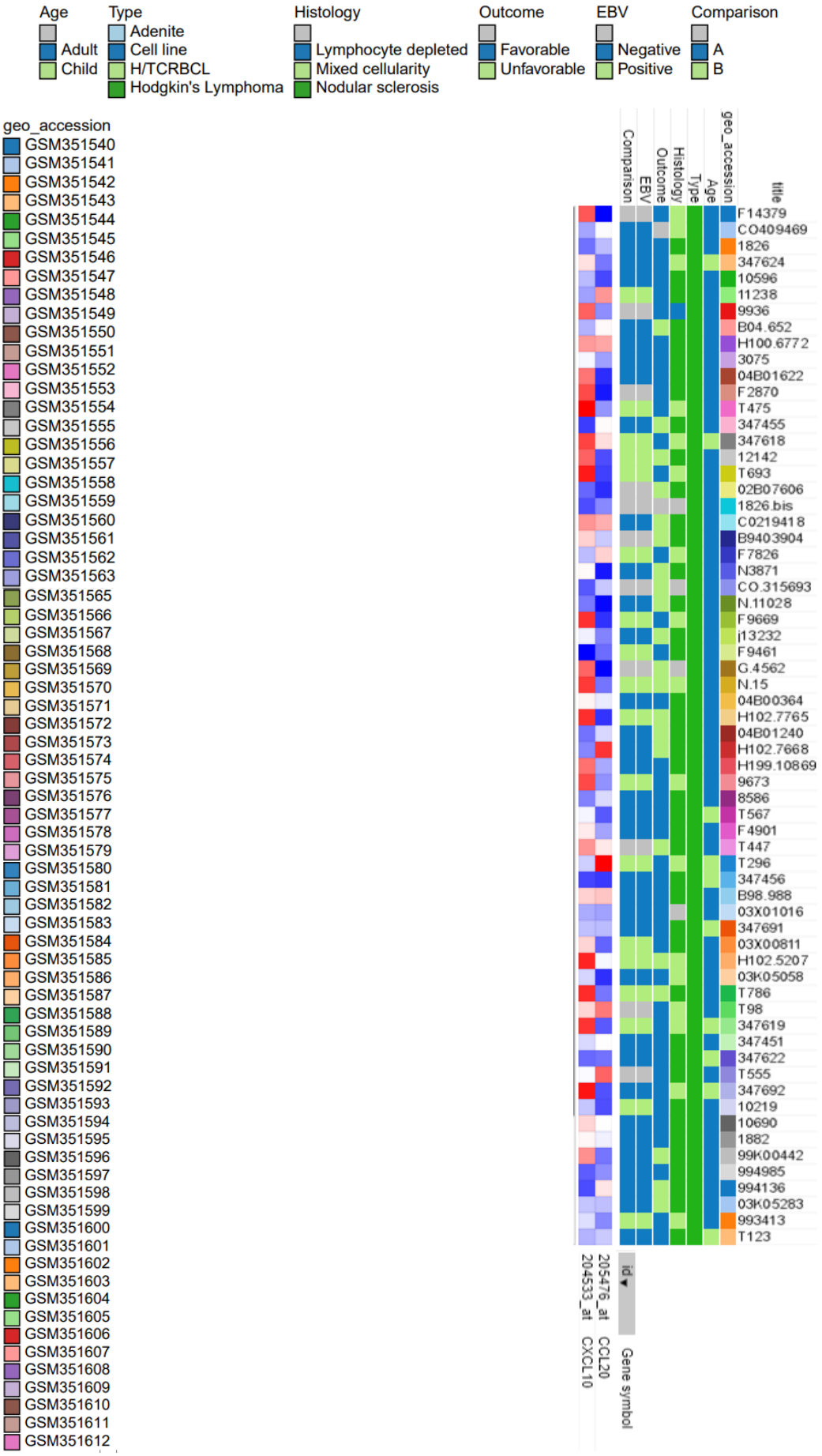

Fig.38 Gene map from Phantasus application with the selected genes of interest.

Conclusion

V. Conclusion

Hodgkin Lymphoma has been a challenge, not least because of the presence of a minority of malignant cells in the tumor. Other challenges still facing pathologists in cHL diagnosis.

The link between EBV and cHL has been uncovered for decades, but still lot of unclear points posing questions. For example, what makes MCcHL the most related subtype to EBV infection? and conversely for NScHL.

EBV encoded latent genes greatly affect cell physiology and promote several deleterious mechanisms within the host cell to go to the extracellular environment and start commanding for further progression and immune evasion.

Revealing the implicated genes and signaling pathways brought us to the conclusion of that EBV genes are enable to exhibit an amount of cross-talk between two compartments and form a network. This highlighting may provide new paths and targets for prevention and treatment of EBV related lymphomas.

References

- *Ahmed HG, Adam TM, Basama NK, Agabeldor AA (2011). Utility of CD3 and CD30 in immunophenotyping of lymphomas among Sudanese patients. J Cancer Sci Ther, 3, 116-9.*
- *Ahmed, W., Tariq, S., & Khan, G. (2018). Tracking EBV-encoded RNAs (EBERs) from the nucleus to the excreted exosomes of B-lymphocytes. Scientific reports, 8(1), 15438. https://doi.org/10.1038/s41598-018-33758-4*
- *Ali S, Olszewski AJ.,2014 jul. Disparate survival and risk of secondary non-Hodgkin lymphoma in histologic subtypes of Hodgkin lymphoma: a population-based study. Leuk Lymphoma. Pp:55,1570–7. Doi: 10.3109/10428194.2013.847938. Epub 2013 Nov 12.*
- *Anders Rehfeld,Malin Nylander , Kirstine Karnov., 2017.Compendium of Histology ; Faculty of Health and Medical Sciences , University of Copenhagen ,Copenhagen Denmark.Pp:396-399. DOI 10.1007/978-3-319-41873-5.*
- *Annarosa Cuccaro, Francesca Bartolomei, Elisa Cupelli, Eugenio Galli, Manuela Giachelia, and Stefan Hohaus. Prognostic Factors in Hodgkin Lymphoma ,2014; 6(1): e2014053doi: 10.4084/MJHID.2014.053*
- *Aravinth, S. P., Rajendran, S., Li, Y., Wu, M., Yi Wong, A. H., & Schwarz, H. (2019). Epstein-Barr virus-encoded LMP1 induces ectopic CD137 expression on Hodgkin and Reed-Sternberg cells via the PI3K-AKT-mTOR pathway. Leukemia & lymphoma, 60(11), 2697–2704. https://doi.org/10.1080/10428194.2019.1607330*
- *Arcipowski, K. M., Stunz, L. L., Graham, J. P., Kraus, Z. J., Vanden Bush, T. J., & Bishop, G. A. (2011). Molecular mechanisms of TNFR-associated factor 6 (TRAF6) utilization by the oncogenic viral mimic of CD40, latent membrane protein 1 (LMP1). [Research Support, N.I.H., Extramural Research Support, Non-U.S. Gov't]. J Biol Chem, 286(12), 9948-9955. doi: 10.1074/jbc.M110.185983*
- *Ashley Rose, Ariel Grajales-Cruz, Alex Lim, Amber Todd, Celeste Bello, Bijal Shah, Julio Chavez, Javier Pinilla-Ibartz, Hayder Saeed,Jose Sandoval-Sus, Leidy Isenalumhe, Lubomir Sokol .Classical Hodgkin Lymphoma: Clinicopathologic Features, Prognostic Factors, and Outcomes from a 28-Year Single Institutional Experience ; Department of Internal Medicine, College of Medicine, University of South Florida, Tampa, FL Department of Malignant Hematology, H. Lee Moffitt Cancer Center and Research Institute, Tampa, FL, 2152-2650, 2020 .https://doi.org/10.1016/j.clml.2020.08.018*
- *Benschop, R., Wei, T., & Na, S. (2009). Tumor necrosis factor receptor superfamily member 21: TNFR-related death receptor-6, DR6. Advances in experimental medicine and biology, 647, 186. https://doi.org/10.1007/978-0-387-89520-8_13*
- *Bentz, G. L., Shackelford, J., & Pagano, J. S. (2012). Epstein-Barr virus latent membrane protein 1 regulates the function of interferon regulatory factor 7 by inducing its sumoylation. Journal of virology, 86(22), 12251–12261. https://doi.org/10.1128/JVI.01407-12*

References

- *Bhargava, P., & Kadin, M. E. (2011). Chapter 5 - Immunohistology of Hodgkin Lymphoma Immunohistology of Hodgkin Lymphoma. Diagnostic Immunohistochemistry, (Third Edition), Editor(s): David J. Dabbs 137–155. doi:10.1016/b978-1-4160-5766-6.00009-1*
- *Bhattacharjee, S., Ghosh Roy, S., Bose, P., & Saha, A. (2016). Role of EBNA-3 Family Proteins in EBV Associated B-cell Lymphomagenesis. [Review]. Front Microbiol, 7, 457. doi: 10.3389/fmicb.2016.00457*
- *Bohle V, Doring C, Hansmann ML, Kuppers R.,2013. Role of early B-cell factor 1 (EBF1) in*
- *Cader, F. Z., Vockerodt, M., Bose, S., Nagy, E., Brundler, M. A., Kearns, P., & Murray, P. G. (2013). The EBV oncogene LMP1 protects lymphoma cells from cell death through the collagen-mediated activation of DDR1. Blood, 122(26), 4237–4245. https://doi.org/10.1182/blood-2013-04-499004*
- *Cairong Zhu, Bryan A. Bassig, Kunchong Shi, Peter Boyle, Huan Guo, and Tongzhang Zheng.Different time trends by gender for the incidence of Hodgkin's lymphoma among young adults in the USA: a birth cohort phenomenon. 2014 Aug; 25(8): 923–931. doi: 10.1007/s10552-014-0391-5*
- *Carbone A, Gloghini.,2016. Atlas genetics cytogenetics oncology haematology. http://documents.irevues.inist.fr/handle/2042/62470*
- *Chang ET, Frøslev T, Sørensen HT, Pedersen.,2011. A nationwide study of aspirin, other non-steroidal anti-inflammatory drugs, and Hodgkin lymphoma risk in Denmark. Br J Cancer 105(11):1776–1782. doi: 10.1038/bjc.2011.443*
- *Chetaille B, Bertucci F, Finetti P, Esterni B, Stamatoullas A, Picquenot JM, Copin MC, Morschhauser F, Casasnovas O, Petrella T, Molina T, Vekhoff A, Feugier P, Bouabdallah R, Birnbaum D, Olive D, Xerri L. Molecular profiling of classical Hodgkin lymphoma tissues uncovers variations in the tumor microenvironment and correlations with EBV infection and outcome. Blood. 2009 Mar 19;113(12):2765-3775. doi: 10.1182/blood-2008-07-168096. Epub 2008 Dec 18. PMID: 19096012.*
- *Chetaille, B., Bertucci, F., Finetti, P., Esterni, B., Stamatoullas, A., Picquenot, J. M., Copin, M. C., Morschhauser, F., Casasnovas, O., Petrella, T., Molina, T., Vekhoff, A., Feugier, P., Bouabdallah, R., Birnbaum, D., Olive, D., & Xerri, L. (2009). Molecular profiling of classical Hodgkin lymphoma tissues uncovers variations in the tumor microenvironment and correlations with EBV infection and outcome. Blood, 113(12), 2765–3775. https://doi.org/10.1182/blood-2008-07-168096*
- *Chiu, Y. F., Sugden, A. U., & Sugden, B. (2013). Epstein-Barr viral productive amplification reprograms nuclear architecture, DNA replication, and histone deposition. Cell host & microbe, 14(6), 607–618. https://doi.org/10.1016/j.chom.2013.11.009*
- *Cozzolino, I., Vitagliano, G., Caputo, A., Montella, M., Franco, R., Ciancia, G., Selleri, C., & Zeppa, P. (2020). CD15, CD30, and PAX5 evaluation in Hodgkin's lymphoma on fine-needle aspiration cytology samples. Diagnostic cytopathology, 48(3), 211–216. https://doi.org/10.1002/dc.24366*
- *D. Maloney, T. Liles, D. Czerwinski, C. Waldichuk, J. Rosenberg, A. Grillo-Lopez, R. Levy, Phase I clinical trial using escalating single-dose infusion of chimeric anti-CD20*

monoclonal antibody (IDEC-C2B8) in patients with recurrent B-cell lymphoma, Blood 84 (1994) 2457–2466.

- *de Oliveira, K. A., Kaergel, E., Heinig, M., Fontaine, J. F., Patone, G., Muro, E. M., Mathas, S., Hummel, M., Andrade-Navarro, M. A., Hübner, N., & Scheidereit, C. (2016). A roadmap of constitutive NF-κB activity in Hodgkin lymphoma: Dominant roles of p50 and p52 revealed by genome-wide analyses. Genome medicine, 8(1), 28. https://doi.org/10.1186/s13073-016-0280-5*
- *De Re, V., Caggiari, L., De Zorzi, M., Fanotto, V., Miolo, G., Puglisi, F., . . . Mascarin, M. (2020). Epstein-Barr virus BART microRNAs in EBV- associated Hodgkin lymphoma and gastric cancer. [Review]. Infect Agent Cancer, 15, 42. doi: 10.1186/s13027-020-00307-6*
- *Desouki, M. M., Post, G. R., Cherry, D., & Lazarchick, J. (2010). PAX-5: a valuable immunohistochemical marker in the differential diagnosis of lymphoid neoplasms. Clinical medicine & research, 8(2), 85–87. https://doi.org/10.3121/cmr.2010.891*
- *Division of Pathology & Data Analytics.,2013,2013,2014. Classical Hodgkin lymphoma-Nodular sclerosis type, virtual pathology; Leeds Institute of Medical Research, University of Leeds.https://www.virtualpathology.leeds.ac.uk/*
- *doi:10.1016/j.bbrc.2010.04.092*
- *doi: 10.1016/j.canrad.2011.09.001*
- *DOI: https://doi.org/10.4049/jimmunol.1003944*
- *Dolcetti R. (2015). Cross-talk between Epstein-Barr virus and microenvironment in the pathogenesis of lymphomas. Seminars in cancer biology, 34, 58–69. https://doi.org/10.1016/j.semcancer.2015.04.006*
- *Elke Wandel, Anja Saalbach, Doreen Sittig, Carl Gebhardt and Gabriela Aust. Thy-1 (CD90) Is an Interacting Partner for CD97 on Activated Endothelial Cells.February 1, 2012, 188 (3) 1442-1450*
- *Ellen T Chang , Tongzhang Zheng, Edward G Weir, Michael Borowitz, Risa B Mann, Donna Spiegelman, Nancy E Mueller.,2004. Aspirin and the risk of Hodgkin's lymphoma in a population-based case-control study. J Natl Cancer Institute 96(4):305–315. DOI: 10.1093/jnci/djh038*
- *Emily M Bowen , Ruth M Pfeiffer , Martha S Linet , Wayne T Liu , Dennis D Weisenburger , D Michal Freedman, Elizabeth K Cahoon .,2016. Relationship between ambient ultraviolet radiation and Hodgkin lymphoma subtypes in the United States. Br J Cancer 114(7):826–831. DOI: 10.1038/bjc.2015.383*
- *Engels EA, Hildesheim.,2018. Immunologic factors. In: Schottenfeld and Fraumeni cancer epidemiology and prevention. Oxford University Press, Oxford. DOI:10.1093/acprof:oso/9780195149616.003.0027*
- *Engert, A. Younes (eds.)., 2020.Hodgkin Lymphoma, Hematologic Malignancies, Department of Internal Medicine: Lymphoma Service, university Hospital: Cologne Memorial Sloan Kettering Cancer , Köln, Nordrhein-Westfalen Germany Center NY, USA , 3th edition , pp.3-52. https://doi.org/10.1007/978-3-030-32482-7_1*

References

- *Faramarz Naeim, P. Nagesh Rao, Sophie X. Song, Ryan T. Phan, Chapter 56 - Nodular Lymphocyte Predominant Hodgkin Lymphoma, Editor(s): Faramarz Naeim, P. Nagesh Rao, Sophie X. Song, Ryan T. Phan, Atlas of Hematopathology (Second Edition), Academic Press, 2018, Pages 784-785,ISBN 9780128098431, https://doi.org/10.1016/B978-0-12-809843-1.00056-5.*
- *Ferlay J, Ervik M, Lam F, Colombet M, Mery L, Piñeros M, Znaor A, Soerjomataram I, Bray F.,2018. Global Cancer Observatory: Cancer Today. Lyon, France: International Agency for Research on Cancer. Available from: https://gco.iarc.fr/today, accessed [25 March 2019].*
- *Gewurz, B. E., Mar, J. C., Padi, M., Zhao, B., Shinners, N. P., Takasaki, K., Bedoya, E., Zou, J. Y., Cahir-McFarland, E., Quackenbush, J., & Kieff, E. (2011). Canonical NF-kappaB activation is essential for Epstein-Barr virus latent membrane protein 1 TES2/CTAR2 gene regulation. Journal of virology, 85(13), 6764–6769. https://doi.org/10.1128/JVI.00422-11*
- *Gomez-Gelvez JC, Smith LB.,2015. Reed-Sternberg-like cells in non-Hodgkin lymphomas. Arch Pathol Lab Med. Pp 139:1205–10. DOI: 10.5858/arpa.2015-0197-RAI*
- *Gravelle, P., Burroni, B., Péricart, S., Rossi, C., Bezombes, C., Tosolini, M., Damotte, D., Brousset, P., Fournié, J. J., & Laurent, C. (2017). Mechanisms of PD-1/PD-L1 expression and prognostic relevance in non-Hodgkin lymphoma: a summary of immunohistochemical studies. Oncotarget, 8(27), 44960–44975. https://doi.org/10.18632/oncotarget.16680*
- *Green, M. R., Rodig, S., Juszczynski, P., Ouyang, J., Sinha, P., O'Donnell, E., Neuberg, D., & Shipp, M. A. (2012). Constitutive AP-1 activity and EBV infection induce PD-L1 in Hodgkin lymphomas and posttransplant lymphoproliferative disorders: implications for targeted therapy. Clinical cancer research : an official journal of the American Association for Cancer Research, 18(6), 1611–1618. https://doi.org/10.1158/1078-0432.CCR-11-1942*
- *Gulley, M. L., Glaser, S. L., Craig, F. E., Borowitz, M., Mann, R. B., Shema, S. J., & Ambinder, R. F. (2002). Guidelines for interpreting EBER in situ hybridization and LMP1 immunohistochemical tests for detecting Epstein-Barr virus in Hodgkin lymphoma. American journal of clinical pathology, 117(2), 259–267. https://doi.org/10.1309/MMAU-0QYH-7BHA-W8C2*
- *Herbert, K. M., & Pimienta, G. (2016). Consideration of Epstein-Barr Virus-Encoded Noncoding RNAs EBER1 and EBER2 as a Functional Backup of Viral Oncoprotein Latent Membrane Protein 1. [Research Support, Non-U.S. Gov't]. mBio, 7(1), e01926-01915. doi: 10.1128/mBio.01926-15*
- *Ho, W. T., Pang, W. L., Chong, S. M., Castella, A., Al-Salam, S., Tan, T. E., Moh, M. C., Koh, L. K., Gan, S. U., Cheng, C. K., & Schwarz, H. (2013). Expression of CD137 on Hodgkin and Reed-Sternberg cells inhibits T-cell activation by eliminating CD137 ligand expression. Cancer research, 73(2), 652–661. https://doi.org/10.1158/0008-5472.CAN-12-3849*

- *Hodgkin lymphoma. Leukemia 27(3):671–679 Edition- publication 2012/11/24. Doi: 10.1038/leu.2012.280. Epub 2012 Oct 1.*
- *Hodgkin Lymphoma: Variant Patterns, Borderlines and Mimics; Department of Pathology, Stanford University School of Medicine, Stanford, 13, 2021. https://doi.org/10.3390/cancers13123021*
- *Isola J., Tanner M.,2004.Chromogenic in situ hybridization in tumor pathology. In: Roulston JE, Bartlett JMS (eds) Molecular diagnosis of cancer. Methods in Molecular Medicine, vol 97. Humana Press. https://doi.org/10.1385/1-59259-760-2:133*
- *Iwakiri, D. (2014). Epstein-Barr Virus-Encoded RNAs: Key Molecules in Viral Pathogenesis. [Review]. Cancers (Basel), 6(3), 1615-1630. doi: 10.3390/cancers6031615*
- *J.-F. Morère, F. Mornex, D. Soulières. Cancer Therapeutics. Paris, Springer-Verlag France .1020 pp (793-794) (2011), ISBN: 9782817800202.*
- *Jensen, K. C., Higgins, J. P., Montgomery, K., Kaygusuz, G., van de Rijn, M., & Natkunam, Y. (2007). The utility of PAX5 immunohistochemistry in the diagnosis of undifferentiated malignant neoplasms. Modern pathology: an official journal of the United States and Canadian Academy of Pathology, Inc, 20(8), 871–877. https://doi.org/10.1038/modpathol.3800831*
- *Kang, M. S., & Kieff, E. (2015). Epstein-Barr virus latent genes. [Research Support, Non-U.S. Gov't Review]. Exp Mol Med, 47, e131. doi: 10.1038/emm.2014.84*
- *Kaseb H, Babiker HM. Hodgkin Lymphoma. StatPearls Publishing; 2021 Jan-. Available from: https://www.ncbi.nlm.nih.gov/books/NBK499969*
- *Kaumudi Konkay, Tara Roshni Paul, Shantveer G. Uppin, and Digumarti Raghunadha Rao. Hodgkin lymphoma: A clinicopathological and immunophenotypic study; 2016 Jan-Mar; 37(1): 59–65. doi: 10.4103/0971-5851.177038*
- *Keegan TH, Glaser SL, Clarke CA, Dorfman RF, Mann RB, DiGiuseppe JA, Chang ET, Ambinder RF (2006) Body size, physical activity, and risk of Hodgkin's lymphoma in women. Cancer Epidemiol Biomarkers Prev 15(6) :1095–1101*
- *KEGG PATHWAY Database. Latent Membrane Protein 1. URL : https://www.kegg.jp/kegg-bin/highlight_pathway?scale=1.0&map=map05169&keyword=LMP1*
- *Kieser, A., & Sterz, K. R. (2015). The Latent Membrane Protein 1 (LMP1). Current topics in microbiology and immunology, 391, 119–149. https://doi.org/10.1007/978-3-319-22834-1_4*
- *Küppers, Ralf .Origin of Hodgkin Lymphoma. ;Hematology (Seventh Edition) (2018), 1204 1211. doi:10.1016/B978-0-323-35762-3.00074-3*
- *Liu, C. D., Lee, H. L., & Peng, C. W. (2020). B Cell-Specific Transcription Activator PAX5 Recruits p300 To Support EBNA1-Driven Transcription. Journal of virology, 94(7), e02028-19. https://doi.org/10.1128/JVI.02028-19*
- *Liu, M., Guo, S., Hibbert, J. M., Jain, V., Singh, N., Wilson, N. O., & Stiles, J. K. (2011). CXCL10/IP-10 in infectious diseases pathogenesis and potential therapeutic implications.*

Cytokine & growth factor reviews, 22(3), 121–130. https://doi.org/10.1016/j.cytogfr.2011.06.001

- *Luo, Y., Liu, Y., Wang, C., & Gan, R. (2021). Signaling pathways of EBV-induced oncogenesis. Cancer cell international, 21(1), 93. https://doi.org/10.1186/s12935-021-01793-3*
- *Maja Ludvigsen , Peter Kamper , Stephen J. Hamilton-Dutroit , Knud Bendix , Michael B. Møller , Francesco A. d'Amore, Bent Honore. Relationship of intratumoural protein expression patterns to age and Epstein-Barr virus status in classical Hodgkin lymphoma. Department of Biomedicine, Aarhus University, Aarhus; Department of Haematology, Aarhus University Hospital, Aarhus; Institute of Pathology, Aarhus University Hospital, Aarhus; Department of Pathology, Odense University Hospital, Odense, Denmark. European Journal of Haematology 95 (137–149),2014 doi:10.1111/ejh.12463*
- *Mohr CF, Kalmer M, Gross C, Mann MC, Sterz KR, Kieser A, Fleckenstein B, Kress AK. The tumor marker Fascin is induced by the Epstein-Barr virus-encoded oncoprotein LMP1 via NF-κB in lymphocytes and contributes to their invasive migration. Cell Commun Signal. 2014 Jul 11;12:46. doi: 10.1186/s12964-014-0046-x. PMID: 25105941; PMCID: PMC4222691.*
- *Mondul AM, Weinstein SJ, Layne TM, Albanes D.,2017. Vitamin D and cancer risk and mortality: state of the science, gaps, and challenges. Epidemiol Rev 39(1):28–48. DOI: 10.1093/epirev/mxx005*
- *National Institute of Public Health.,2017. Algiers region tumor registry 2019 edition, pp 20-23. https://www.sante.gov.dz/*
- *Notarte, K. I., Senanayake, S., Macaranas, I., Albano, P. M., Mundo, L., Fennell, E., . . . Murray, P. (2021). MicroRNA and Other Non-Coding RNAs in Epstein-Barr Virus-Associated Cancers. [Review]. Cancers (Basel), 13(15). doi: 10.3390/cancers13153909*
- *Nutt SL, Kee BL.,2007.The transcriptional regulation of B cell lineage commitment. Immunity 26(6) :715–725 Edition- publication 2007/06/227. doi: 10.1016/j.immuni.2007.05.010.*
- *O'Malley, D. P., Dogan, A., Fedoriw, Y., Medeiros, L. J., Ok, C. Y., & Salama, M. E. (2019). American Registry of Pathology Expert Opinions: Immunohistochemical evaluation of classic Hodgkin lymphoma. Annals of diagnostic pathology, 39, 105–110. https://doi.org/10.1016/j.anndiagpath.2019.02.001*
- *Paul Murray and Andrew Bell,C. Münz (ed.).,2015.Epstein Barr Virus Volume 1, Current Topics in Microbiology and Immunology,pp:390 .DOI 10.1007/978-3-319-22822-8_12*
- *Payandeh, Z., Bahrami, A. A., Hoseinpoor, R., Mortazavi, Y., Rajabibazl, M., Rahimpour, A., Taromchi, A. H., & Khalil, S. (2019). The applications of anti-CD20 antibodies to treat various B cells disorders. Biomedicine & pharmacotherapy = Biomedecine & pharmacotherapie, 109, 2415–2426. https://doi.org/10.1016/j.biopha.2018.11.121*
- *Pierce JM, Mehta A. Diagnostic, prognostic and therapeutic role of CD30 in lymphoma. Expert Rev Hematol. 2017 Jan;10(1):29-37. doi: 10.1080/17474086.2017.1270202. Epub 2016 Dec 21. PMID: 27927047.*

References

- *Pina-Oviedo S, Moran CA.,2016. Primary mediastinal classical Hodgkin lymphoma. Adv Anat Pathol. Sep;23(5):285-309. Doi: 10.1097/PAP.0000000000000119.*
- *Portis T, Dyck P, Longnecker R.,2003. Epstein-Barr Virus (EBV) LMP2A induces alterations in gene transcription similar to those observed in Reed-Sternberg cells of Hodgkin lymphoma. Blood 102:4166. Doi: 10.1182/blood-2003-04-1018*
- *Portis T, Longnecker R.,2004. Epstein-Barr virus (EBV) LMP2A alters normal transcriptional regulation following B-cell receptor activation. Virology 318(2):524–533 Edition publication 2004/02/20. DOI: 10.1016/j.virol.2003.09.017*
- *Portlock, C. S., Donnelly, G. B., Qin, J., Straus, D., Yahalom, J., Zelenetz, A., Noy, A., O'Connor, O., Horwitz, S., Moskowitz, C., & Filippa, D. A. (2004). Adverse prognostic significance of CD20 positive Reed-Sternberg cells in classical Hodgkin's disease. British journal of haematology, 125(6), 701–708. https://doi.org/10.1111/j.1365-2141.2004.04964.x*
- *Price, A. M., & Luftig, M. A. (2015). To be or not IIb: a multi-step process for Epstein-Barr virus latency establishment and consequences for B cell tumorigenesis. PLoS pathogens, 11(3), e1004656. https://doi.org/10.1371/journal.ppat.1004656*
- *Rajendran, S., Ho, W. T., & Schwarz, H. (2016). CD137 signaling in Hodgkin and Reed-Sternberg cell lines induces IL-13 secretion, immune deviation and enhanced growth. [Research Support, Non-U.S. Gov't]. Oncoimmunology, 5(6), e1160188. doi: 10.1080/2162402X.2016.1160188*
- *Ranuhardy D, Suzanna E, Sari RM, Hadisantoso DW, Andalucia R, Abdillah A. CD30, CD15, CD50, and PAX5 Expressions as Diagnostic Markers for Hodgkin Lymphoma (HL) and Systemic Anaplastic Large Cell Lymphoma (sALCL). Acta Med Indones. 2018 Apr;50(2):104-109. PMID: 29950528.*
- *Rassidakis, G. Z., Medeiros, L. J., Viviani, S., Bonfante, V., Nadali, G. P., Vassilakopoulos, T. P., Mesina, O., Herling, M., Angelopoulou, M. K., Giardini, R., Chilosi, M., Kittas, C., McLaughlin, P., Rodriguez, M. A., Romaguera, J., Bonadonna, G., Gianni, A. M., Pizzolo, G., Pangalis, G. A., Cabanillas, F., … Sarris, A. H. (2002). CD20 expression in Hodgkin and Reed-Sternberg cells of classical Hodgkin's disease: associations with presenting features and clinical outcome. Journal of clinical oncology: official journal of the American Society of Clinical Oncology, 20(5), 1278–1287. https://doi.org/10.1200/JCO.2002.20.5.1278*
- *Revue Algérienne d'Hématologie, n° 10-11, décembre 2015*
- *Ritu Lakhtakia , Ikram Burneyn., 2015 May. A Historical Tale of Two Lymphomas , Sultan Qaboos Univ Med J.; 15(2): e202–e206. Published online 2015 May 28. https://www.ncbi.nlm.nih.gov/pmc/articles/PMC4450782/*
- *Romana Idrees, Zubair Ahmad, Asim Qureshi, Aamir Ahsan, Shahid Pervez .Is fascin really a useful marker in distinguishing between classical Hodgkin's lymphoma and various types of Non-Hodgkin's lymphomas in difficult cases?. 2010 ;63:571e574. doi:10.1136/jcp.2009.075127*

References

- *S.D. Hudnall, R. Küppers (eds.).,2018. Precision Molecular Pathology of Hodgkin Lymphoma, Molecular Pathology Library, page,1th edition, pp:13-26;35-42 https://doi.org/10.1007/978-3-319-68094-1_1S.D.*
- *Saadettin Kılıçkap, İbrahim Barışta, Şükran Ülger, İsmail Çelik, Uğur Selek,Ferah Yıldız, Ayşe Kars, Yavuz Özışık, and Gülten Tekuzman. Clinical Features and Prognostic Factors of Hodgkin's Lymphoma: A Single Center Experience; 2013 Jun; 30(2): 178–185. doi: 10.5152/balkanmedj.2012.110*
- *Saadettin Kılıçkap, İbrahim Barışta,Şükran Ülger, İsmail Çelik,Uğur Selek, Ferah Yıldız, Ayşe Kars, Yavuz Özışık and Gülten Tekuzman .Clinical Features and Prognostic Factors of Hodgkin's Lymphoma: A Single Center Experience . 2013 Jun; 30(2): 178–185.doi: 10.5152/balkanmedj.2012.110*
- *Saha, A., & Robertson, E. S. (2013). Impact of EBV essential nuclear protein EBNA-3C on B-cell proliferation and apoptosis. Future microbiology, 8(3), 323–352. https://doi.org/10.2217/fmb.12.147*
- *Santos, M., & Lima, M. M. (2017). CD20 role in pathophysiology of Hodgkin's disease. Revista da Associacao Medica Brasileira (1992), 63(9), 810–813. https://doi.org/10.1590/1806-9282.63.09.810*
- *Saridakis, V., Sheng, Y., Sarkari, F., Holowaty, M. N., Shire, K., Nguyen, T., Zhang, R. G., Liao, J., Lee, W., Edwards, A. M., Arrowsmith, C. H., & Frappier, L. (2005). Structure of the p53 binding domain of HAUSP/USP7 bound to Epstein-Barr nuclear antigen 1 implications for EBV-mediated immortalization. Molecular cell, 18(1), 25–36. https://doi.org/10.1016/j.molcel.2005.02.029*
- *Shengchen Lin, Matthew D. Taylor, Pankaj K. Singh and Shengyu Yang. How does fascin promote cancer metastasis? Federation of European Biochemical Societies; 1434–1446 ª 2020doi:10.1111/febs.15484*
- *Sheren Younes, Rebecca B. Rojansky, Joshua R. Menke , Dita Gratzinger and Yasodha Natkunam . Pitfalls in the Diagnosis of Nodular Lymphocyte Predominant*
- *Shin-ichi Nakatsuka, and Katsuyuki Aozasab. Epidemiology and Pathologic Features of Hodgkin Lymphoma. Department of Clinical Laboratory, National Hospital Organization Osaka Minami Medical Center; Department of Pathology, Osaka University Graduate School of Medicine, Osaka, Japan Received December 12, 2005; accepted March 31, 2006 https://link.springer.com/content/pdf/10.1532/IJH97.05184.pdf*
- *Stanfield, B. A., & Luftig, M. A. (2017). Recent advances in understanding Epstein-Barr virus. F1000Research, 6, 386. https://doi.org/10.12688/f1000research.10591.1*
- *Steidl C, Connors JM and Gascoyne RD: Molecular pathogenesis of Hodgkin's lymphoma: Increasing evidence of the importance of the microenvironment. J Clin Oncol 29: 1812 1826, 2011.*
- *Stephan Mathas, Sylvia Hartmann, Ralf Küppers., 2016.Hodgkin lymphoma: Pathology and Biology, Seminars in Hematology.http://dx.doi.org/10.1053/j.seminhematol.2016.05.007*

References

- *Swerdlow SH, Campo E, Harris NL, Jaffe ES, Pileri SA, Stein H et al.,2008. Classification of tumours of haematopoietic and lymphoid tissues, 4th edn. IARC Press, Lyon. http://apps.who.int/bookorders/anglais/detart1.jsp?codlan=1&codcol=70&codcch=4002*
- *Szymula, A., Palermo, R. D., Bayoumy, A., Groves, I. J., Ba Abdullah, M., Holder, B., & White, R. E. (2018). Epstein-Barr virus nuclear antigen EBNA-LP is essential for transforming naïve B cells, and facilitates recruitment of transcription factors to the viral genome. PLoS pathogens, 14(2), e1006890. https://doi.org/10.1371/journal.ppat.1006890*
- *T. Clark Brelje, Robert L.,2005. Chapter10-Sorenson, lymphoid system HISTOLOGY GUIDE, virtual microscopy laboratory , Medical School ,University of Minnesota ,Minneapolis, MN. https://histologyguide.com/*
- *Thida AM, Tun AM. Lymphocyte Depleted Hodgkin Lymphoma. Treasure Island (FL): StatPearls Publishing; 2021 Jan-. Available from: https://www.ncbi.nlm.nih.gov/books/NBK556042/*
- *Treetipsatit, J., Rimzsa, L., Grogan, T., Warnke, R. A., & Natkunam, Y. (2014). Variable expression of B-cell transcription factors in reactive immunoblastic proliferations: a potential mimic of classical Hodgkin lymphoma. The American journal of surgical pathology, 38(12), 1655–1663. https://doi.org/10.1097/PAS.0000000000000266*
- *Triebwasser C, Wang R, DeWan AT Catherine Metayer, Libby Morimoto, Joseph L Wiemels , Nina Kadan-Lottick , Xiaomei Ma l.,2016 Dec. Birth weight and risk of paediatric Hodgkin lymphoma :findings from a population-based record linkage study in California. Eur J Cancer 69:19–27. Doi: 10.1016/j.ejca.2016.09.016. Epub 2016 Nov 1.*
- *Tsai, K., Thikmyanova, N., Wojcechowskyj, J. A., Delecluse, H. J., & Lieberman, P. M. (2011). EBV tegument protein BNRF1 disrupts DAXX-ATRX to activate viral early gene transcription. PLoS pathogens, 7(11), e1002376. https://doi.org/10.1371/journal.ppat.1002376*
- *Uniprot Database. Latent Membrane Protein 1. URL : https://www.uniprot.org/uniprot/P03230*
- *Uniprot Database. Latent Membrane Protein 2. URL: https://www.uniprot.org/uniprot/P13285*
- *van der Weyden, C. A., Pileri, S. A., Feldman, A. L., Whisstock, J., & Prince, H. M. (2017). Understanding CD30 biology and therapeutic targeting: a historical perspective providing insight into future directions. Blood cancer journal, 7(9), e603. 2. https://doi.org/10.1038/bcj.2017.85*
- *Völker, HU.Peuples., Becker, E., Müller-Hermelink, HK. and M.Cheikh. Extraganglionic manifestation of classical Hodgkin lymphoma in the ENT region. ENT 68, 32-39 (2020). https://doi.org/10.1007/s00106-019-00781-4*
- *Weiss, L. M., & O'Malley, D. (2013). Benign lymphadenopathies. Modern pathology: an official journal of the United States and Canadian Academy of Pathology, Inc, 26 Suppl 1, S88–S96. https://doi.org/10.1038/modpathol.2012.176*

- *Weniger, M. A., & Küppers, R. (2016). NF-κB deregulation in Hodgkin lymphoma. Seminars in cancer biology, 39, 32–39. https://doi.org/10.1016/j.semcancer.2016.05.001*
- *Wolk A, Gridley G, Svensson M (2001) A retrospective study of obesity and cancer risk. Cancer Causes Control 12(1):13–21*
- *Wu, S., Xie, P., Welsh, K., Li, C., Ni, C. Z., Zhu, X., Reed, J. C., Satterthwait, A. C., Bishop, G. A., & Ely, K. R. (2005). LMP1 protein from the Epstein-Barr virus is a structural CD40 decoy in B lymphocytes for binding to TRAF3. The Journal of biological chemistry, 280(39), 33620–33626. https://doi.org/10.1074/jbc.M502511200*
- *Xin Huang1, Ilja Nolte, Zifen Gao, Hans Vos, Bouke Hepkema, Sibrand Poppema, Anke van den Berg, Arjan Diepstra. Epidemiology of Classical Hodgkin Lymphoma and Its Association with Epstein Barr Virus in Northern China. Department of Pathology and Medical Biology, University Medical Center Groningen. PLoS ONE 6(6): e21152(2011) doi: 10.1371/journal.pone.0021152.*
- *Yin, H., Qu, J., Peng, Q., & Gan, R. (2019). Molecular mechanisms of EBV-driven cell cycle progression and oncogenesis. [Review]. Med Microbiol Immunol, 208(5), 573-583. doi: 10.1007/s00430-018-0570-1*
- *Yongzhi Men, Xuemei Sun, Daolin Wei, and Ziwei Yu .Primary extranodal head and neck classical Hodgkin lymphoma: A rare clinical case report. 2016 Aug; 12(2): 1007–1011. doi: 10.3892/etm.2016.3374*
- *Yoshihito Ishiura , Norihiro Kotani , Ryusuke Yamashita , Harumi Yamamoto , Yasunori Kozutsumi , Koichi Honke. Anomalous expression of Thy1 (CD90) in B-cell lymphoma cells and proliferation inhibition by anti-Thy1 antibody treatment. 396 (2010) 329–334*
- *Younes A, Carbone A, Johnson P, Dabaja B, Ansell S, Kuruvilla L. De Vita VTJ, Lawrrence TS, Rosemberg SA (eds),.2014. De Vita, Hellman, and Rosenberg's Cancer: Principles & Practice of Oncology: Wolters Kluwer Health/Lippincott Williams & Wilkins. https://books.google.dz/*
- *Young, L. S. (2021). Epstein–Barr Virus (Herpesviridae). 267-277. doi: 10.1016/b978-0-12-809633-8.21278-8*

Appendix

APPENDIX

APPENDIX I

Table 01: General description of the lymph node **(Rehfeld et *al*.,2017; Clark Brelje and Sorenson.,2005)**

	Subdivision	**Function**	**Light microscopy**
Capsule			
Parenchyma	Subcapsular sinus	Space underneath the capsule that receives lymph from afferente lymphotic vessels	The wall of the sinus is a discontinuous layer of flattened endothelial-like cells
	Trabeculae	connective tissue that extends inward from the capsule.	
	Trabecular sinuses	spaces alongside trabeculae in which lymph flows from the subcapsular sinus into the cortex.	
Cortex			Dark , due to abundant basophilic lymphocytes
Parenchyma	**Outer cortex** • Nodules: Spherical clusters of LB , the germinal center	Differentiation of B lymphocytes into plasma cells	Follicular lymphatic tissue with primary and secondary lymphatic follicles
	Inner cortex (paracortex) • Thymus-dependant cortex	T cell reservoir in the node	Diffuse lymphatic tissue. High endothelial venules (HEVs).
	• High endothelial venules HEV	Venules with exceptionally large endothelial cells through which lymphocytes in the blood enter the node	
Stroma			Reticular connective tissue: meshwork of reticular fibers covered by reticular cells

Medulla			Light , due to fewer cells and abundant lymphatic sinuses
Parenchyma	Medullary cords	Site of antibody production	Plasma cells, B lymphocytes, and macrophages. The wall of the sinus is a discontinuous layer of flattened endothelial-like cells
	Medullary sinuses	Filtration of lymph	
Stroma			Reticular connective tissue: Meshwork of reticular fibers, covered by reticular cells

Appendix II

II.1.3 Non-Biological Material:

1.3.1 Gross examination:

1.3.1.1 Instruments provided:

1. Gloves
2. Blade
3. Cutting board
4. Scaipel
5. Large scissors
6. Dissecting scissors
7. Ruler
8. Forceps
9. Cassetes
10. Sized container for fixative solution.

1.3.1.2 Reagents provided :

- 10% neutral buffered formalin

Fig. 02 On the left: Instruments used for grossing. **On the right:** 10% neutral buffered formalin

1.3.2 Tissue processing and preparation material

1.3.2.1 Instruments provided

- Leica TP 1020 Processor (Leica TP 1020)
- Leica Histocore Arcadia Embedding Center w/ H Paraffin Dispenser & C Cold Plate
- Metal Leica Microtome, (RM2125 RTS)
- Leica Flattening Table (HI1220)
- Nüve Oven (FN500)
- LABOPUR Ductless fume hoods.

Other instruments :

- Tissue Embedding Molds
- Water bath container

- Forceps

Fig.03 Instruments provided for tissue processing and sample preparation. **(Original photos)**

1.3.2.2 Reagents provided

- Ethanols at 100°, 80°, 70°
- Xylenes
- Paraffin

1.3.3 Histochemical Hematoxylin & Eosin (H&E) staining material

1.3.3.1 Instruments provided

- For routine H&E staining Dako CoverStainer is provided
- Staining jars
- Slide Holders
- Coverslipps
- Light microscope

1.3.3.2 Reagents provided

- Ethanols at 70°; 95°; 100°.
- Xylenes.
- Eosin solution. (0.02%)
- Harris Hematoxylin solution
- Ammonia solution (0.2%)
- Acid Alchol (1%)
- Mounting media

Fig. 04 Dako CoverStainer. **(Original photo)**

Fig.05 Reagents provided for the H&E staining procedure. **(Original photos)**

1.3.4 Immunohistochemistry material

1.3..4.1 Instruments provided:

- Micro Pipettes (10ul, 100ul, 1000ul).
- Staining jars.
- Slide Holders.
- Coverslipps.
- Humidity chamber.
- Hydrophobic pen
- Sized glass containers.
- Dako PT Link.
- For routine IHC : Dako AutostainerLink 48 and VENTANA BenchMark ULTRA.
- Light Microscope.

1.3.4.2 Reagents provided

- Ethanols 70°,80°,90°.

- Xylenes.
- Dako EnVision™ FLEX reagents (See list bellow)
- Mayer Hematoxylin solution.

SM801 — EnVision™ FLEX PEROXIDASE-BLOCKING REAGENT

EnVision™ FLEX Peroxidase-Blocking Reagent
3 x 40 mL, ready-to-use
Phosphate buffer containing hydrogen peroxide, 15 mmol/L NaN_3 and detergent.

SM802 — EnVision™ FLEX /HRP

EnVision™ FLEX /HRP
3 x 40 mL, ready-to-use
Dextran coupled with peroxidase molecules and goat secondary antibody molecules against rabbit and mouse immunoglobulins. In buffered solution containing stabilizing protein and preservative.

DM827 — EnVision™ FLEX DAB+ CHROMOGEN

EnVision™ FLEX DAB+ Chromogen
3 x 3 mL
3,3'-diaminobenzidine tetrahydrochloride in organic solvent.
The color of this reagent may vary from strong violet to colorless without having any influence on the performance of the kit.

SM803 — EnVision™ FLEX SUBSTRATE BUFFER

EnVision™ FLEX Substrate Buffer
12 x 20 mL
Buffered solution containing hydrogen peroxide and preservative.

DM828 — EnVision™ FLEX TARGET RETRIEVAL SOLUTION HIGH pH (50x)

EnVision™ FLEX Target Retrieval Solution, High pH (50x)
9 x 30 mL, 50x concentrated
Tris/EDTA buffer, pH 9

DM831 — EnVision™ FLEX WASH BUFFER (20x)

EnVision™ FLEX Wash Buffer (20x)
4 x 1 L, 20x concentrated
Tris-buffered saline solution containing Tween 20, pH 7.6 (±0.1).

K8005
DM829 — EnVision™ FLEX TARGET RETRIEVAL SOLUTION LOW pH (50x)

EnVision™ FLEX Target Retrieval Solution, Low pH (50x)
3 x 30 mL, 50x concentrated
Citrate buffer, pH 6.1

K8006
DM830 — EnVision™ FLEX ANTIBODY DILUENT

EnVision™ FLEX Antibody Diluent
120 mL, ready-to-use
Tris buffer, pH 7.2, containing 15 mmol/L NaN_3, and protein.

Fig.06 Materials provided for manual Immunohistochemistry. **(Original photos)**

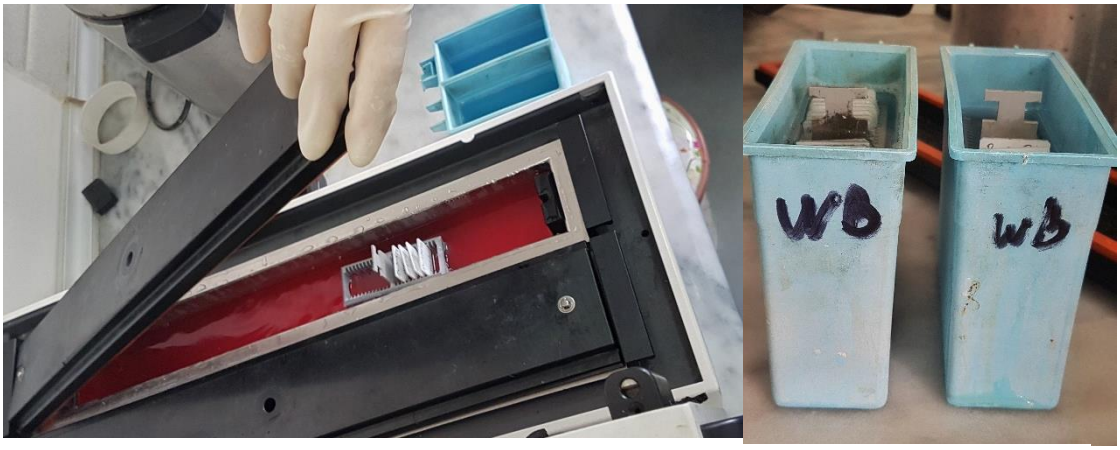

Fig. Heat Induced-Epitope Retreival (HIER) procedure. **(Original photos)**

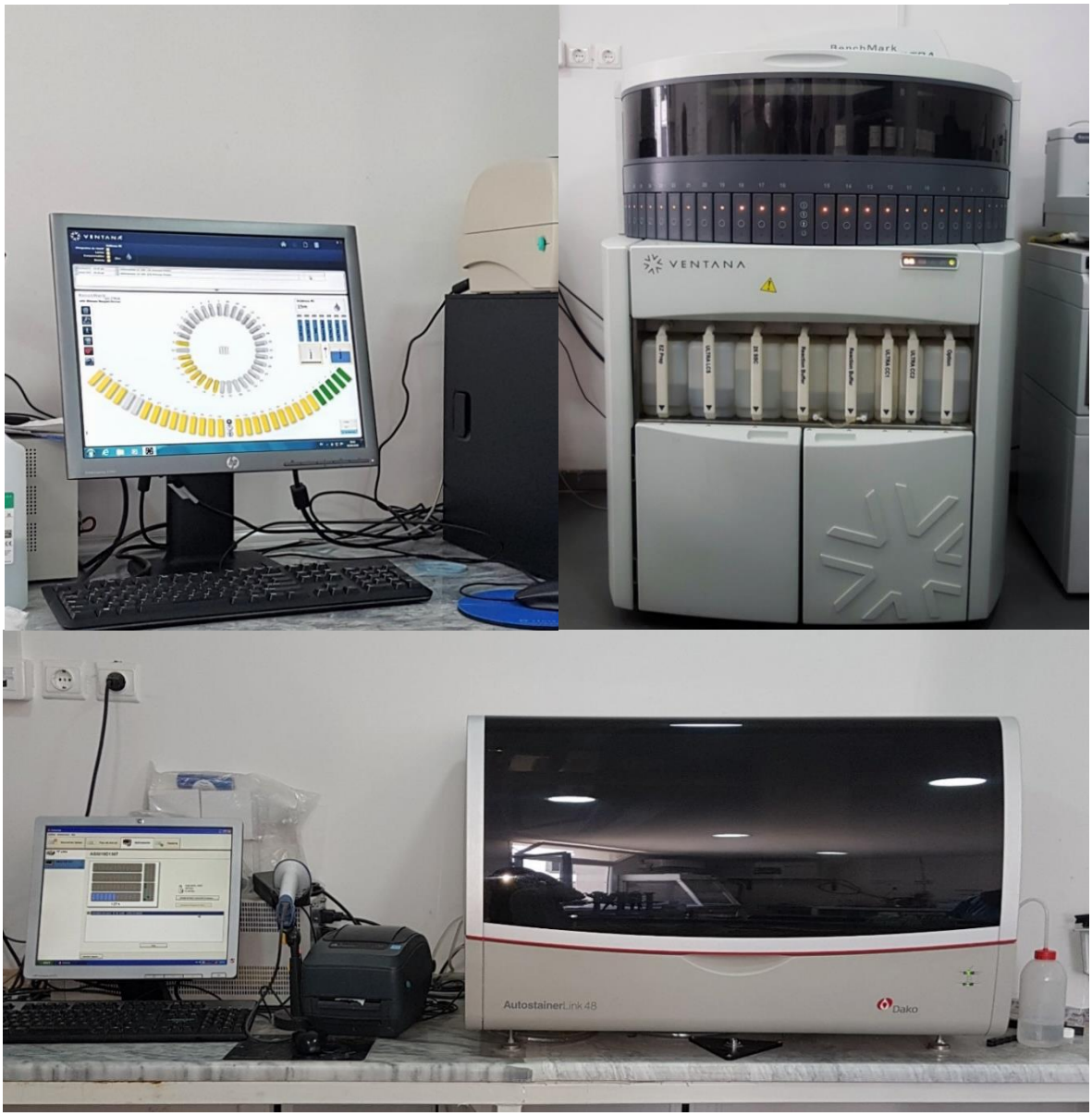

Fig.07 Utilized Autostainers for routine Immunohistochemistry. The upper photo shows the VENTANA BenchMark ULTRA system with the associated software. The lower photo shows the Dako AutostainerLink 48 with the associated software. **(Original photos)**

Fig.08 Dako EnVision™ FLEX Reagents for Immunohistochemistry. **(Original photos)**

Fig.09 Dako EnVision™ FLEX TARGET RETRIEVAL SOLUTION HIGH pH (50x). **(Original photos)**

1.3.5 Chromogenic In Situ Hybridization material

1.3.5.1 Instruments provided

- Hybridizer
- Humidity chamber
- Adjustable calibrated micro pipettes (10ul, 100ul, 1000ul)
- Coverslips
- Water bath.

- Retractable Ballpoint
- Coplin jars
- Staining jars
- Slides holders
- Light microscope.

1.3.5.2 Reagents provided

- Ethanols 70°; 95°; 100°.
- Xylenes
- Hydrogen peroxide (H2O2) 30%
- Pepesin
- Fixogum Rubber Cement
- Heat pretreatment solution EDTA
- DAB reagent (AP-Red Solution B “SB1b” + AP-Red Solution A”SB1a”)
- Nuclear Blue Solution (CS2)
- Mounting Solution

Fig.10 Instruments provided for CISH technique. The right side photo shows the Hybridizer. The up left photo shows the humidity chamber. The low left photo shows the water bath. **(Original photos)**

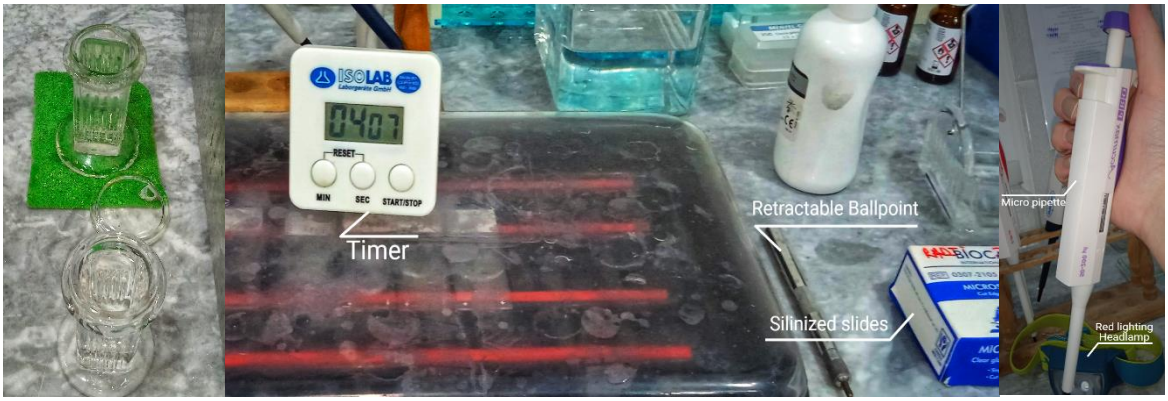

Fig.11 Other provided material for CISH technique. **(Original photos)**

Fig.12 Reagents provided for CISH technique. **(Original photos)**

Methods

- **Fixation:**

Fixation is a crucial step for the observation and interpretation of the specimens. it is done by immersing the organ in a fixative liquid; a 10% formaldehyde, the fixation time shall be at least 48 h at room temperature and may last several days.

The histological goal of fixation is to immobilize cells in a state close to the living state; This fixation leads to a hardening of the organ which allows the various tissue formations to be held in place; not only for the H&E and immunohistochemistry, but also to protect the cells against bacterial attacks, distortions and retractions.

- **Gross examination:**

The gross examination allowed to select the regions of interest for the microscopic examination: damaged zones, zones of healthy macroscopic aspect and limits of excision.

A complete, non-fragmented node biopsy or excisional biopsy of a sufficiently large pathological node is required to diagnose HL cases.

Sampling of the selected portion should be done as gently as possible in order not to degrade tissue organization.

Once obtained, Excisional biopsies and biopsy cores are measured and immediately placed in cassettes with the patient's ID; then immersed in a large volume of 10% formalin (at least 5X the volume of the sample).

Fig.13 Macroscopic examination of a lymph node; cassette placement and fixation in buffered formalin. **(Original photos)**

- **Tissue Processing:**

- **Dehydration and Embedding**

The aim of this step is to remove the intracellular water and obtain a rigidity to the sample, to be able to make a thin tissue section afterwards without losing the initial cellular structure at the time of the rupture of the plasma membrane (exit of rough water).

Tissue processing is done by the Leica TP 1020 Biosystems **(See non-biological material)**, an automatic tissue processor by which the processing is carried out in 3 steps: dehydration, clearing and infiltration of tissue samples with alcohol (Ethanol), solvents (Xylene) and paraffin

Wax. The Tissue Processing machine comprises a set of 12 baths arranged in a circle, allowing an automatic transfer where the duration of each bath differs from the other.

The tissues contained in cassettes are dehydrated by passage in ethanol, this alcohol is subsequently replaced by xylene (miscible with paraffin); then, impregnation step of the tissues is done on 3 successive baths of molten paraffin Wax at 60° then cooled.

Embedding: this step is carried out using an "Embedding center" .The specimen is placed in a mold then filled with molten paraffin. The sample is carefully oriented in the mold in order to determine the "plane of section", which is important, either for diagnosis or for a research purpose. A cassette then is placed on the top of the mold after partially cooling it on a cold plate, more paraffin is added on. Once cooled, a solid block is obtained, and the attached mold can be removed to move to microtomy.

Fig.14 Embedding and paraffin wax block making steps. **(Original photos)**

- **Sectioning/ Microtomy:**

Fig. 15 Histological sections of 1 to 3µm are made with the microtome; the section is spread out on a slide which is then identified and dried on a hot plate. **(Original photos)**

This step is achieved by using precision knives (microtome) in order to cut the Paraffin embedded tissue into sections of 1–3 µm (depends on the use). The paraffin block is placed in the microtome holder. Ribbons obtained are floated on a water bath maintained at 37°C to stretch the paraffin section. Depending on the use, a microscope glass slide with the patient's ID is placed under the selected tissue section and removed from the water bath. Tissue sections are then deposited on a hot plate at 72°C to melt paraffin and eliminate water residues from the tissue.

- **H&E staining :**

- **Dako CoverStainer**

Dako CoverStainer automates every step of the H&E process from baking, dewaxing and staining through to the dehydrated, coverslipped and dried slide that is ready for examination by the pathologist. It is divided into 3 sections, top, middle and bottom sections with 38 reagent station (20 reagent bottles in the bottom station and 18 reagent station in the middle station). The middle station contains the rack-loading tray, the heating chamber on the right, the robot and the elevator on the left. The top section comprises a touch screen to monitor the instrument, a Dako coverslipper module and a drying unit. **(See Fig.03 above)**

The Dako CoverStainer is turned on by the user and the first step is to place the slides in the rack and introduce them in the rack-loading tray. The instructions are followed on the touchscreen. The instrument works as follow :

the robot picks up the slide rack and places it in the heating unit, the heating unit for ten minutes incubation at 65°C. When baking is done the robot will pick up the slide rack and transfer it according to the protocol out in the reagents station and start incubating by transfering the slides rack to the dip tank that follows, after the H&E staining, the slides rack gets transfered to the elevator that takes it up to the coverslipping module to start the mounting procedure, the rack containing stained and mounted tissue sections is then transfered directy to the to the drying unit which tends to dry the slides for ten minutes. Once done the slides rack is transferred to the exit station. An alarm system indicates that the slides are ready to pick. The obtained slides are directly oriented to a microscopic evaluation by the pathologist.

H&E NOTES:

- Each step in the H&E staining protocol is followed by rinsing with running water.
- Tissue sections should not dry.

- **Immunohistochemistry**

Dilution of:

- **Antigen Retrieval solution**

STEP 1 Calculs : For the EnVision™ FLEX Target Retrieval Solution (TARS) bottle, 50x concentrated in a volume of 30 mL, we apply the Rule Of Three to obtein the concentration we need **50×30= 1500 mL**

That means : **30mL (TARS) ⟶ 1500 mL (Distilled Water)**

1mL (TARS) ⟶ 50 mL (Distilled Water)

Thus, EnVision™ FLEX Target Antigen Retreival Solution must be diluted at 1:50. In our case, the PT Link tanks has a capacity to contain 1500mL (1.5L), this quantity is recommended by the Dako EnVision™ FLEX catalog.

STEP 2 In a sized container, transfer 30mL of EnVision™ FLEX Target Antigen Retreival Solution (code K8004,K8005).

STEP 3 Gradually add distilled water until accomplishing the volume to 1500mL.

- **Substrate-Chromogen solution preparation**

STEP 1 Depending on the number of slides to be stained, transfer enough 1 mL aliquots of Substrate Buffer into an appropriately sized container.

STEP 2 For each 1 mL of buffer, add one drop (20 µL) of Liquid DAB+ Chromogen. Mix immediately.

Marker	HIER solution	Dilution	pH
CD30	Citrate buffer	1:50	6.1
CD15	Citrate Plus (10x)	1:10	6.1
CD20	Tris/EDTA	1:50	9
PAX5	Citrate buffer	1:50 or 1:10	6.1
EBV-LMP	Tris/EDTA	1:50	9
CD3	Tris/EDTA	1:50	9

Table.02. Required Heat Induced Epitope Retrieval (HIER) instructions for each marker prior staining procedure.

Marker	Manufacturer	Clonality	Ig-Isotype	Localization	Dilution range	Incubation period
CD30	DAKO (IR602)	Ber-H2	IgG1, kappa.	Membrane and/or cytoplasm.	Ready to use	30 minutes
CD15	Histo-Line Laboratories (RA0119-C.5)	Leu-M1 (MMA)	IgM, Kappa	Cell surface and granular paranuclear	1:50	30 minutes
CD20	DAKO (IR604)	L26	IgG2a, kappa.	Cytoplasmic side of the cell surface membrane.	Ready to use	30 minutes
PAX5	DAKO (M7307)	DAK-Pax5	IgG1, kappa.	Nuclear	1:15-1:30	20 minutes
EBV-LMP	DAKO (IR753)	CS.1-4	G1, kappa.	Cytoplasm and membrane	Ready to use	30 minutes
CD3	DAKO (IR503)	Polyclonal (UCHT1)	-	cytoplasm and/or membrane	Ready to use	30 minutes

Table.03 Characteristics of the utilized antibodies for this study

IHC NOTES:

- The tissue sections should not dry out during the treatment or during the following immunohistochemical staining procedure.
- Each step in the staining protocol is followed by rinsing with distilled for 30 seconds (except for HIER procedure)
- PT Link is pre-heated at 65°C to prevent the alteration of the tissue and the membrane integrity.
- Due to an effective washing procedure and the presence of stabilizing proteins in the Dako reagents, extra blocking steps to reduce non-specific background staining are unnecessary.
- 20-30 minutes' incubations help to increase sensitivity.
- Incubations are carried out in a humidified chamber to prevent evaporation and drying of the tissue sections.
- Slides are wiped after each step.
- The prepared DAB+ substrate-chromogen solution is stable approximately 5 days when stored at 2-8°C

Chromogenic In Situ Hybridization

STEP 1: Specimen Pretreatment

Spread the 4 micron FFPT sections on positively charged slides than incubate for 10-15 min in the oven at 92°C (drying) and for 10min at 70°C in the hot plate.

Dewax the slides in xylene 2x5min, moreover for the hydration immersed them through decreasing concentration ethanol (100%, 90%, and 70%), 3 min each then washed them in distilled water tow times. After using any reagent, the slides undergo a location of interest's areas using a Retractable Ballpoint.

Incubate the slides 5min in H2O2 at 30% on a humidity chamber to inhibit endogenous peroxidase, after that to pass for the second big step, the slides are washed in distilled water tow times, 1 min each at ambient temperature(AT).

STEP 2: digestion with pepsin

In humidity chamber, apply 1-2 drops of pepsin enzyme covering the area of interest, then incubate in hybridizer 3-5min at 37°C, wash in distilled water at AT then to unmask the target antigen (EBER) by removing excess formalin (formaldehyde bonds formed around the nucleus) incubate the slides for 15min in heat pretreatment solution EDTA at 90°C(which has already placed in water bath at 98°C), wash in distilled water at AT.

Dehydrate in 70%,90%,100% ethanol ,1 min each, then air dry sections.

STEP 3: EBV Probe

Apply 10ul of probe (Zyto Fast EBV Probe) to cover the entire section by covering the slide with 22mm×22mm coverslip (avoid trapped bubbles), fix it with Fixogum rubber cement.

Under the darkness, place the sections in a hybridizer, incubate for 2h by wish: the denaturation (5min at 75°C) and hybridization (1hat 55°C) continue with automatic process.

STEP 4: Post-hybridization and detection

Cautiously, peel the rubber cement than incubate inside wash buffer TBS for 5min at AT in order to facilitate the detachment of the coverslips without damage to the sections. For a second time immerse in another jar of TBS buffer which had been placed into a water bath at 55°C, 5min to eliminate the excess of cement.

Wash in TBS buffer for 5min at AT than apply1-2 drops of mouse anti-Dig antibody (AB1), incubate in hybridization chamber 30min at 37°C (under darkness).

Wash slides in TBS buffer three times, 1min each at AT.

Apply 1-2 drops of HRP (AB2) than incubate for 3min at 37°C (in hybridizer under darkness), wash in TBS buffer three times, 1min at AT.

Apply DAB reagent: blend 1 ml of AP-Red Solution B with 1-2 drops of AP-Red Solution A, incubate 20min at 37°C (in hybridizer under darkness) . wash in distilled water three times 1min each at AT.

Counterstain sections for 2 min with Nuclear Blue Solution (CS2), wash under cold water for 2min, immerse in 70%,90%,100% ethanol, 30s each, then in xylene tow times, 30sec each.

Air dry sections for 2min. apply coverslip(24mm×32mm) and incubate for 30 min.

Reading of stained sections under t light microscope.

Patients	Age	Subtype	CD15	CD30	CD20/HRS cells	CD20/B cells	CD3	PAX5	EBV-LMP1
Patient 1	29	NScHL							
Patient 2	55	MCcHL							
Patient 3	65	NScHL							
Patient 4	26	NScHL							
Patient 5	21	NScHL							
Patient 6	43	MCcHL							
Patient 7	35	NScHL							
Patient 8	44	NScHL							
Patient 9	33	NScHL							
Patient 10	73	LRcHL							
Patient 11	36	NScHL							
Patient 12	27	NScHL							
Patient 13	61	MCcHL							
Patient 14	3	MCcHL							
Patient 15	41	NScHL							
Patient 16	6	MCcHL							
Patient 17	61	NScHL							
Patient 18	10	MCcHL							
Patient 19	36	MCcHL							
Patient 20	41	NScHL							
Patient 21	35	NScHL							

P

N

Table.04 Immunohistochemistry distribution tests within the 21 patients

Appendix IV

ID	Gene.Symbol	Gene.Title	log2(fold change)	log(10Pvalue)
200766_at	ENTPD6	ectonucleoside triphosphate diphosphohydrolase 6 (putative)	0.394	4.023
201193_at	C2CD2L	C2CD2-like	0.396	3.945
201296_s_at	ANKMY2	ankyrin repeat and MYND domain containing 2	0.433	3.946
201564_s_at	RHOT1	ras homolog family member T1	0.445	3.879
201704_at	KLHL24	kelch-like family member 24	0.462	3.601
201739_at	CAST	calpastatin	0.469	3.665
201779_s_at	RNF111	ring finger protein 111	0.474	3.796
201780_s_at	MIR6513 /// TMBIM1	microRNA 6513 /// transmembrane BAX inhibitor motif containing 1	0.485	3.98
202087_s_at	RHOQ	ras homolog family member Q	0.489	3.702
202304_at	WDFY3	WD repeat and FYVE domain containing 3	0.491	3.697
202441_at	RAB1A	RAB1A, member RAS oncogene family	0.504	4.591
202687_s_at	ZCCHC6	zinc finger, CCHC domain containing 6	0.51	3.803
202688_at	FNDC3A	fibronectin type III domain containing 3A	0.516	4.413
202812_at	ERLIN1	ER lipid raft associated 1	0.533	4.958
202902_s_at	DICER1	dicer 1, ribonuclease type III	0.54	4.348
202912_at	SH3BP2	SH3-domain binding protein 2	0.541	3.752
202922_at	TSPAN4	tetraspanin 4	0.556	4.19
202923_s_at	CA11	carbonic anhydrase XI	0.563	3.699
202953_at	MSX1	msh homeobox 1	-0.563	3.631
202974_at	AKAP10	A kinase (PRKA) anchor protein 10	0.569	3.903
203042_at	SCARA3	scavenger receptor class A, member 3	-0.57	3.631
203097_s_at	CYFIP1	cytoplasmic FMR1 interacting protein 1	0.591	4.189
203123_s_at	CD46	CD46 molecule, complement regulatory protein	0.594	4.752
203665_at	ATG7	autophagy related 7	0.596	3.724
203971_at	ASAH1	N-acylsphingosine amidohydrolase (acid ceramidase) 1	0.596	3.73
204043_at	GCLC	glutamate-cysteine ligase, catalytic subunit	0.608	3.974
204059_s_at	ATP10D	ATPase, class V, type 10D	0.617	4.538
204079_at	AOAH	acyloxyacyl hydrolase (neutrophil)	0.619	3.6
204137_at	TPST2	tyrosylprotein sulfotransferase 2	0.628	4.969
204194_at	DENND1B	DENN/MADD domain containing 1B	0.64	4.097
204224_s_at	INSIG2	insulin induced gene 2	0.665	5.766

204232_at	CASP10	caspase 10, apoptosis-related cysteine peptidase	0.666	5.673
204417_at	WSB1	WD repeat and SOCS box containing 1	0.671	4.018
204757_s_at	MEGF9	multiple EGF-like-domains 9	0.675	5.837
204834_at	ARHGAP12	Rho GTPase activating protein 12	0.676	5.231
204929_s_at	OLFM1	olfactomedin 1	-0.683	3.623
204961_s_at	GALC	galactosylceramidase	0.686	3.943
205098_at	BACH1	BTB and CNC homology 1, basic leucine zipper transcription factor 1	0.694	4.397
205467_at	RHOQ	ras homolog family member Q	0.697	4.335
205488_at	IRAK3	interleukin-1 receptor-associated kinase 3	0.714	4.105
205552_s_at	LAMP2	lysosomal-associated membrane protein 2	0.718	3.835
205591_at	GCLC	glutamate-cysteine ligase, catalytic subunit	0.718	4.604
205639_at	NAGK	N-acetylglucosamine kinase	0.733	4.54
205692_s_at	CTSD	cathepsin D	0.739	3.786
205922_at	IDH1	isocitrate dehydrogenase 1 (NADP+), soluble	0.74	3.906
205932_s_at	MR1	major histocompatibility complex, class I-related	0.741	3.673
205936_s_at	RNF13	ring finger protein 13	0.749	4.684
206011_at	LGALS8	lectin, galactoside-binding, soluble, 8	0.756	5.45
206631_at	CASP1	caspase 1, apoptosis-related cysteine peptidase	0.76	3.776
206692_at	TCF7L2	transcription factor 7-like 2 (T-cell specific, HMG-box)	0.763	3.843
207565_s_at	CASP1	caspase 1, apoptosis-related cysteine peptidase	0.765	3.752
207571_x_at	GPR137B	G protein-coupled receptor 137B	0.765	4.246
207606_s_at	SGK1	serum/glucocorticoid regulated kinase 1	0.767	5.042
208783_s_at	RGL1	ral guanine nucleotide dissociation stimulator-like 1	0.768	4.114
208850_s_at	CITED2	Cbp/p300-interacting transactivator, with Glu/Asp-rich carboxy-terminal domain, 2	0.774	5.514
208908_s_at	RAPGEF2	Rap guanine nucleotide exchange factor (GEF) 2	0.775	5.158
208923_at	TNFSF10	tumor necrosis factor (ligand) superfamily, member 10	0.781	3.6
208936_x_at	THEMIS2	thymocyte selection associated family member 2	0.788	4.75
209263_x_at	RNF13	ring finger protein 13	0.794	4.49
209357_at	VNN2	vanin 2	0.811	3.613

209566_at	SAT1	spermidine/spermine N1-acetyltransferase 1	0.815	4.583
209568_s_at	SLC11A2	solute carrier family 11 (proton-coupled divalent metal ion transporter), member 2	0.818	4.727
209726_at	APOL3	apolipoprotein L, 3	0.828	3.673
209906_at	GSAP	gamma-secretase activating protein	0.83	3.624
209933_s_at	GAA	glucosidase, alpha; acid	0.837	4.158
209949_at	THEMIS2	thymocyte selection associated family member 2	0.85	5.749
210321_at	MPP1	membrane protein, palmitoylated 1, 55kDa	0.852	4.179
210785_s_at	TCN2	transcobalamin II	0.865	4.058
211250_s_at	FSCN1	fascin actin-bundling protein 1	-0.897	3.667
211368_s_at	CTSS	cathepsin S	0.898	3.909
211434_s_at	NCF1	neutrophil cytosolic factor 1	0.902	3.781
212117_at	CTSL	cathepsin L	0.905	4.523
212120_at	CD38	CD38 molecule	0.91	4.049
212224_at	ADAP2	ArfGAP with dual PH domains 2	0.911	4.591
212598_at	THY1	Thy-1 cell surface antigen	-0.914	3.776
212670_at	GSAP	gamma-secretase activating protein	0.917	4.266
212761_at	SECTM1	secreted and transmembrane 1	0.919	3.637
212798_s_at	NPL	N-acetylneuraminate pyruvate lyase (dihydrodipicolinate synthase)	0.93	3.842
212830_at	HIST2H2AA3 /// HIST2H2AA4	histone cluster 2, H2aa3 /// histone cluster 2, H2aa4	0.94	4.773
212888_at	CCR1	chemokine (C-C motif) receptor 1	0.949	4.1
213142_x_at	TNFSF10	tumor necrosis factor (ligand) superfamily, member 10	0.951	3.756
213238_at	RBM47	RNA binding motif protein 47	0.975	5.119
213396_s_at	CD300A	CD300a molecule	0.976	3.801
213440_at	PTGER2	prostaglandin E receptor 2 (subtype EP2), 53kDa	0.976	4.477
213624_at	HIST2H2AA3 /// HIST2H2AA4	histone cluster 2, H2aa3 /// histone cluster 2, H2aa4	0.981	4.653
213716_s_at	ELN	elastin	-1.002	3.77
213902_at	OAS1	2'-5'-oligoadenylate synthetase 1, 40/46kDa	1.012	3.94
213988_s_at	C3AR1	complement component 3a receptor 1	1.012	4.744
214084_x_at	FGL2	fibrinogen-like 2	1.02	4.001
214290_s_at	NCF2	neutrophil cytosolic factor 2	1.022	4.105
217078_s_at	TNFRSF21	tumor necrosis factor receptor superfamily, member 21	-1.047	4.321

217730_at	FCER1G	Fc fragment of IgE, high affinity I, receptor for; gamma polypeptide	1.048	3.784
218035_s_at	NCF1 /// NCF1B /// NCF1C	neutrophil cytosolic factor 1 /// neutrophil cytosolic factor 1B pseudogene /// neutrophil cytosolic factor 1C pseudogene	1.049	4.108
218217_at	HMOX1	heme oxygenase (decycling) 1	1.053	4.144
218231_at	CD300A	CD300a molecule	1.053	5.731
218232_at	HK3	hexokinase 3 (white cell)	1.071	3.686
218280_x_at	KCNJ10	potassium inwardly-rectifying channel, subfamily J, member 10	1.083	3.888
218404_at	VAMP5	vesicle-associated membrane protein 5	1.086	3.634
218673_s_at	GCH1	GTP cyclohydrolase 1	1.114	3.972
218761_at	SCPEP1	serine carboxypeptidase 1	1.114	5.629
218856_at	SLC31A1	solute carrier family 31 (copper transporter), member 1	1.144	4.595
218980_at	CCRL2	chemokine (C-C motif) receptor-like 2	1.179	4.184
219159_s_at	ADM	adrenomedullin	1.193	4.979
219358_s_at	SMPDL3A	sphingomyelin phosphodiesterase, acid-like 3A	1.22	4.48
219416_at	GZMA	granzyme A (granzyme 1, cytotoxic T-lymphocyte-associated serine esterase 3)	1.237	4.522
219696_at	FHOD3	formin homology 2 domain containing 3	-1.253	3.665
219938_s_at	C1QA	complement component 1, q subcomponent, A chain	1.258	3.774
220034_at	GZMH	granzyme H (cathepsin G-like 2, protein h-CCPX)	1.376	4.225
220933_s_at	ME1	malic enzyme 1, NADP(+)-dependent, cytosolic	1.421	4.155
221087_s_at	C1QB	complement component 1, q subcomponent, B chain	1.515	4.25
221210_s_at	PSTPIP2	proline-serine-threonine phosphatase interacting protein 2	1.529	3.619
221985_at	SNX10	sorting nexin 10	1.531	4.623
222148_s_at	ALDH1A1	aldehyde dehydrogenase 1 family, member A1	1.66	5.091

Table.05 List of the top DEGs from GEO2R web tool.(DEGs =114)